

2010

SYNTHESIS AND CHARACTERIZATION OF ELECTROSPUN GELATIN/DENDRIMER SCAFFOLD ENCAPSULATED WITH A SILVER AS A POTENTIAL ANTIMICROBIAL WOUND DRESSING

Alpana Dongargaonkar
Virginia Commonwealth University

Follow this and additional works at: <http://scholarscompass.vcu.edu/etd>

 Part of the [Biomedical Engineering and Bioengineering Commons](#)

© The Author

Downloaded from

<http://scholarscompass.vcu.edu/etd/2318>

This Thesis is brought to you for free and open access by the Graduate School at VCU Scholars Compass. It has been accepted for inclusion in Theses and Dissertations by an authorized administrator of VCU Scholars Compass. For more information, please contact libcompass@vcu.edu.

School of Engineering
Virginia Commonwealth University

This is to certify that the thesis prepared by Alpana Ajit Dongargaonkar entitled
SYNTHESIS AND CHARACTERIZATION OF ELECTROSPUN
GELATIN/DENDRIMER SCAFFOLD ENCAPSULATED WITH SILVER AS A
POTENTIAL ANTIMICROBIAL WOUND DRESSING has been approved by her
committee as satisfactory completion of the thesis requirement for the degree of Master
of Science in Biomedical Engineering

Dr. Hu Yang, Ph.D., Thesis Director, School of Engineering

Dr. Gary L. Bowlin, Ph.D., School of Engineering

Dr. Thomas W. Haas, Ph.D., School of Engineering

Dr. W. Andrew Yeudall, Ph.D., School of Dentistry

Dr. Gerald E. Miller, Ph.D., Department Chair, School of Engineering

Dr. Rosalyn Hobson, Ph.D., Associate Dean of Graduate Studies, School of Engineering

Dr. Russell D. Jamison, Ph.D., Dean, School of Engineering

Dr. Douglas F. Boudinot, Ph.D., Dean of the School of Graduate Studies

December 09, 2010.

© Alpana Ajit Dongargaonkar 2010

All Rights Reserved

SYNTHESIS AND CHARACTERIZATION OF ELECTROSPUN
GELATIN/DENDRIMER SCAFFOLD ENCAPSULATED WITH SILVER AS A
POTENTIAL ANTIMICROBIAL WOUND DRESSING

A Thesis submitted in partial fulfillment of the requirements for the degree of Master of
Science in Biomedical Engineering at Virginia Commonwealth University

By

Alpana Ajit Dongargaonkar
Bachelor of Technology, ICFAI Institute of Science and Technology, India, 2007

Director: Hu Yang, Ph.D., Assistant Professor, Biomedical Engineering

Virginia Commonwealth University
Richmond, Virginia

Acknowledgement

I would like to express my deep and sincere gratitude to my research advisor Dr. Hu Yang, for his immense support, guidance and encouragement throughout the course of my Masters education. Dr. Yang has been a constant source of inspiration and motivation and I consider myself extremely lucky to have him as my advisor. I sincerely thank the School of Engineering, Virginia Commonwealth University for giving me an opportunity to study here. I would also like to thank the members of my thesis committee Dr. Gary Bowlin, Dr. Andrew Yeudall and Dr. Thomas Haas for reviewing and evaluating my research. I thank Dr. Bowlin and his lab members for assisting me in electrospinning and other lab equipments for characterization. I also thank Dr. Ping Xu and his lab members for their assistance in performing the antimicrobial assay. I warmly thank my fellow lab mates Khushboo Sharma, Alicia Smith-Freshwater, Quan Yuan, Olga Zolotarskaya, Gunjan Saxena and Christopher Holden for their assistance and invaluable suggestions for research as well as coursework towards my Masters degree. It has been a memorable experience working with all of you, thanks.

I am extremely grateful to my wonderful friends and roommates, Rahul, Khushboo, Aditi, Yamini and Sudharshana for their love and emotional support. Last but not the least, I am most grateful to my loving parents, Anupama and Ajit Dongargaonkar and grandmom, Pushpa Gokhale for having faith in me; without their love and support I would not have been able to reach here.

Table of Contents

	Page
Acknowledgements	ii
List of Tables	vi
List of Figures	vii
 Chapter	
1 Introduction	1
2 Background	3
2.1 Phases of wound healing	3
2.1.1 Hemostasis.....	3
2.1.2 Inflammatory phase	3
2.1.3 Proliferative phase	4
2.1.4 Maturation or Remodeling phase.....	4
2.2 Factors affecting wound healing	5
2.3 Drugs, growth factors and other therapeutics to enhance the efficacy of the dressing	5
2.4 Wound dressings	6
2.4.1 Traditional and modern dressings.....	7
2.4.2 Drug delivery for wound healing	9
2.5 Dendrimers	10
2.5.1 Synthesis of dendrimers	10
2.5.2 Polyamidoamine (PAMAM) dendrimers	11
2.6 Electrospun gelatin/dendrimer scaffold with silver	13

3	Experimental Materials and Methods	15
3.1	Materials.....	15
3.2	Equipment	16
3.3	Experimental methods	17
3.3.1	Preparation of gelatin-dendrimer conjugates.....	17
3.3.2	Preparation of sample solutions for electrospinning.....	17
3.3.3	Electrospinning	17
3.3.4	Crosslinking.....	19
3.4	Characterization	19
3.4.1	Ninhydrin Assay	19
3.4.2	Scanning electron microscopy (SEM)	20
3.4.3	Tensile testing.....	21
3.4.4	Porosity measurements.....	21
3.4.5	Permeability and pore size measurements.....	21
3.4.6	Adsorption and swelling studies	22
3.4.7	In vitro degradation studies	23
3.4.8	Antimicrobial activity of silver.....	23
3.4.9	Silver release studies	24
3.4.10	Statistical analysis	25
4	Results and Discussion	26
4.1	Preparation and characterization of gelatin-dendrimer conjugates ...	26
4.2	Morphology, fiber diameter and mechanical properties	27
4.3	Scaffold porosity, permeability, swelling and degradation studies ..	33

4.4 Antimicrobial assay	37
4.5 Silver release kinetics	38
4.6 Conclusions	41
5 Summary and Future Work	42
Literature Cited	44
Appendices	49

List of Tables

	Page
Table 1: Classification of wound dressings.....	7
Table 2: List of materials.....	15
Table 3: List of equipment	16
Table 4: Solutions prepared for electrospinning scaffolds.....	18
Table 5: Tensile studies and fiber diameter of the non-crosslinked scaffolds.....	31
Table 6: Tensile studies and fiber diameter of the scaffolds crosslinked by the solution method	31
Table 7: Antimicrobial activity against <i>Staphylococcus aureus</i>	37
Table 8: Antimicrobial activity against <i>Pseudomonas aeruginosa</i>	38
Table 9: Summary table	42

List of Figures

	Page
Figure 1: Phases of wound healing.	4
Figure 2: Divergent method for synthesis of dendrimers	10
Figure 3: Convergent method for synthesis of dendrimers	11
Figure 4: Generation 2.0 PAMAM dendrimer	12
Figure 5: Generation 1.5 PAMAM dendrimer	12
Figure 6: Schematic diagram of electrospinning	18
Figure 7: Standard curve of gelatin (Ninhydrin assay)	20
Figure 8: Standard curve for silver	25
Figure 9: Reaction mechanism- conjugation of dendrimer to gelatin.....	26
Figure 10: SEM images of the non-crosslinked scaffolds.....	28
Figure 11: SEM images of the scaffolds crosslinked by the solution method.....	29
Figure 12: Fiber diameter of scaffolds (non-crosslinked and crosslinked by solution method.....	30
Figure 13: Graphical representation of stress, strain and modulus (A: Stress, B: Strain, C: Modulus).....	32
Figure 14: Porosity of the scaffolds crosslinked by the solution method	34
Figure 15: Permeability of the scaffolds crosslinked by the solution method	34
Figure 16: Pore size of the scaffolds crosslinked by the solution method	34
Figure 17: Swelling studies of the scaffolds crosslinked by the solution method.....	35
Figure 18: Degradation of the scaffolds crosslinked by the solution method	36
Figure 19: Antimicrobial activity against <i>Staphylococcus aureus</i>	39
Figure 20: Antimicrobial activity against <i>Pseudomonas aeruginosa</i>	40

Figure 21: Silver release kinetics	41
--	----

Abstract

SYNTHESIS AND CHARACTERIZATION OF ELECTROSPUN GELATIN/DENDRIMER SCAFFOLD ENCAPSULATED WITH SILVER AS A POTENTIAL ANTIMICROBIAL WOUND DRESSING

By Alpana Ajit Dongargaonkar

A thesis submitted in partial fulfillment of the requirements for the degree of Master of Science
in Biomedical Engineering at Virginia Commonwealth University.

Virginia Commonwealth University, 2010

Director: Hu Yang, Ph.D., Assistant Professor, Biomedical Engineering

A novel nanofiber scaffold was fabricated and characterized as a potential antimicrobial wound dressing. Half generation polyamidoamine (PAMAM) dendrimer G3.5 was covalently conjugated to gelatin. Gelatin alone or with gelatin-dendrimer conjugates was electrospun into nanofiber scaffolds. Gelatin is a derivative of natural collagen, and it is biocompatible, non-toxic and inexpensive, making it a desirable component in a wound dressing. Dendrimers are synthetic polymers comprising of a central core, internal branches and reactive surface groups. They

provide a structurally controlled architecture for drug release. Silver was incorporated into the scaffold in situ due to its broad spectrum of antimicrobial properties. The scaffolds were further crosslinked by photo curable PEG-diacrylate in solution or vapor to gain structure stability. The fabricated scaffolds with various compositions displayed a wide range of structure characteristics and properties in terms of fiber morphology, swelling and degradation, mechanical properties, antimicrobial activity and silver release kinetics. The scaffolds showed a similar fiber structure and morphology. It was found that the fiber diameter of the scaffolds containing silver was greater than scaffolds without silver. The porosity of the crosslinked scaffolds ranged from 67.56% to 90.42% and also exhibited a high capacity of swelling and adsorption. The results of the antimicrobial assay showed that scaffolds containing silver could effectively inhibit growth of bacteria at the end of 48 h. In vitro silver release studies demonstrated that silver could be released in a controlled manner over an extended period of time.

CHAPTER 1 INTRODUCTION

Skin is the outermost layer of the body and therefore most easily susceptible to injuries or wounds. Wounds may result from a variety of sources like accidents, surgical procedures, burns, trauma, ulcers or diseases like diabetes. They need to be treated properly to ensure effective and rapid healing. Chronic wounds affect approximately 1.5 to 3 million Americans every year and account for \$7 billion in healthcare worldwide (Margolis et al. 2002). Also, as the number of people suffering from diabetes is increasing, diabetic foot ulcers occur in almost 25% of the patients with diabetes (Centegra).

A number of new materials that hold great promise towards wound treatment have been developed. Biocompatible materials like hydrogels, hydrocolloids, foams, scaffolds and gauze are being actively studied for developing effective wound dressing products. Recently, electrospun nanofiber scaffolds have become a subject of attention for development of composite wound dressings. Such electrospun scaffolds can be generated from natural and synthetic biopolymers. They mimic the extracellular matrix, are biocompatible, biodegradable with highly porous structures providing space for cell in growth and air and moisture exchange. Also, therapeutics such as drugs and growth factors can be incorporated into the scaffolds for enhanced treatment.

The objective of this thesis was to synthesize and design a gelatin-dendrimer nanofiber scaffold with silver encapsulated as a potential antimicrobial wound dressing. Gelatin is a substance native to the human body. It is non-toxic, inexpensive and bio-compatible. Dendrimers are highly branched molecules comprising of a central core, internal branches and reactive surface groups. They provide a structurally stable architecture for drug delivery and controlled drug release. Silver is known for its antimicrobial properties and its use has been revived due to the emergence of antibiotic resistant organisms.

The experimental protocol involved the preparation of gelatin-dendrimer conjugates and preparation of solutions for electrospinning scaffolds. Eight different solutions were prepared for electrospinning consisting of gelatin and gelatin-dendrimer with different concentrations of silver, 0.825 mg/ml, 1.65 mg/ml and 3.3 mg/ml. To improve their structural stability, the scaffolds were crosslinked by solution or vapor of PEG-diacrylate in the presence of

dimethoxyphenylacetophenone (photo-initiator) upon irradiation. The morphology, structure and fiber diameter of the scaffolds were examined by scanning electron microscopy (SEM). The crosslinked scaffolds were further characterized by determining the mechanical strength, porosity, permeability and swelling ratio. The antimicrobial activity of the scaffolds was investigated against two common wound pathogens: gram-positive *Staphylococcus aureus* and gram-negative *Pseudomonas aeruginosa*. Data were collected at 4 h, 24 h and 48 h time points. It was observed that the scaffolds with all concentrations of silver could inhibit the growth of bacteria efficiently at the end of 48 h. The in-vitro release kinetics of silver was studied by Inductively coupled plasma-optical emission spectroscopy (ICP-OES).

CHAPTER 2 BACKGROUND

2.1 Phases of wound healing

A wound in the skin can be generated by physical or thermal damages or as a result of a medical condition (Boateng et al. 2008). Wounds may be classified as acute or chronic wounds. Acute wounds are injuries that heal within 8 to 12 weeks with minimum scar formation, whereas chronic wounds do not heal within 12 weeks (Boateng et al. 2008; Harding et al. 2002; Nicholas 2002).

Normal wound healing is a natural, biological process that leads to the growth and regeneration of tissue (Boateng et al. 2008). It involves platelets, neutrophils, macrophages, lymphocytes, fibroblasts, epithelial cells, growth factors and etc (Epstein et al. 1999). The normal process of wound healing consists of four phases namely: (i) Hemostasis, (ii) Inflammatory phase, (iii) Proliferative phase, and (iv) Maturation or remodeling phase (Ratner 2004). A schematic diagram of the process is shown in Figure 1 and the phases are described as:

2.1.1 Hemostasis

The immediate reaction of our body, to a cut or injury to the skin, is bleeding from the injured blood vessels (Boateng et al. 2008). Bleeding activates the platelets and clotting factors that play an important role in hemostasis. The clotting cascade is activated and fibrinogen and thrombin form a stable fibrin clot to prevent further bleeding. Further, the clot protects the underlying injured tissue (Martin 1997; Ratner 2004). Platelets secrete certain cytokines and growth factors such as platelet derived growth factor (PDGF) and transforming growth factor- β (TGF- β) to help in the healing process (Epstein et al. 1999).

2.1.2 Inflammatory phase

The inflammatory phase is characterized by swelling and redness at the area of injury. Neutrophils, lymphocytes and macrophages play an important role in inflammation by phagocytizing the bacteria and micro-organisms (Keast and Orsted). The release of plasma proteins at the wound site also causes vasodilation of the blood vessels (Boateng et al. 2008). Macrophages produce chemotactic and growth factors like interleukin-1 (IL-1), platelet derived

growth factor, transforming growth factor- β (TGF- β), epidermal growth factor, fibroblast growth factor and insulin-like growth factor which promote the proliferative phase of wound healing (Faler et al. 2006; Keast and Orsted).

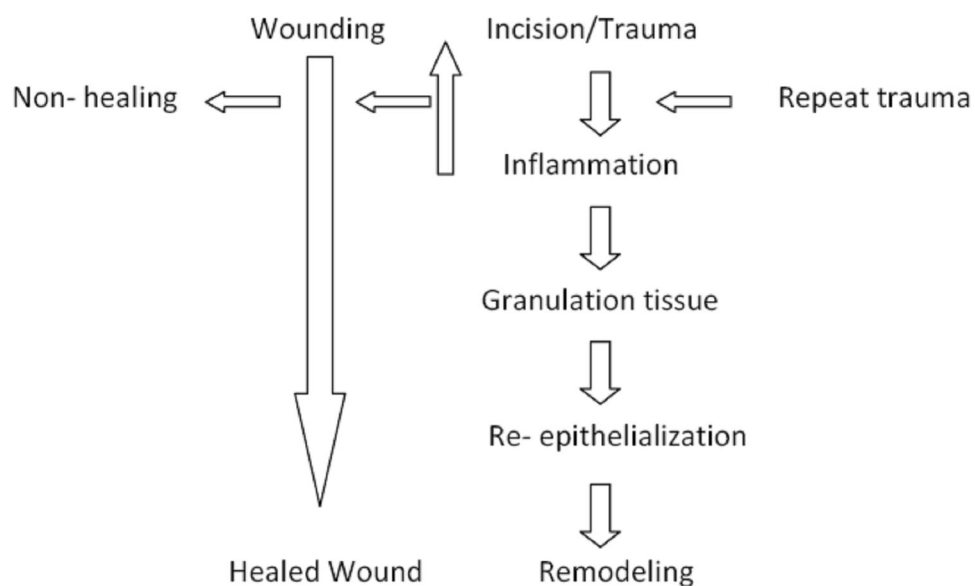
2.1.3 Proliferative phase

The proliferative phase begins when fibroblasts enter the wound site and involves extracellular matrix (ECM) deposition, angiogenesis and epithelialization (Faler et al. 2006). Fibroblasts secrete collagen which is helpful for cell migration and proliferation (Faler et al. 2006). Epithelialization occurs with formation of new blood vessels.

2.1.4 Maturation or remodeling phase

This is the last phase of the healing process and may take from about several months to years to complete depending on wound type (Boateng et al. 2008). Fibroblasts facilitate the formation of a collagen network and remodeling to strengthen the scar.

Figure 1: Phases of wound healing (Re-drawn from (Percival and Keith 2010))



2.2 Factors affecting wound healing

There are various factors that can result in an impaired wound healing (Guo and DiPietro 2010) and generally lead to a pathological wound (Boateng et al. 2008). Such factors can be classified as local and systemic factors (Guo and DiPietro 2010). Local factors are those that directly affect the wound (Guo and DiPietro 2010) such as infection, ischemia, oxygenation, topical agents, or foreign bodies (Guo and DiPietro 2010; Kerstein 1997; Waldorf and Fewkes 1995), whereas systemic factors are related to the health state of an individual, such as age, nutrition, diseases (diabetes, fibrosis, jaundice etc.), medications, smoking, or immunocompromised disorders (cancer, radiotherapy) (Guo and DiPietro 2010). Bacteria like *Pseudomonas aeruginosa*, *Staphylococcus aureus*, *Streptococcus pyogenes* and *Proteus*, *Clostridium* and *Coliform* species are common wound pathogens and unfavourable (Boateng et al. 2008; Guo and DiPietro 2010). Studies have shown that skin graft healing was affected by *P. aeruginosa* and *S. aureus* and the presence of *S. aureus* was found in 94% of the ulcers (Gilliland et al. 1988). Production of excess collagen results in the formation of keloid scars (Martin 1997). Age also affects the healing process since aging decreases the ability to combat infection (Boateng et al. 2008). Also, poor nutrition such as vitamin, mineral and protein deficiency impair and delay the wound healing process (Hemila and Douglas 1999; Patel 2005; Rojas and Phillips 1999). Diseases like diabetes affect wound healing due to poor blood circulation and also they may delay inflammation and production of collagen (Boateng et al. 2008).

2.3 Drugs, growth factors and other therapeutics to enhance the efficacy of the dressing

Apart from developing dressings to protect wounds, research is being conducted to incorporate therapeutics into wound dressings. These incorporated agents play an active part in the wound repair process. For example, antimicrobial agents can be included to inhibit growth of micro-organisms (Boateng et al. 2008).

As antimicrobial agents are able to inhibit growth of micro-organisms and prevent infection in the wound area, they are mainly for diabetic foot ulcers (Nelson et al. 2006; O'Meara et al. 2000), or wounds resulting from surgery or accidents (Harihara et al. 2006), where the risk of infection is high (Boateng et al. 2008). Commonly used antimicrobial agents are povidone-iodine with fabric dressings, silver with synthetic dressings, gentamycin with collagen dressings and

ofloxacin with silicone gel sheets (Boateng et al. 2008). The delivery of antibiotics to the wound site through wound dressings is preferred over systemic administration since the dosage required for the latter may lead to toxic reactions in the body or may be ineffective due to poor blood circulation to the extremities (Boateng et al. 2008) (e.g., diabetic foot ulcers). In addition, delivery of antibiotics through wound dressings decreases the occurrence of bacterial resistance and interference with the wound repair process (Doillon and Silver 1986).

Growth factors play an active role in cell division, migration, differentiation and proliferation (Boateng et al. 2008). They can be incorporated into wound dressing to enhance the healing process by (i) increasing the activity of inflammatory cells and fibroblasts at the wound site and (ii) stimulating cellular proliferation and angiogenesis, which, in turn, affects the production and degradation of the extracellular matrix (Greenhalgh 1996; Komarcevic 2000). Various growth factors that have been identified to play a role in wound healing are epidermal growth factor (EGF), platelet derived growth factor (PDGF), fibroblast growth factor (FGF), transforming growth factor- β (TGF- β) and insulin like growth factor (IGF-1) (Greenhalgh 1996; Steenfos 1994). Different dressings have been investigated for delivering specific growth factors. Collagen dressings have been shown to effectively deliver EGF (Grzybowski et al. 1999) and PDGF (Koempel et al. 1998) and hydrogel dressings have been shown to deliver TGF- β (Puolakkainen et al. 1995). Research done by Park et al. (Park et al. 2004) showed that wound healing was more effective when a collagen dressing containing antibiotics and FGF was used as compared to collagen dressing with antibiotic only.

2.4 Wound dressings

An ideal wound dressing is one that promotes wound healing and provides optimal environment for wound healing to take place (Shanmugasundaram et al. 2006). The desired characteristics of a wound dressing are (Ngan 2005):

- Maintaining optimum temperature and environment for wound healing
- Protecting the wound from any injury and infection by bacteria or other micro-organisms
- Controlling the moisture content
- Providing mechanical support to the wound site

- Absorbing wound exudates and keeping wound area clean
- Sterility and non-toxicity

Wound dressings can be classified based on the type of material, function and physical form of the dressing (Boateng et al. 2008):

Table 1: Classification of wound dressings (Boateng et al. 2008; Ngan 2005; Paul and Sharma 2004)

Type of Dressing	Characteristics	Example(s)
Passive Products	Comprise of traditional dressings	Gauze and tulle dressings
Interactive Products	These are dressings composed from polymers which allow moisture and oxygen exchange but can keep bacteria out. These are mostly applied to wounds that produce low exudates	Hydrogels and foam dressings
Bioactive Products	These comprise of dressings which deliver substances that can enhance the wound healing process	Alginates, chitosan, collagens and hydrocolloids

2.4.1 Traditional and modern dressings

Wound dressings have evolved over the period of time from raw applications like medicinal plants/herbs, honey and etc., to commercially designed dressings (Boateng et al. 2008). Although medicinal herbs and plants have been shown to demonstrate antimicrobial activity and reduce inflammation, their direct application may be harmful as they could contain micro-organisms which would be a source of infection (Boateng et al. 2008). Therefore, it is important to maintain an aseptic environment for wound healing to take place and use sterile wound dressings (Boateng et al. 2008). The research done by Winter in the 1960s led to the development of an approach to maintaining a moist environment for enhanced wound repair (Winter 1962). This boosted the development of advanced dressings with added functionalities to enhance wound healing (Sai and Babu 2000).

Traditional dressings consist of gauze, bandages or materials woven from fabric (Boateng et al. 2008; Sai and Babu 2000). They are dry dressings and hence moisture content can easily

evaporate through them, thus not providing a moist environment for healing. They cannot inhibit entry of micro-organisms and also its adherence to the wound causes difficulty in removing the dressing. To overcome these drawbacks, tulle dressings, gauze meshes impregnated with paraffin, have been developed. They can be removed from skin with less pain (Boateng et al. 2008; Sai and Babu 2000). However, traditional dressings need to be changed frequently and are less cost effective than synthetic/modern dressings (Harding et al. 2000). Due to these disadvantages, modern or synthetic dressings are being actively researched and developed for wound treatment.

Synthetic or modern wound dressings are classified based on the starting material used. They include hydrocolloids, alginate, hydrogel, foam, biological dressings (Boateng et al. 2008). Hydrocolloid dressings are formed from colloidal (gel-like) substances added to adhesive compounds. They can be obtained in the form of thin films or sheets and are useful for treating light to moderately exuding wounds (Boateng et al. 2008). In the original state, hydrocolloid dressings are impermeable to water vapor. However, in the presence of wound exudates, the dressings change their structure to a gel-like covering hence becoming more permeable to water and oxygen (Thomas and Loveless 1997). They do not cause any pain upon removal and are particularly useful in pediatric wound care (Thomas 1992). Alginate dressings are composed of calcium alginate and are useful in moderate to heavily exuding wounds like bleeding (Boateng et al. 2008; Paul and Sharma 2004). They can be used in the form of fibers or foams (Boateng et al. 2008). Similar to hydrocolloids, alginate dressings also can form a gel upon contact with the wound exudates. Upon application, ion exchange takes place between the exudates and alginate fibers to help form a protective gel (Thomas 2000). This helps control the moisture content and minimizes the pain during removal of the dressing (1994; Boateng et al. 2008; Gilchrist and Martin 1983).

Hydrogels are hydrophilic substances composed of synthetic polymers and have high swelling capacity (Boateng et al. 2008; Sai and Babu 2000). They occur in the form of amorphous gel or as an elastic sheet. Hydrogel in the form of elastic sheet contains crosslinked polymers so that it can retain water (Boateng et al. 2008; Sai and Babu 2000). They do not react with biological tissues, are permeable to water and metabolites (Wichterle and Lim 1960), provide a moist and

cool environment at the surface of the wound to reduce pain (Boateng et al. 2008; Sai and Babu 2000) and promote reepithelization of wounds (Debra and Cheri 1998). Foam dressings are sheets composed of polymer solutions like polyurethane (Chardack et al. 1962), which provide a moist environment and thermal insulation at the wound site (Boateng et al. 2008). These dressings are highly porous in nature, can absorb large amounts of fluid and hence can be used for low, moderate or heavily exuding wounds (Thomas 1990). Biological dressings comprise dressings derived from natural tissues or tissue engineered products consisting of combination of polymers such as collagen, hyaluronic acid, chitosan and elastin (Bartlett 1981). The major characteristics that make them attractive components for wound healing, are biodegradability, biocompatibility, non-toxicity and an active role in promoting new tissue formation (Boateng et al. 2008; Kollenberg 1998; Ueno et al. 1999).

2.4.2 Drug delivery for wound healing

Drug delivery systems have been developed to increase the effectiveness of therapeutic drugs through controlled release. Local drug delivery can be achieved by encapsulating the drug into biopolymer matrices or by covalent attachment to dendrimer surface groups or other polymers (Saltzman and Olbricht 2002). Controlled delivery of antibiotics to the wound site is beneficial because it reduces the need to deliver high doses of antibiotics systemically (Boateng et al. 2008). Dressings made from natural or synthetic biopolymers can be incorporated with drugs and growth factors for effective healing. Many polymeric dressings have been evaluated for controlled drug delivery including hydrogels based on poly(vinyl alcohol), poly(lactide-co-glycolide), poly(vinyl pyrrolidone), poly(hydroxyl-alkylmethacrylates) and alginate, polymeric matrices prepared from hyaluronic acid, collagen or chitosan and synthetic dressings which include silicone gel sheets (Boateng et al. 2008).

Controlled drug release at wounds is governed by swelling of the polymer matrix, diffusion of the drug, degradation of the scaffold or the combination of the above (Boateng et al. 2008; Sill and von Recum 2008). Diffusion of the drug and degradation of the scaffold are desirable but also disadvantageous because it may result in accumulation of the drug in large doses which can be toxic (Sill and von Recum 2008).

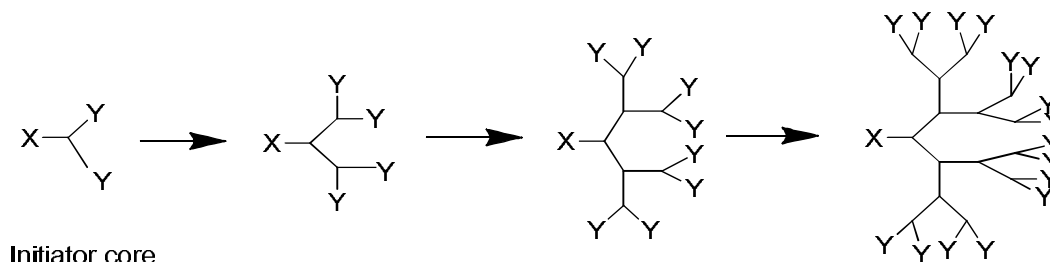
2.5 Dendrimers

Dendrimers are a group of highly branched polymers suitable for numerous applications in nanomedicine and nanotechnology. Dendrimers were first developed by Tomalia et al (Tomalia et al. 1985). The term ‘dendrimer’ is derived from the Greek word ‘dendron’ meaning tree. They are globular in structure and comprise a central core, internal branches and many reactive surface groups. There are many properties of dendrimers that make them attractive for biomedical applications: (i) they are monodisperse macromolecules (consistent size and form); (ii) they have low polydispersity index; (iii) they are highly soluble and miscible due to their branched structure; (iv) drug molecules can be encapsulated in their central core or covalently attached to their surface groups; and (v) their structurally stable architecture permits controlled drug release (Klajnert and Bryszewska 2007).

2.5.1 Synthesis of dendrimers

Dendrimers can be synthesized by two major methods: divergent synthesis and convergent synthesis (Klajnert and Bryszewska 2007). In the divergent synthesis method (Figure 2), the dendrimer advances in the outward direction from a core molecule. The core molecule reacts with monomer molecules resulting in first generation of the dendrimer. Subsequent reactions with many monomers lead to the formation of successive generations of the dendrimer. The divergent method can be used for producing large quantities of dendrimers but faces difficulty in purifying the final product.

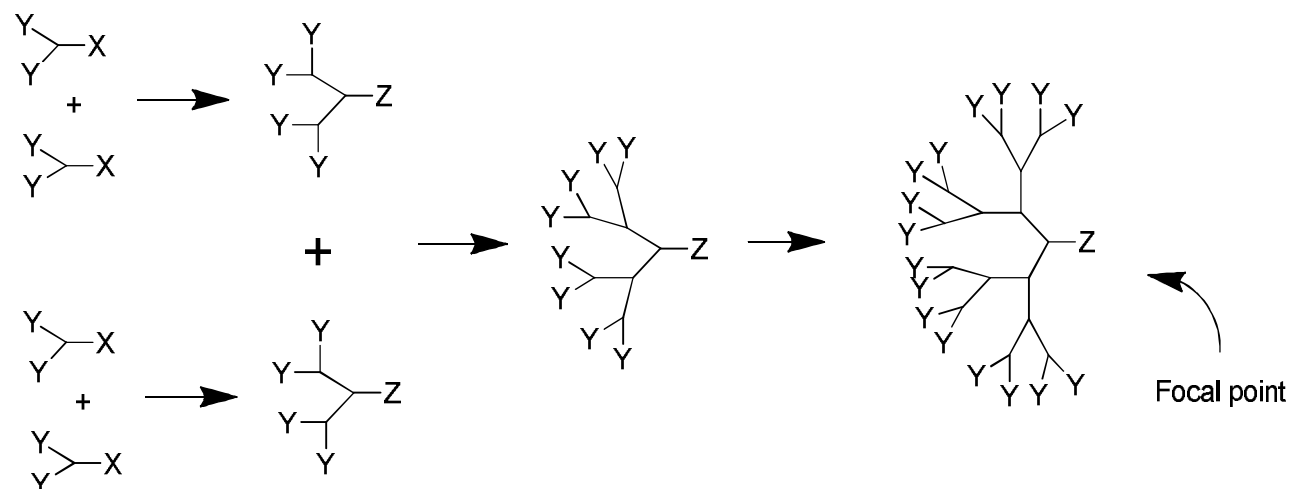
Figure 2: Divergent method for synthesis of dendrimers



In the convergent synthesis method (Figure 3), the dendrimer progresses inwards towards the core molecule. Two or more dendrons attached to the monomer molecules react with the core

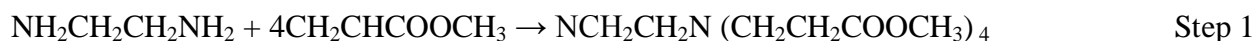
molecule to form the dendrimer. The structure resulting from convergent synthesis has less defects and the final product is easier to purify. Due to steric hindrance, high generations of dendrimers are difficult to form by the convergent synthesis.

Figure 3: Convergent method for synthesis of dendrimers



2.5.2 Polyamidoamine (PAMAM) dendrimers

PAMAM dendrimers can be synthesized by divergent synthesis to have an ethylenediamine (EDA) or an ammonia core with methyl acrylate and ethylene diamine branches (Klajnert and Bryszewska 2007; Tomalia et al. 1985). The reaction scheme for the synthesis is illustrated below (Klajnert and Bryszewska 2007):



Full generation (cationic) PAMAM dendrimers have terminal amine groups, whereas half generations (anionic) have terminal carboxyl groups as shown in Figure 4 and Figure 5, respectively (Klajnert and Bryszewska 2007). As the number of generations increase, the number of reactive surface groups is doubled (Klajnert and Bryszewska 2007).

Figure 4: Generation 2.0 PAMAM dendrimer

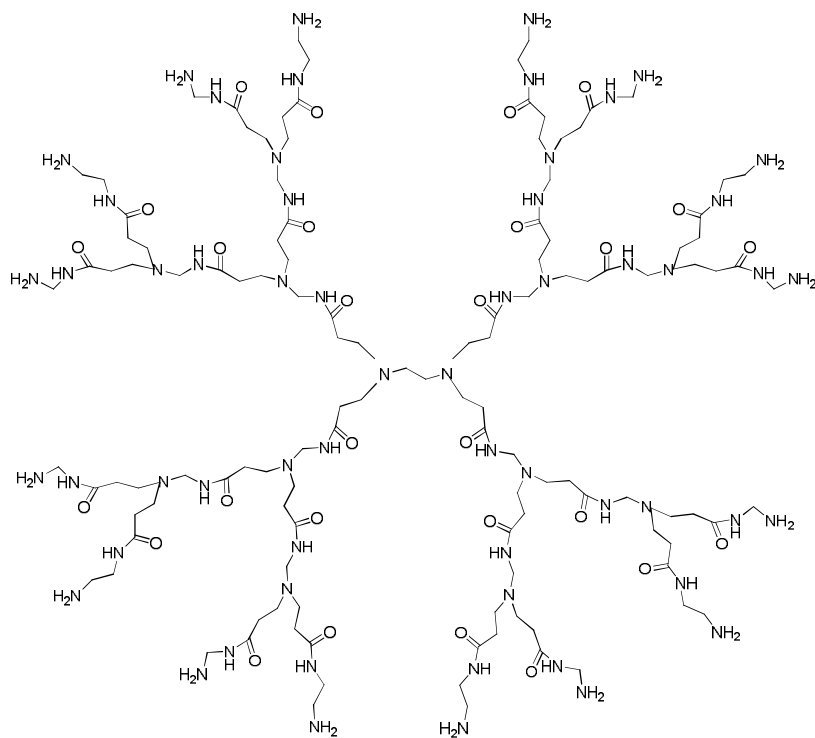
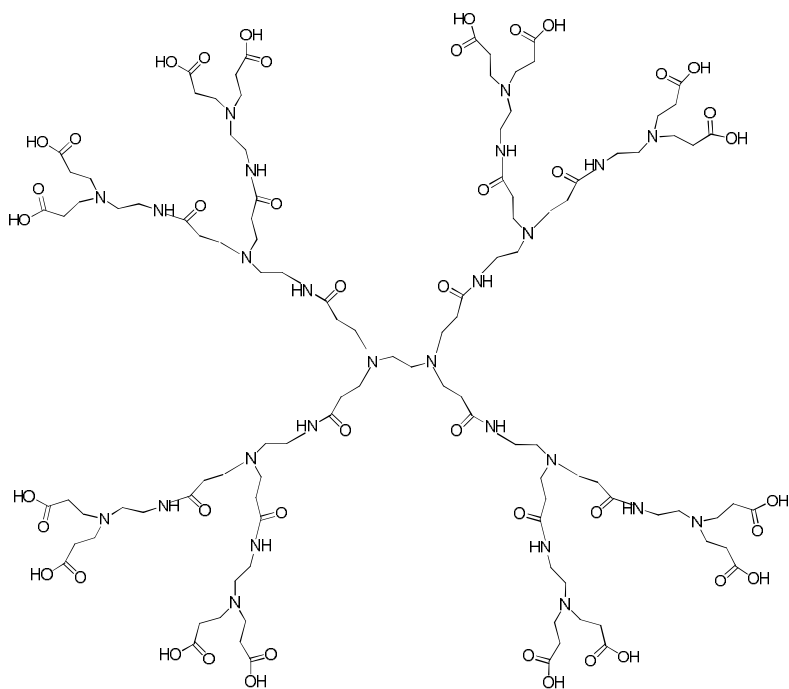


Figure 5: Generation 1.5 PAMAM dendrimer



2.6 Electrospun gelatin/dendrimer scaffold with silver

Electrospinning is a popular technique used for the fabrication of nanoscale structures for various applications like wound dressings, drug delivery vehicles and tissue engineered scaffolds (Huang et al. 2004). The scaffolds produced from natural, biodegradable polymers have very small fiber diameter ranging from nano to micrometers which is suitable to replicate the structural morphology of the natural extracellular matrix of native tissues and organs (Huang et al. 2004).

In this study, gelatin was the major component used since it is a natural biopolymer derived from collagen. It is biocompatible, biodegradable and can be commercially available at a relatively low cost (Zhang et al. 2005). It is popularly used in the field of medicine as a sealant for vascular prosthesis and as a wound dressing. However, gelatin is easily soluble in water and electrospun gelatin fibers can easily lose their structural stability in an aqueous medium. Hence, gelatin based scaffolds need to be crosslinked or incorporated with stabilizing polymers to retain its mechanical integrity as a tissue engineered construct (Zhang et al. 2005). Dendrimer can be covalently bound to gelatin and electrospun into a scaffold for drug encapsulation and drug delivery.

Silver was selected as an antimicrobial agent due to its broad range of antimicrobial activity against gram-positive and gram-negative bacteria (Hromadka et al. 2008). It can also inhibit antibiotic resistant bacteria like methicillin-resistant *Staphylococcus aureus* (MRSA) and vancomycin-resistant *enterococci* (VRE) when used at proper concentrations (Warriner and Burrell 2005). Silver can kill micro-organisms by multiple mechanisms, it can change the structure and function of a bacterial cell by altering its protein structure or rupture the bacterial cell wall or block the respiratory pathway (Warriner and Burrell 2005). Silver based wound dressings and creams are used for wound healing and to maintain a microbe free environment at the wound site (Warriner and Burrell 2005). Silver based dressings are particularly used in burn wounds, chronic leg ulcers, diabetic wounds and traumatic injuries (Ip et al. 2006). There are various ways by which silver can be incorporated in the dressing such as silver nitrate, silver sulfadiazine, silver calcium phosphate or in the form of nanocrystalline silver (Warriner and Burrell 2005). The silver can be released from the dressing by means of diffusion to the surface of the wound (Agarwal et al. 2009).

Apart from the advantages of including silver in a dressing, there are certain difficulties faced with current topical silver dressings such as slow rate of release, staining at the wound area, rapid consumption of silver ions and patient comfort (Warriner and Burrell 2005). Due to these issues, silver based dressings need to be investigated and an optimum concentration of silver introduced into the dressing needs to be selected.

CHAPTER 3 EXPERIMENTAL MATERIALS AND METHODS

3.1 Materials

Table 2: List of materials

Material	Abbreviation
Polyamidoamine (PAMAM) dendrimer generation 3.5, 10 wt% solution in methanol	G3.5
Gelatin from porcine skin- Type A	
Sodium bicarbonate	NaHCO ₃
1-Ethyl-3-(3-dimethylaminopropyl)carbodiimide	EDC
N-Hydroxysuccinimide	NHS
Ethyl ether (anhydrous)	
Ethanol (denatured)	
Poly (ethylene glycol) diacrylate (M _n =575 g/mol)	PEG-diacrylate
Dimethoxyphenylacetophenone, 99%	DMPA
Ninhydrin, 97%	
De-ionized water	DI water
Silver acetate	
1,1,1,3,3,3 Hexafluoro-2-propanol	HFP
Sodium chloride	NaCl
Peptone	
Tryptone	
Yeast extract	
Agar	
Phosphate buffered saline	PBS
Aqueous silver standard for ICP-OES	

3.2 Equipment

Table 3: List of equipment

Equipment name	Purpose
Rotary evaporator, LABOROTA 4000 (Heidolph)	To distill low boiling point chemicals from a mixture of compounds
Flexi-dry MP controlled rate freezer (FTS Systems, Inc.)	To freeze dry the sample
Weighing scale	To measure the quantity of chemicals
Long wave ultra-violet lamp, model B (UVP)	For UV irradiation
Ultra violet visible (UV-Vis) spectrophotometer (Genesys 6, Thermo electron Corporation)	To measure the absorbance value or standard curve
Electrospinner	To electrospin scaffolds
MTS Bionix 200 - Mechanical testing system	To measure stress, strain and modulus
Scanning electron microscope model EVO 550	To take images of the scaffold and measure the fiber diameter by Image Tool
Autoclave	To sterilize medium
Incubator	To control temperature and humidity of microbial culture
Hood	To maintain sterile conditions
Eppendorf centrifuge model-5415D	To separate mixture of compounds based on density
Varian vista MPX, ICP-OES	To measure the concentration of metals in a sample by inductively coupled plasma-optical emission spectroscopy

3.3 Experimental methods

3.3.1 Preparation of gelatin-dendrimer conjugates

The protocol used for the preparation of gelatin-dendrimer conjugate was a slight modification to that used by Alicia Smith Freshwater (Smith-Freshwater 2009). Gelatin was conjugated with half generation PAMAM dendrimer G3.5. Briefly, 120 μ l of G3.5 in methanol stock solution was dried by rotary evaporation and re-dissolved in 2 ml of distilled water. This solution was vortexed thoroughly and mixed with 3 mg of NHS and 5 mg of EDC while stirring for 24 h to achieve surface activated G3.5 (i.e., G3.5-NHS). To prepare the gelatin solution, 20 mg of gelatin was added to 20 ml of 0.1N NaHCO_3 solution and completely dissolved by stirring at 80°C until it formed a clear solution. At 24 h, the gelatin solution was added to G3.5-NHS solution and kept in an ice bath for 4 h. It was then centrifuged for 20 min at 10 rpm and the supernatant was added drop wise to 50 ml of ethyl ether and refrigerated for 24 h. It was then centrifuged for 20 min at 10 rpm and the precipitate was collected. The precipitate was further purified by rapid dialysis using 12-14 kDa MWCO dialysis tubing. The purified solution was lyophilized by FTS to obtain gelatin-dendrimer conjugates.

3.3.2 Preparation of sample solutions for electrospinning

Eight different sample solutions were prepared using HFP as a solvent. The types of scaffolds electrospun and their constituents are summarized in Table 4. The reason for electrospinning eight different scaffolds with varying amounts of silver was to compare the characteristics of these scaffolds against each other and to determine the optimum silver composition against infection. The solutions were mixed thoroughly for 24 h on a shaker plate prior to electrospinning.

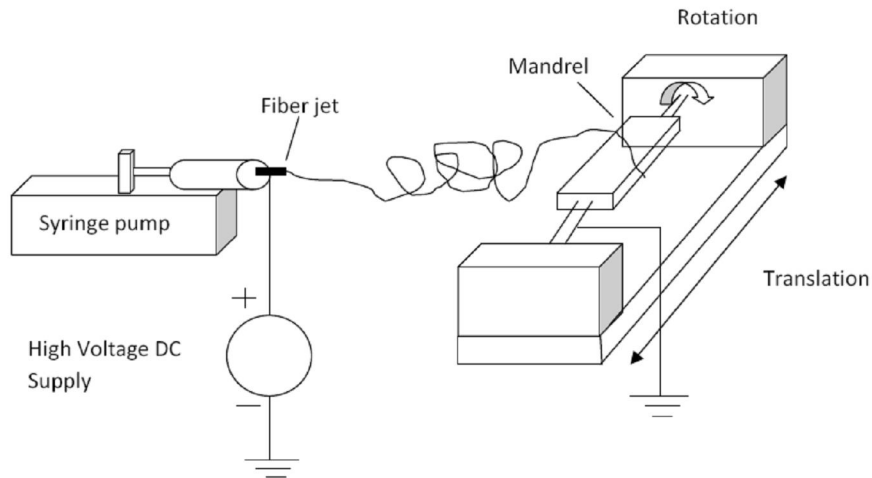
3.3.3 Electrospinning

A schematic diagram of the electrospinning technique is illustrated in Figure 6. In the electrospinning process, electrical charge is applied to draw fine fibers from the solution. The solution for electrospinning is loaded into a syringe and a positively charged electrode is attached to the needle of the syringe. The voltage applied results in an electric field and the drop of

Table 4: Solutions prepared for electrospinning scaffolds (The solutions were prepared in 10 ml of HFP)

Scaffold	Gelatin (mg/ml)	Gelatin-dendrimer conjugate (mg/ml)	Silver acetate (mg/ml)
S1	100	0	0
S2	100	0	3.3
S3	100	0	1.65
S4	100	0	0.825
S5	96	4	0
S6	96	4	3.3
S7	96	4	1.65
S8	96	4	0.825

Figure 6: Schematic diagram of electrospinning (Re-drawn from (Sill and von Recum 2008))



polymer solution at the tip of the needle is altered into a conical shape known as the Taylor cone. As the strength of the electric field increases, the polymer solution jet is elongated to form long, thin fibers as a result of solvent evaporation. The fibers are collected on a collector or mandrel that is grounded. The mandrel undergoes translation and rotation for the uniform deposition of the scaffold.

Particularly, the electrospinning solution was loaded into a 10 ml Becton Dickinson syringe and placed in a KD Scientific syringe pump for electrospinning. The syringe pump was set to deliver the solution at a rate of 5 ml/h. A voltage of 25 kV was applied to the needle of the syringe by a high voltage power supply (Spellman CZE1000R, Spellman High Voltage Electronics Corporation). The mandrel chosen for collecting the fibers was a flat, stainless steel mandrel 7.5 cm x 2.5 cm x 0.5 cm (L x W x T). It was placed approximately 125 mm from the needle tip and rotated at ~500 rpm for uniform collection of the fibers. After electrospinning was completed, the scaffold was carefully removed from the mandrel, placed in a fume hood for degassing and stored in a moisture free environment.

3.3.4 Crosslinking

After electrospinning, the scaffolds were crosslinked to increase structure stability and mechanical properties. For each scaffold, 100 μ l of PEG diacrylate, 4 mg of dimethoxyphenylacetophenone (photo-initiator) and 2 ml of ethanol were used to prepare the crosslinking solution. The solution was poured onto a scaffold of 7.5 cm x 5 cm and of varied thickness and allowed to stay for about 30 min. The scaffold was then held under UV light for 2 min on each side. This method is referred to as the solution method. As an alternative method, vapors were used for crosslinking the scaffolds. The solution was heated in a water bath and the scaffold was crosslinked by the vapors. It was then held under UV light for 2 min on each side. This method is referred to as the vapor method. The scaffolds crosslinked by the vapor method did not retain their structure in aqueous medium and could be only characterized for morphology, fiber diameter, and tensile properties. Their data is shown in Appendix C.

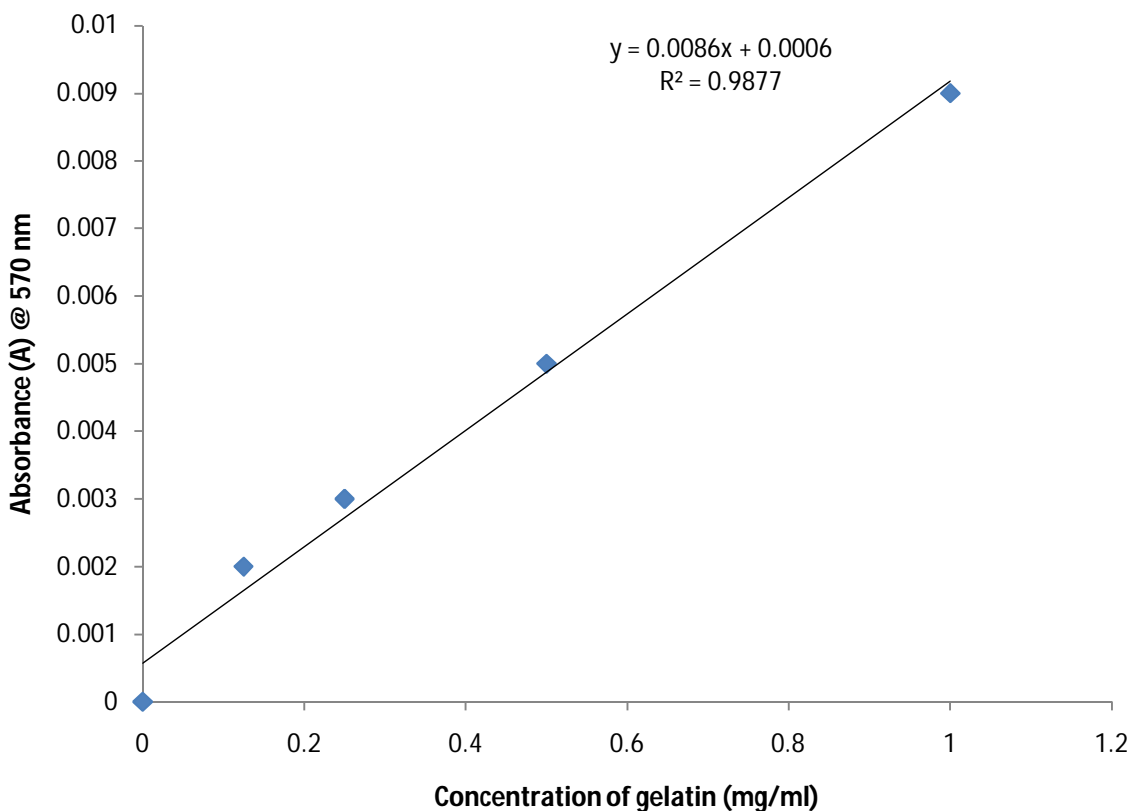
3.4 Characterization

3.4.1 Ninhydrin assay

Ninhydrin assay was performed to confirm the conjugation of dendrimer to gelatin. The ninhydrin stock solution was prepared by dissolving 30 mg of ninhydrin in 10 ml of ethanol. Five different concentrations of gelatin were prepared and mixed with 1 ml ninhydrin solution and a standard curve (Figure 7) was obtained using UV-Vis spectrophotometer. 1 mg of G3.5-gelatin conjugate was mixed with 1 ml of DI water and 1 ml of ninhydrin solution. This mixture

was heated to approximately 80°C for 5-10 min and cooled to 20-25°C and the absorbance was measured at 570 nm. The absorbance value of G3.5-gelatin conjugate mixed with ninhydrin was compared to the standard curve of gelatin mixed with ninhydrin.

Figure 7: Standard curve of gelatin (Ninhydrin assay)



3.4.2 Scanning electron microscopy (SEM)

SEM images of the scaffolds were taken to characterize the structure and morphology of the scaffolds. A small piece of sample from each scaffold was cut and gold sputter coated. Images were taken by Scanning Electron Microscope Model 550 at a magnification of 1200x. A scale bar of 10 μm is presented on each figure. Fiber diameter was calculated by using the UTHSCSA Image tool Version 3.0 to measure 30 randomly chosen fibers.

3.4.3 Tensile testing

Tensile studies of the scaffold were performed to analyze the mechanical properties of the scaffolds. Tensile studies were done on the MTS Bionix 200®- Mechanical testing system with a 100 N load cell. Six dog-bone shaped samples were cut out from each scaffold using a punch die. The thickness of the samples was measured in inches and the scaffolds were placed in the metal grips of the mechanical testing system moving at a rate of 10 mm/min. Stress, strain, modulus and energy to break were measured by the MTS Testworks software (version 4.04A).

3.4.4 Porosity measurements

Scaffold porosity was measured by taking out 1 cm x 1 cm samples from the scaffold and measuring the mass in g and thickness which ranged from 0.032 cm to 0.33 cm. Porosity was calculated by the formula:

$$P = \left[1 - \frac{V_g}{V_a} \right] \times 100$$

Where, V_g = Mass of scaffold/ Density of collagen (1.41 g/cm³)

V_a = Apparent volume of the square section 1 cm x 1 cm x thickness

Three samples (n=3) were used from each type of scaffold for the porosity measurements.

3.4.5 Permeability and pore size measurements

Permeability was measured by an apparatus designed by Scott Sell (Sell et al. 2008). 12 mm discs were punched out from the scaffolds and the time taken for 10 ml of water to pass through the disc was noted.

Permeability was calculated as (Carr and Hardin 1987):

$$\tau = \frac{Q\mu T}{tAP}$$

Where, τ = Permeability measured in Darcy

Q=volume flowing through the system

T= scaffold thickness

μ = fluid viscosity (0.89 cP)

t = time taken for 10 ml water to flow through the scaffold (in seconds)

A= cross sectional area of scaffold (πr^2)

P= applied pressure (ρgh) in atm

Where, ρ = density of water (1000 kg/m³)

g = gravitational force (9.8 m/s²)

h = total height of the system (m)

The average pore size was calculated as (Carr and Hardin 1987):

$$r = \frac{0.5093}{\tau^{1/2}}$$

Three samples (n=3) were used from each type of scaffold for permeability measurements.

3.4.6 Adsorption and swelling studies

Simulated wound fluid (Parsons et al. 2005) (SWF) was used as the medium for swelling studies and antimicrobial activity to mimic the clinical conditions. SWF consists of 50% calf serum and 50% maximum recovery diluent (0.1% w/v peptone and 0.9% w/v sodium chloride) (Parsons et al. 2005). 2.5cm x 2.5 cm of samples were cut out from each of the scaffolds and weighed (W_d). They were immersed in 5 ml of SWF at room temperature. The samples were taken out of the fluid, blot dried and weighed (W_s) at 10 min, 20 min, 30 min, 60 min, 90 min, 120 min, 24 h and 48 h. The swelling ratio (%) was calculated by the formula (Parsons et al. 2005):

$$\text{Swelling ratio \%} = \left[\frac{W_s - W_d}{W_d} \right] \times 100$$

Three samples (n=3) were used from each type of scaffold for swelling studies.

3.4.7 In vitro degradation studies

The *in vitro* degradability of the scaffolds without silver (S1 and S5) was evaluated. Four different media and conditions were used for the degradation studies: (i) incubation in Dulbecco's modified Eagle's medium (DMEM) supplemented with 10% fetal bovine serum (FBS) at 37°C, (ii) DMEM supplemented with 10% FBS at room temperature, (iii) incubation in SWF at 37°C and (iv) incubation in cell conditioned medium at 37°C (Cell conditioned medium was DMEM supplemented with 10% FBS used for culturing confluent BJ-hTERT fibroblasts for 24 h in 96 x 16 mm sterile petri dish). Nine samples from each scaffold of size 1 cm x 1 cm were weighed and immersed in 1.5 ml of each of the media mentioned above, for 24 h. After 6 h, 12 h and 24 h three samples of each scaffold type were taken out from all media, centrifuged for 20 min, frozen, then lyophilized and weighed. The average ratio of weight loss due to the degradation in each scaffold was calculated using the formula:

$$\text{Ratio of weight loss (\%)} = \left[\frac{W_o - W_d}{W_o} \right] \times 100$$

Where, W_o = initial weight

W_d = weight of the sample after degradation

3.4.8 Antimicrobial activity of silver

The antimicrobial activity of silver was tested against common wound pathogens- gram positive *Staphylococcus aureus* (strain N315) and gram negative *Pseudomonas aeruginosa* (strain PA01). Colony plates of *Staphylococcus aureus* and *Pseudomonas aeruginosa* were cultured from the respective bacterial strains. 1 L of Luria agar was prepared containing 10 g of Tryptone, 5 g of yeast extract, 10 g of NaCl and agar to a final concentration of 1.5%. All the components were dissolved in 1 L of DI water. The medium was autoclaved at 121° C for 15 to 20 min and poured onto sterile petri plates and allowed to dry. Bacterial culture was inoculated using 1 colony in 3-4 ml of SWF and incubated at 37° C overnight. 10 fold serial dilutions of the pure bacterial culture were made in SWF and 10⁵ dilution repeats were prepared in test tubes. 2.5 cm x 2.5 cm sample taken out from each scaffold were inserted into the 10⁵ dilution test tubes and incubated at 37° C.

One test tube containing no scaffold was used as control. 100 µl (0.1 ml) of aliquot was taken out from each of the test tubes at 4 h, 24 h and 48 h and plated on luria agar plates. The plates were incubated at 37° C in the incubator overnight and observed for any bacterial growth thereafter. After incubation, the number of colonies present was counted and colony forming units/ml (cfu/ml) was reported.

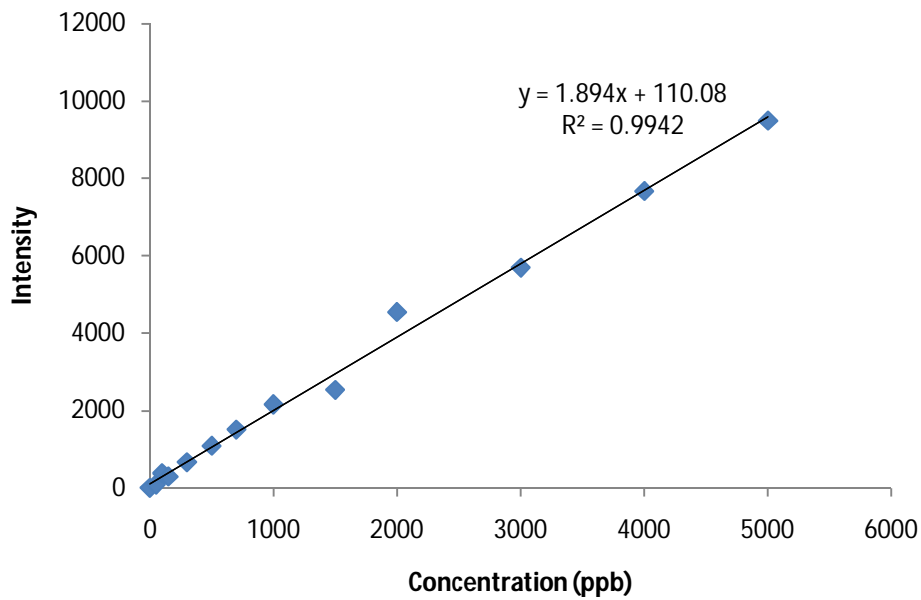
3.4.9 Silver release studies

The silver release from the scaffolds was studied in PBS. 2.5 cm x 2.5 cm of samples were taken out from the scaffolds, weighed and immersed into a capped glass vial containing 20 ml (0.02 L) of PBS. The glass vial was kept on a stir plate and the temperature was maintained at 37°C. At pre-determined time points: 1 h, 2 h, 3 h, 4 h, 24 h, 48 h, 72 h, 96 h, 120 h, 144 h, 168 h, 192 h, 216 h, 240 h and 264 h, 10 ml (0.01 L) of PBS was transferred to a capped tube for silver content analysis. 10 ml of fresh PBS was added to the vial to maintain the volume of the medium for continuous observation. Silver content was analyzed by Inductively Coupled Plasma-Optical Emission Spectroscopy (ICP-OES/ ICP Varian Vista MPX). ICP-OES is a technique used for analysis of trace metals present in a sample. The presence of the metals is detected by electromagnetic radiation emitted by excited atoms or ions, at a wavelength characteristic to a particular metal (Mermet 2005; Stefánsson et al. 2007). The concentration of the metal can be calculated by the intensity of the emission.

Different concentrations of aqueous silver standards were prepared from a stock solution of 1000 ppm (mg/L) silver standard. The intensity values of the known concentration of silver standards and the aliquots were recorded by ICP-OES. The calibration curve of silver (Figure 8) was used as a reference to calculate the concentration of silver in each of the aliquots. The concentration of silver in each aliquot ([concentration]_{to}) was obtained in the units of parts per billion (ppb or µg/L). The amount released at each time point was calculated as follows:

$$\% \text{ Cumulative amount released (t)} = \left[\frac{[\text{concentration}]_t \times 0.02 \text{ L} + [\text{concentration}]_{to} \times 0.01 \text{ L}}{\text{Initial amount of silver in the sample (}\mu\text{g)}} \right] \times 100$$

Figure 8: Standard curve for silver



3.4.10 Statistical analysis

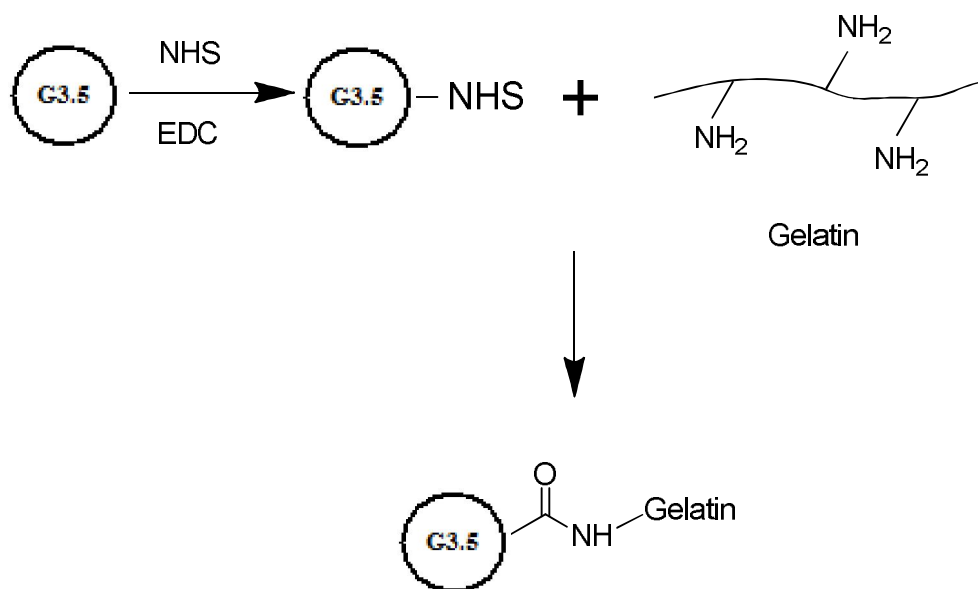
Statistical analysis was performed on mean scaffold fiber diameters, tensile testing values, porosity, permeability, pore size, swelling ratio (%) and degradation. All statistical analysis was based on one way analysis of variance (ANOVA) and Tukey's test for significance, performed on Minitab statistical software. A p-value less than 0.05 was considered statistically significant. Graphical representations of mean data were constructed with Microsoft Excel 2007 with error bars representing standard deviations.

CHAPTER 4 RESULTS AND DISCUSSION

4.1 Preparation and characterization of gelatin-dendrimer conjugates

Coupling of G3.5 to gelatin was based on EDC/NHS chemistry and the reaction mechanism is shown in Figure 9. EDC along with NHS activated the terminal carboxyl groups of G3.5. The carboxyl groups and amine groups form an amide bond, hence coupling dendrimer to the gelatin backbone.

Figure 9: Reaction mechanism- conjugation of dendrimer to gelatin



The conjugation of gelatin and G3.5 was confirmed by the ninhydrin assay. Ninhydrin produces a chromophore when mixed with amine containing compounds and its presence can be detected by measuring the absorbance value by UV-Vis spectrophotometer at a wavelength of 570 nm. As shown in the standard curve of gelatin (Figure 7), 1 mg/ml of pure gelatin mixed with 1 ml of ninhydrin was found to have an absorbance value of 0.009 whereas 1 mg/ml of G3.5-gelatin mixed with 1 ml of ninhydrin solution gave an absorbance value of 0.002. The reduced absorbance was attributed to the decrease in the number of free amine groups and hence confirmed the conjugation of dendrimer to gelatin.

4.2 Morphology, fiber diameter and mechanical properties

Electrospinning technique for fabrication of nanofiber scaffolds is gaining popularity due to its simplicity and ease of use (Kumbar et al. 2008). Electrospun scaffolds exhibit similarity in morphology to natural extra-cellular matrix (ECM), which is beneficial for tissue growth. Electrospinning can produce randomly oriented or aligned, continuous fibers which have high porosity and high surface area (Sill and von Recum 2008).

Pure gelatin alone or with gelatin-dendrimer conjugates was electrospun to form nanofiber scaffolds. The scaffolds were further crosslinked to improve their structural stability. The data shown and discussed in this chapter are based on non-crosslinked scaffolds and scaffolds crosslinked by the solution method. The structure, morphology, mechanical properties and swelling ability of the scaffolds were evaluated. Different concentrations of silver acetate were incorporated in the scaffolds to determine the antimicrobial efficacy and silver release kinetics. SEM images of non-crosslinked scaffolds and scaffolds crosslinked by the solution method are shown in Figure 10 and Figure 11, respectively. It is observed that the scaffolds crosslinked by the solution method retained the nanofiber structure. There are many factors that affect the fiber diameter and morphology, such as concentration of polymer, viscosity, voltage applied, diameter of the needle and the rate at which the polymer solution is delivered (Lee et al. 2008). The fiber diameter of the non-crosslinked scaffolds ranged from 3.15 to 5.88 μm and that of the scaffolds crosslinked by the solution method ranged from 2.64 to 6.98 μm . A graphical representation of the data is shown in Figure 12. Also, statistical differences were analyzed using ANOVA in Minitab statistical software and the data is shown in Appendix A and Appendix B. It was observed that for both non-crosslinked and crosslinked scaffolds by the solution method, the fiber diameter of the gelatin-dendrimer scaffolds (S5, S6, S7, S8) was larger than that of the scaffolds containing gelatin only (S1, S2, S3, S4). Also it was observed that as the silver concentration in the gelatin scaffolds decreased, the fiber diameter decreased but for the gelatin-dendrimer scaffolds as the silver concentration in the gelatin scaffolds increased. Half generation PAMAM dendrimers have a negative charge which could also have an influence on the electric field during electrospinning, thereby affecting the fiber diameter.

Figure 10: SEM images of the non-crosslinked scaffolds (The white block arrows indicate the notation of the scale bar of 10 μm)

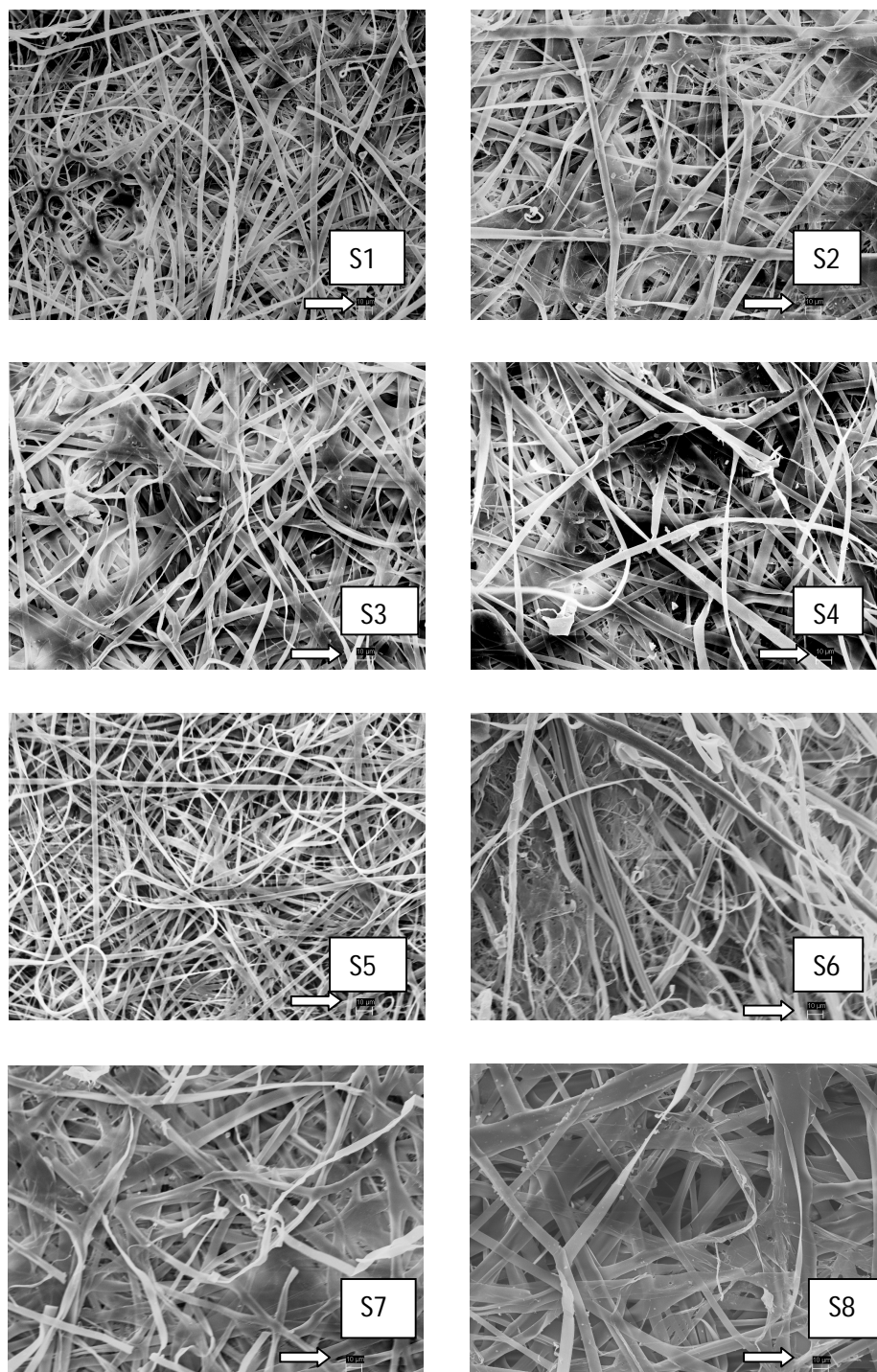


Figure 11: SEM images of the scaffolds crosslinked by the solution method (The white block arrows indicate the notation of the scale bar of 10 μm)

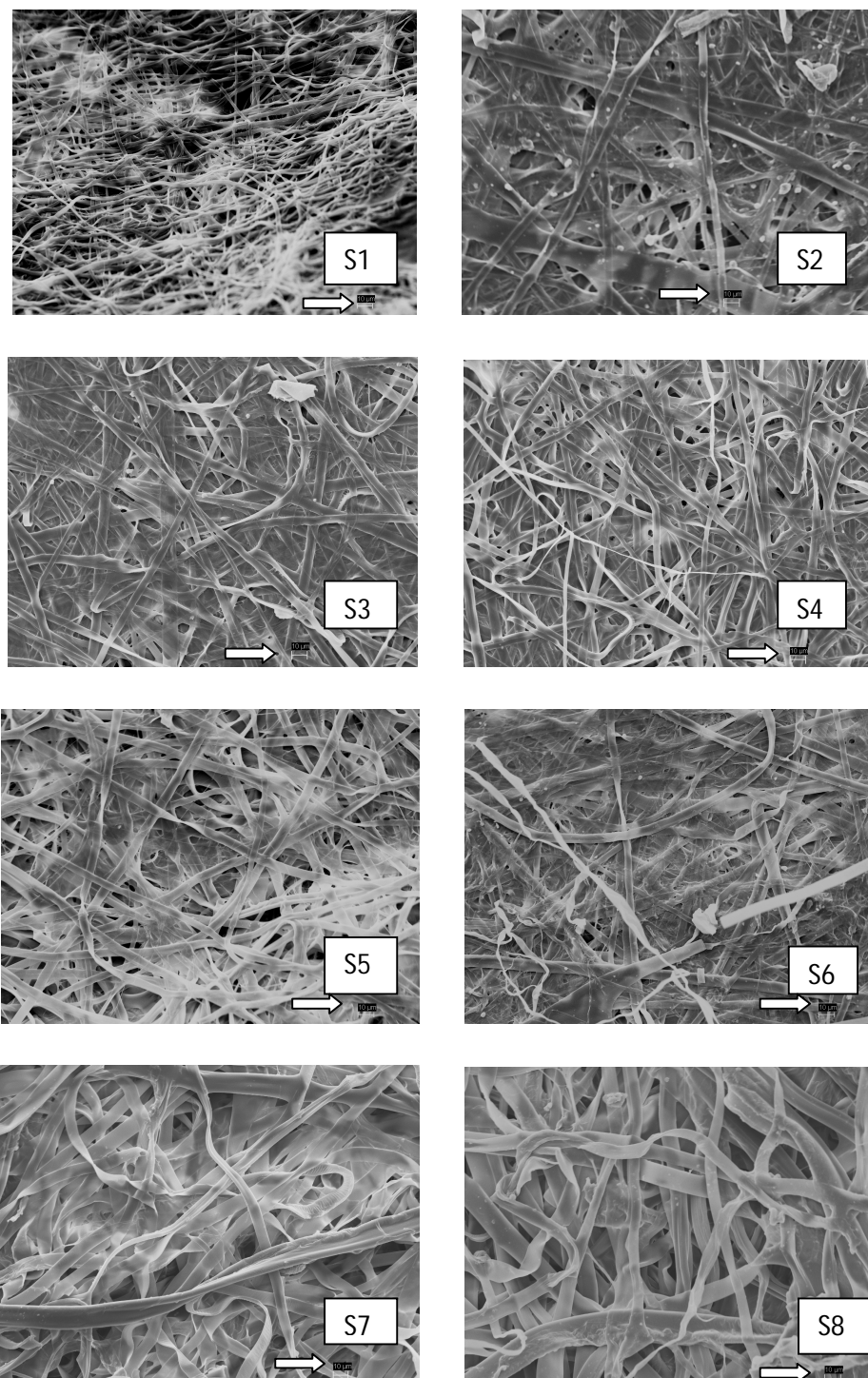
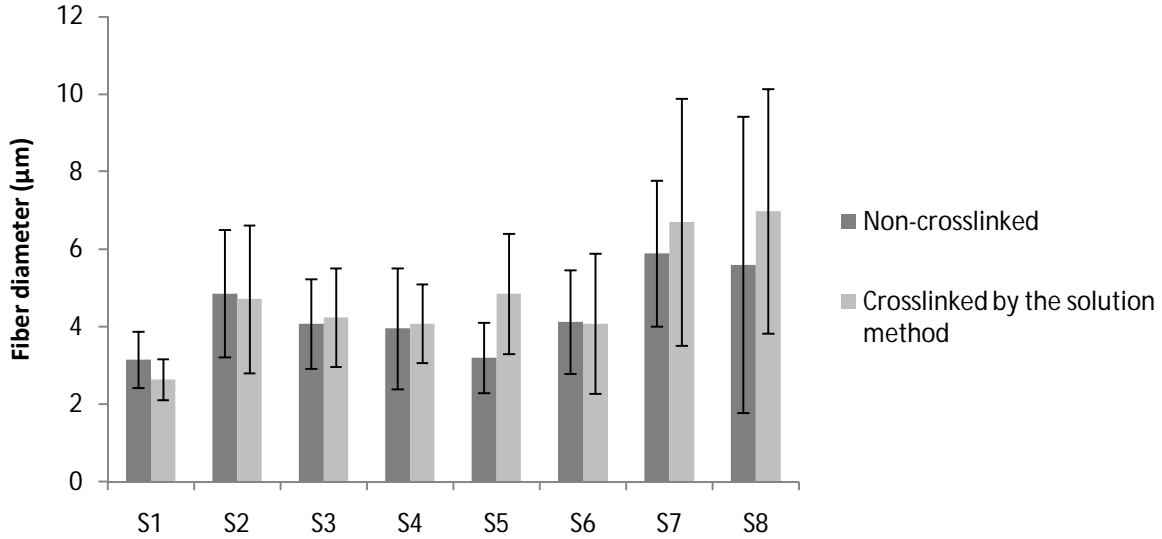


Figure 12: Fiber diameter of scaffolds (non-crosslinked and crosslinked by solution method)



Mechanical properties of a scaffold need to be evaluated for durability, stress resistance, flexibility and elasticity (Boateng et al. 2008). Peak stress, strain at break, energy to break and modulus of all scaffolds were determined by MTS Bionix and Testworks4 software. Tensile strength is the maximum stress a scaffold can withstand before breaking and determines the hardness of the scaffold. It also depends on the type and amount of polymer in the scaffold (Boateng et al. 2008). Strain at break describes the ductility and brittleness of the scaffold and also tells about the elongation of the scaffold at breaking point (Boateng et al. 2008). The mechanical properties and fiber diameter of the non-crosslinked and crosslinked scaffolds by the solution method are shown in Table 5 and Table 6, respectively; and a graphical representation of stress, strain and modulus data is shown in Figure 13. The mean stress of the non-crosslinked scaffolds ranged from 1.063 to 2.087 MPa (Appendix B) and that of crosslinked scaffolds by the solution method ranged from 0.692 to 3.125 MPa with a pooled standard deviation of 0.8616 (Appendix A). Mean stress for crosslinked scaffolds by the solution method is statistically higher in the S1 scaffold type which contained only gelatin. It was observed that the stress values were higher for the non-crosslinked scaffolds as compared to the crosslinked ones except for scaffold S1. This behaviour was also observed in the modulus results. The scaffolds containing silver displayed higher stress values than scaffolds without silver. The mean strain for the non crosslinked scaffolds ranged from 0.015 to 0.040 mm/mm and for the crosslinked scaffolds by

the solution method ranged from 0.020 to 0.067 mm/mm. The strain values for crosslinked scaffolds were higher than the non-crosslinked scaffolds except for scaffold S2.

Further characterization to determine the porosity, permeability, swelling ratio, antimicrobial activity and silver release kinetics was performed only on scaffolds crosslinked by the solution method since they could retain their stability in aqueous medium.

Table 5 : Tensile studies and fiber diameter of the non-crosslinked scaffolds

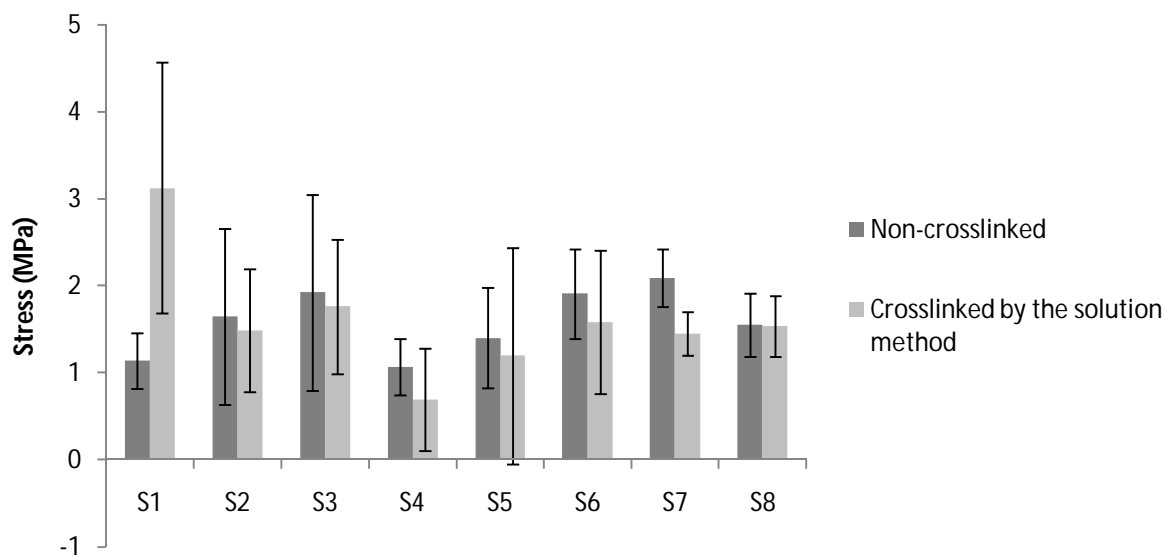
Scaffold	Fiber diameter (μm)	Peak stress (MPa)	Modulus (MPa)	Strain at break (mm/mm)	Energy to break (N*mm)
S1	3.15 ± 0.72	1.136 ± 0.319	47.134 ± 6.463	0.028 ± 0.007	0.203 ± 0.097
S2	4.85 ± 1.64	1.646 ± 1.016	93.636 ± 46.672	0.040 ± 0.038	0.272 ± 0.286
S3	4.07 ± 1.15	1.922 ± 1.128	99.276 ± 45.636	0.022 ± 0.007	0.13 ± 0.050
S4	3.95 ± 1.96	1.063 ± 0.323	64.841 ± 15.302	0.018 ± 0.007	0.107 ± 0.064
S5	3.20 ± 0.90	1.399 ± 0.578	80.525 ± 20.326	0.022 ± 0.005	0.183 ± 0.090
S6	4.12 ± 1.34	1.908 ± 0.519	66.580 ± 18.809	0.037 ± 0.009	0.476 ± 0.173
S7	5.88 ± 1.88	2.087 ± 0.335	104.835 ± 18.741	0.027 ± 0.006	0.332 ± 0.174
S8	5.59 ± 3.83	1.549 ± 0.363	100.319 ± 27.641	0.015 ± 0.005	0.137 ± 0.079

Table 6: Tensile studies and fiber diameter of the scaffolds crosslinked by the solution method

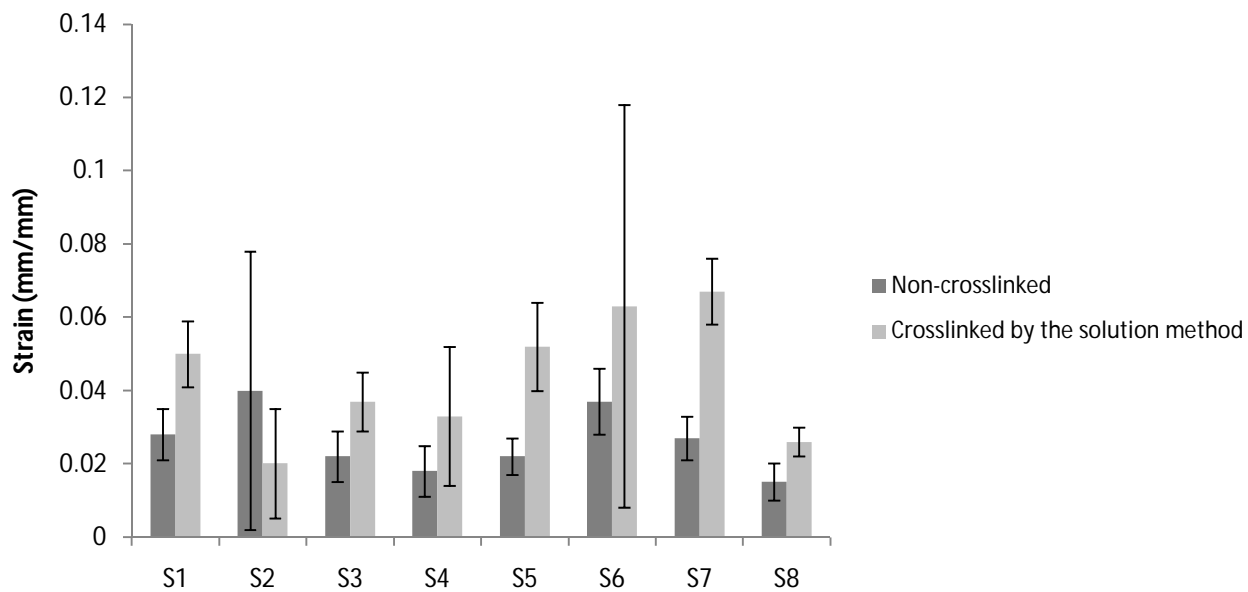
Scaffold	Fiber diameter (μm)	Peak stress (MPa)	Modulus (MPa)	Strain at break (mm/mm)	Energy to break (N*mm)
S1	2.64 ± 0.53	3.125 ± 1.443	80.835 ± 24.326	0.050 ± 0.009	0.060 ± 0.366
S2	4.71 ± 1.90	1.485 ± 0.703	92.709 ± 35.127	0.020 ± 0.015	0.011 ± 0.075
S3	4.24 ± 1.27	1.760 ± 0.774	58.330 ± 20.242	0.037 ± 0.008	0.306 ± 0.205
S4	4.08 ± 1.02	0.692 ± 0.587	38.271 ± 12.854	0.033 ± 0.019	0.115 ± 0.140
S5	4.85 ± 1.55	1.196 ± 1.246	53.443 ± 53.337	0.052 ± 0.012	0.278 ± 0.319
S6	4.08 ± 1.80	1.581 ± 0.826	59.370 ± 27.612	0.063 ± 0.055	0.422 ± 0.203
S7	6.7 ± 3.19	1.447 ± 0.250	33.804 ± 8.913	0.067 ± 0.009	0.646 ± 0.102
S8	6.98 ± 3.16	1.533 ± 0.348	69.395 ± 21.298	0.026 ± 0.004	0.192 ± 0.062

Figure 13: Graphical representation of stress, strain and modulus (A: Stress, B: Strain, C: Modulus)

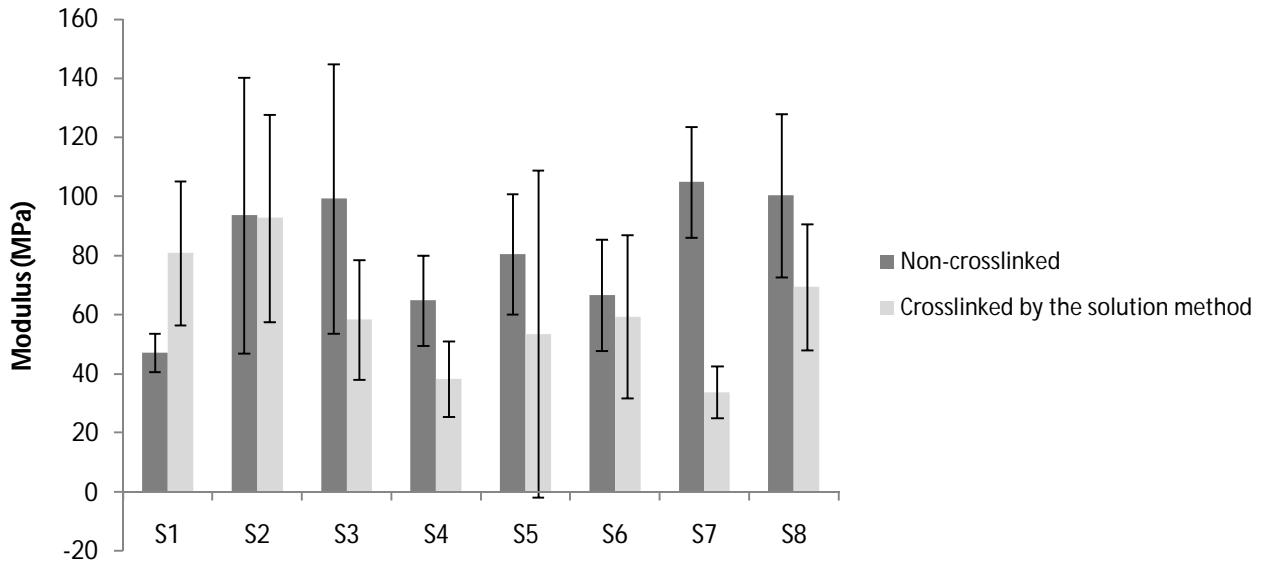
A



B



C



4.3 Scaffold porosity, permeability, swelling and degradation studies

The porosity, permeability and swelling ability of the scaffolds were evaluated to verify their capability for medium exchange. Porosity is the measure of void space within the scaffolds. The graphical data for porosity is shown in Figure 14 and the statistical analysis for the data is shown in Appendix A. The porosity of the scaffolds crosslinked by the solution method ranged from 67.56 to 90.42% which is suitable as a tissue engineered scaffold for adequate moisture and oxygen exchange to underlying cells (Freed et al. 1994). The porosity of scaffold S8 was significantly higher than the porosity of scaffolds S3, S4 and S5 and highest among all the porosity values. Permeability is the measure of the ease of flow of fluid through the scaffold. Permeability ranged from 0.1673 to 2.428 Darcy and is depicted in Figure 15. Also the statistical analysis for permeability and pore size data is shown in Appendix A. It is observed that the gelatin-dendrimer scaffolds containing silver had lower permeability values as compared to the gelatin scaffolds containing silver but the statistical analysis shows that the data is not statistically significant. This lower permeability values of the gelatin-dendrimer scaffolds containing silver may be due to their higher fiber diameter. Pore size of the scaffolds show a similar trend to what was found in permeability as shown in Figure 16.

Figure 14: Porosity of the scaffolds crosslinked by the solution method

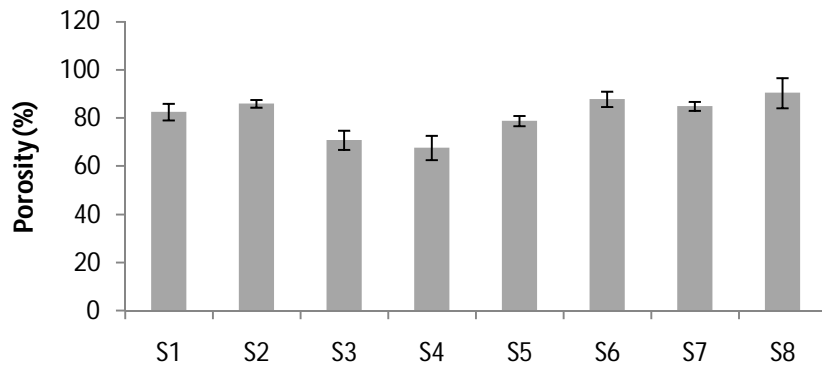


Figure 15: Permeability of the scaffolds crosslinked by the solution method

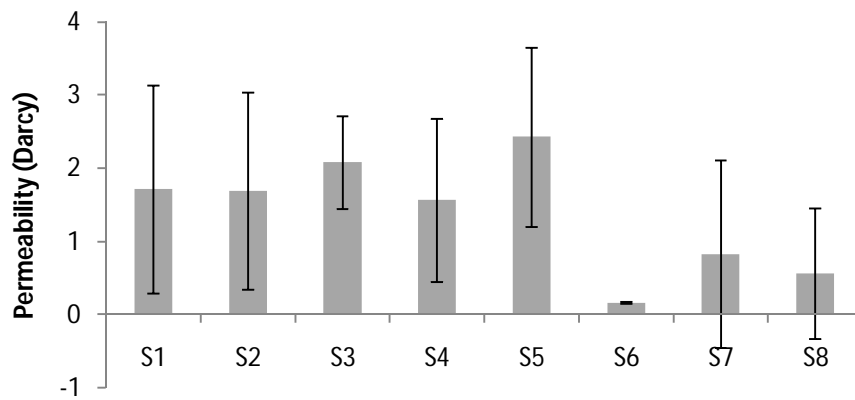
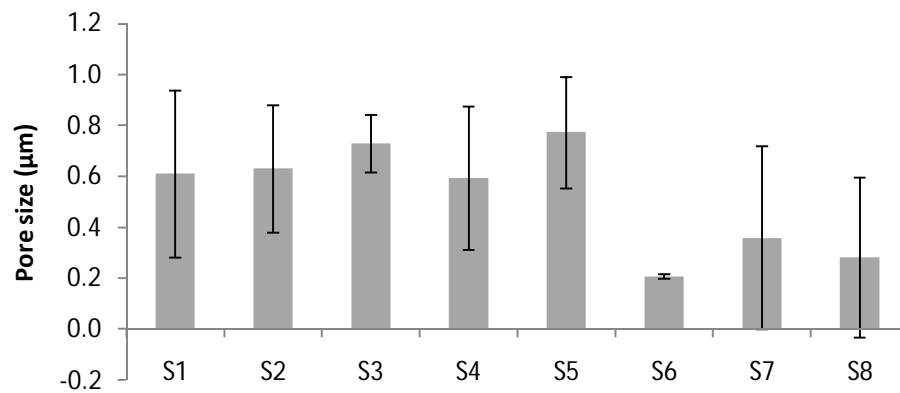
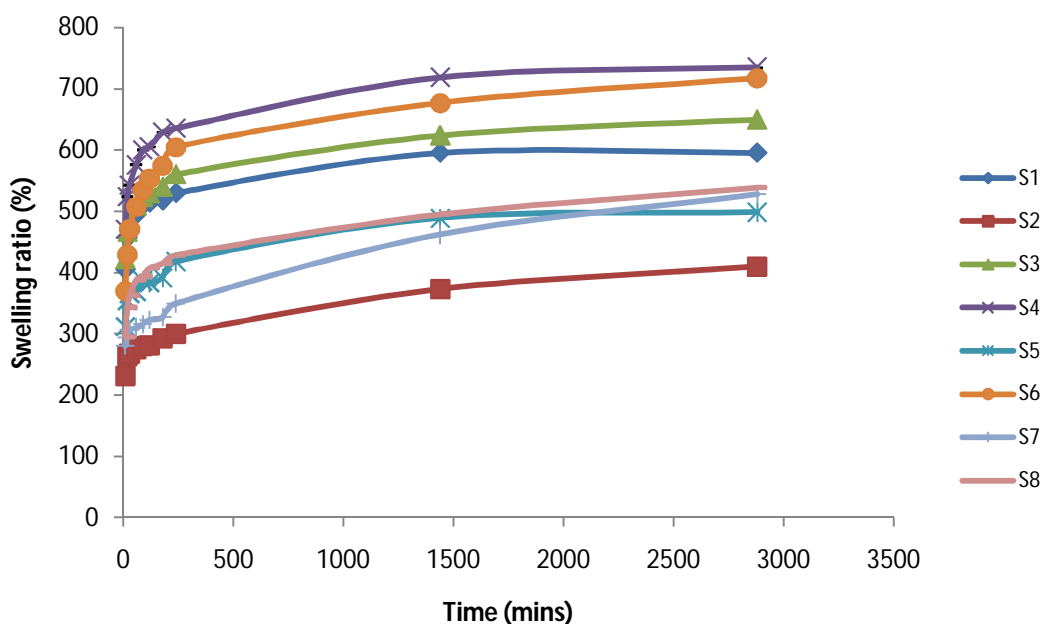


Figure 16: Pore size of the scaffolds crosslinked by the solution method



Adsorption and swelling studies were done to determine the swelling capacity of the scaffolds. Wounds that have extensive bleeding and heavy amounts of exudate require dressings to absorb quickly and maintain a clean environment at the wound site. The swelling studies were carried out in the SWF to replicate the clinical conditions. A graphical representation of the data is shown in Figure 17 and a statistical analysis of the swelling ratio values at 48 h is shown in Appendix A. All the scaffolds demonstrated a good swelling and absorbing capacity. The swelling ratio varied from 415 to 626 % at the end of 48 h (2880 min). It is observed that scaffold S4 had the highest swelling ratio.

Figure 17: Swelling of the scaffolds crosslinked by the solution method (in SWF at room temperature)

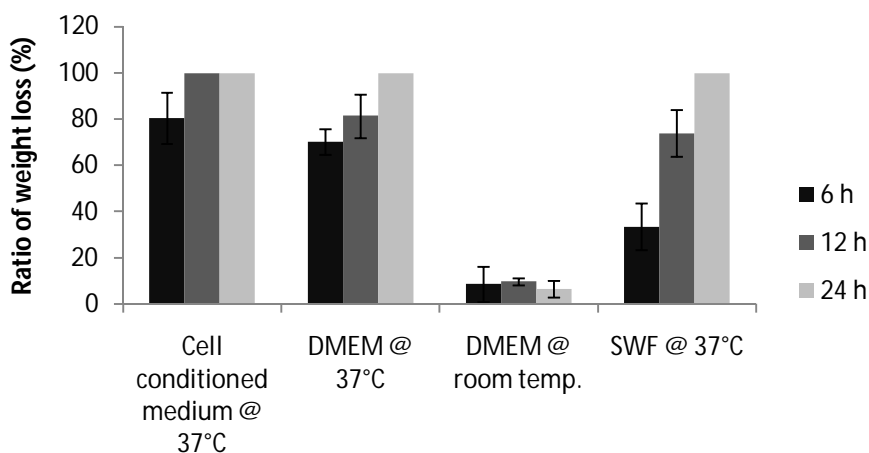


Gelatin is easily soluble and therefore scaffolds containing gelatin need to be evaluated for degradation. The scaffolds without silver (S1 and S5) were evaluated for degradation studies to observe the effect of temperature and other factors, if any, on the rate of degradation of the scaffold. It was observed that temperature did play a role in the rate of degradation as shown in Figure 18 for scaffold S1 and S5. A statistical analysis of the data is shown in Appendix A. For both the scaffolds, the weight loss (%) was significantly lower when tested at room temperature as compared to incubation at 37°C. The type of medium also affected the rate of degradation.

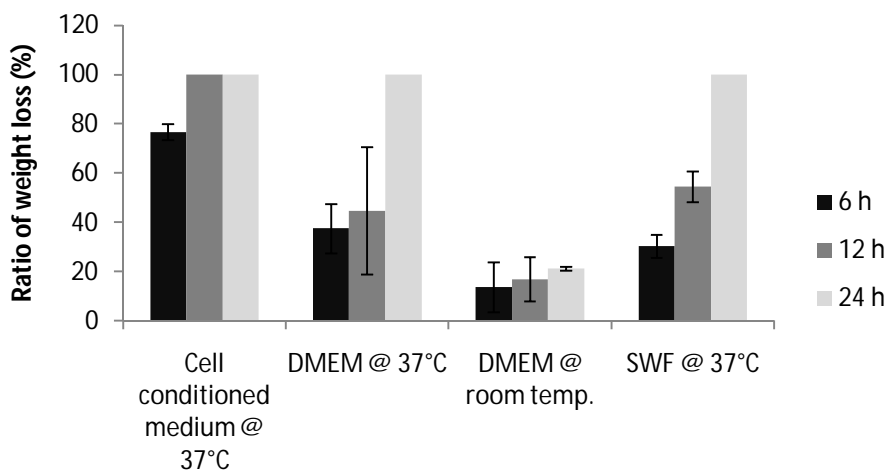
Both the scaffolds degraded completely at the end of 24 h in all media at 37°C, with the weight loss being highest during incubation in cell conditioned medium. It was also observed that S5 which contained gelatin-dendrimer conjugate had lesser degradation than S1 which contained only gelatin when incubated in same media at 37°C.

Figure 18: Degradation of the scaffolds crosslinked by the solution method

Scaffold S1



Scaffold S5



4.4 Antimicrobial assay

The scaffolds crosslinked by solution method were tested for antimicrobial efficacy against two common wound pathogens, gram positive *Staphylococcus aureus* and gram negative *Pseudomonas aeruginosa*. Gram positive bacteria do not contain any outer membrane but have a thick peptidoglycan layer and stain dark blue or violet by Gram's staining. In contrast, gram negative bacteria contain an outer membrane but have a thin peptidoglycan layer and stain pink by Gram's staining. The results for colony forming units/ml and the images of the petri plates are shown in Table 7, Table 8, Figure 19 and Figure 20. It is observed that the growth of both bacteria increased in a span of 48 h for the culture test tubes with no sample (control) and those containing scaffold samples without silver (S1 and S5). For *Staphylococcus aureus*, it was observed that at the end of 4 h, bacterial growth was completely inhibited in the test tubes containing S2, S3, S5 and S6, but there was some growth in the test tubes containing S4 and S8. Overall it was observed that all the scaffold samples containing silver inhibited the growth of *Staphylococcus aureus* by the end of 48 h. For *Pseudomonas aeruginosa*, it was observed that all the scaffold samples containing silver inhibited the growth of bacteria by the end of 48 h.

Table 7: Antimicrobial activity against *Staphylococcus aureus*

Scaffold type	4 h	24 h	48 h
Control (untreated)	10×10^7 cfu/ml	24×10^7 cfu/ml	Bacterial lawn
S1	5.1×10^7 cfu/ml	6×10^7 cfu/ml	Bacterial lawn
S2	No colonies	No colonies	No colonies
S3	No colonies	No colonies	No colonies
S4	0.7×10^7 cfu/ml	No colonies	No colonies
S5	6×10^7 cfu/ml	Bacterial lawn	Bacterial lawn
S6	No colonies	No colonies	No colonies
S7	No colonies	No colonies	No colonies
S8	1.5×10^7 cfu/ml	No colonies	No colonies

Table 8: Antimicrobial activity against *Pseudomonas aeruginosa*

Sample type	4 h	24 h	48 h
Control (untreated)	Bacterial lawn	Bacterial lawn	Bacterial lawn
S1	Bacterial lawn	Bacterial lawn	Bacterial lawn
S2	No colonies	No colonies	No colonies
S3	No colonies	No colonies	No colonies
S4	No colonies	No colonies	No colonies
S5	Bacterial lawn	Bacterial lawn	Bacterial lawn
S6	No colonies	No colonies	No colonies
S7	No colonies	No colonies	No colonies
S8	No colonies	No colonies	No colonies

4.5 Silver release kinetics

Silver release kinetics were measured by means of diffusion of silver into PBS medium and analyzing the silver content by ICP-OES. A graphical representation of cumulative release of silver (%) over time is shown in Figure 21. It is observed that all the scaffolds containing silver show a similar drug release pattern over a span of 264 h (short term). Silver release was slow and a very small amount of silver was released at the end of 264 h. It is also observed that larger amount of silver is released from gelatin-dendrimer scaffolds as compared to gelatin scaffolds containing equal amounts of silver (i.e. S2 and S6, S3 and S7, S4 and S8). This may be due to the larger fiber diameter of gelatin-dendrimer scaffolds. Fibers with larger diameter have a greater surface area for diffusion. Comparison of the antimicrobial assay and silver release kinetics revealed that even a low amount of silver released could inhibit any bacterial growth by 48 h.

Figure 19: Antimicrobial activity against *Staphylococcus aureus*

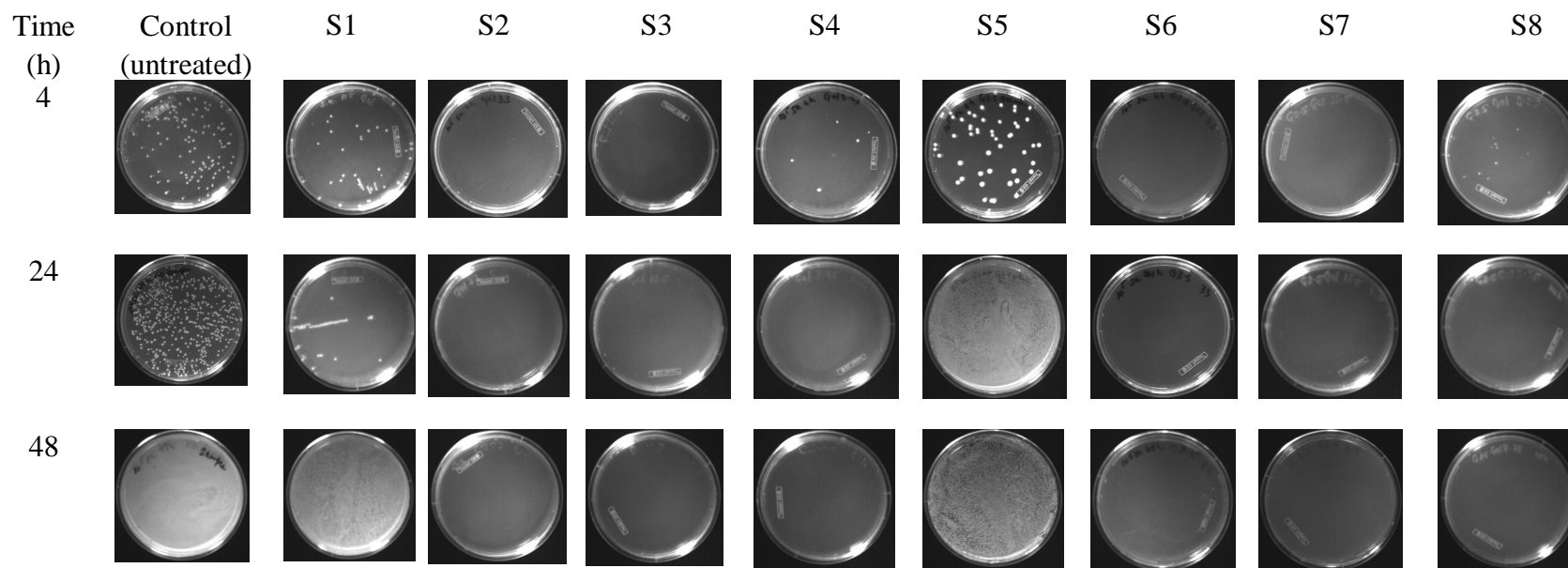


Figure 20: Antimicrobial activity against *Pseudomonas aeruginosa*

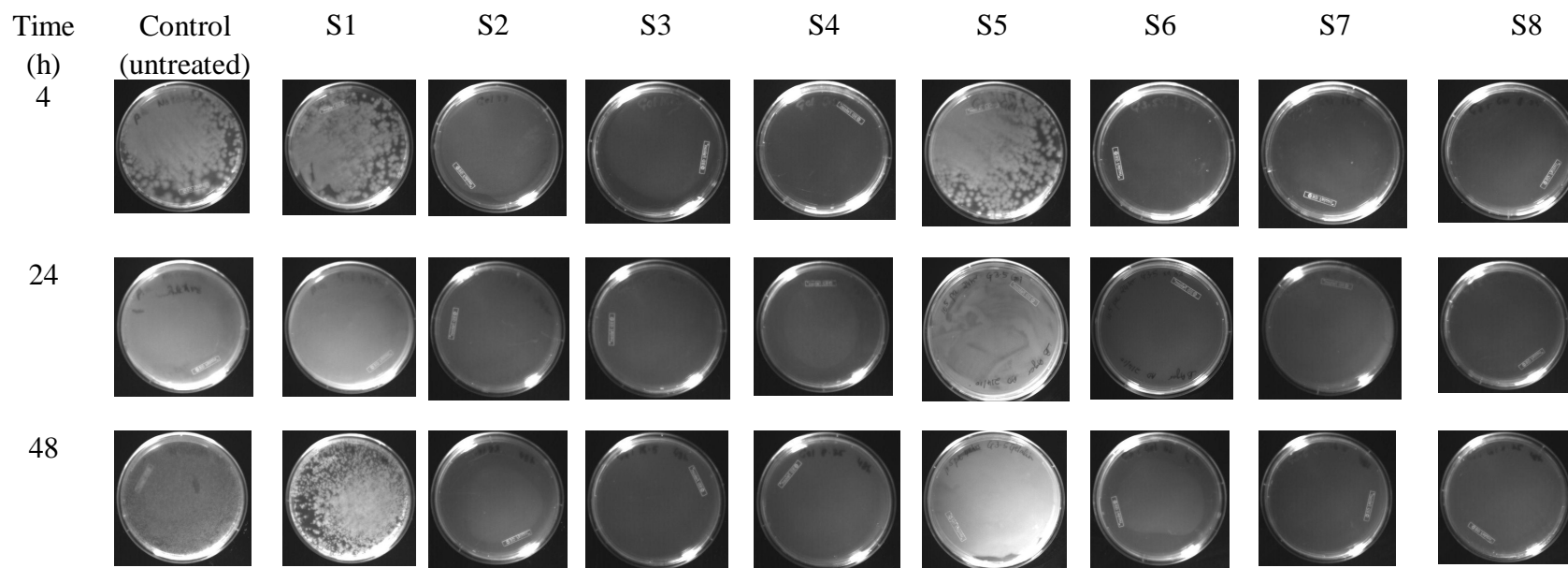
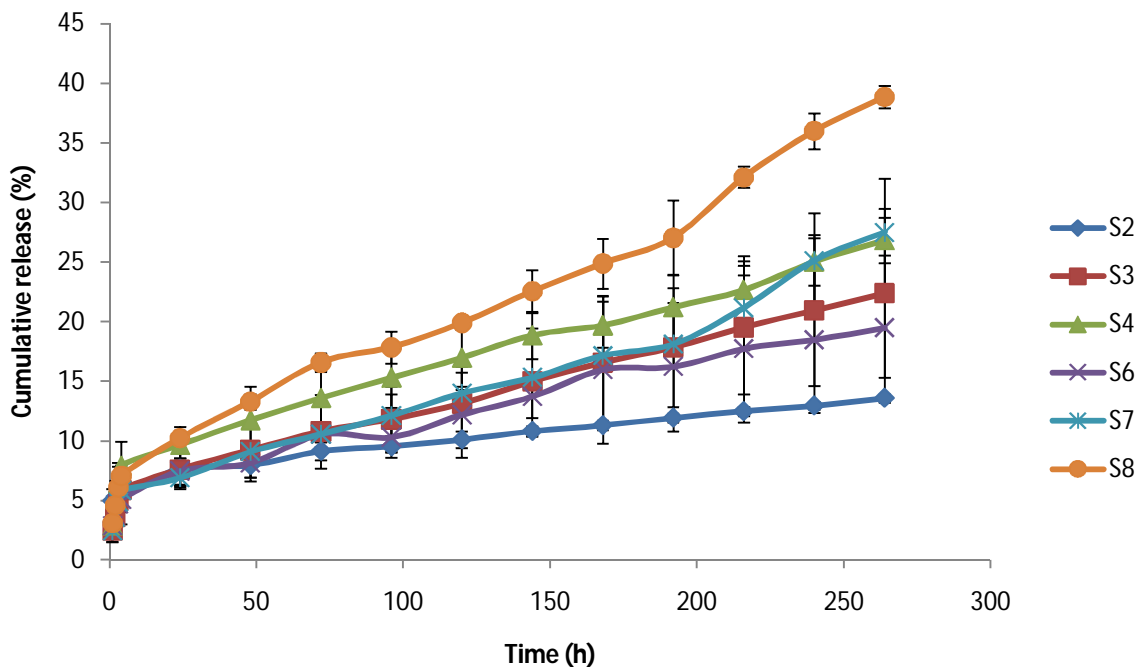


Figure 21: Silver release kinetics



4.6 Conclusions

This work demonstrated that silver containing nanofiber dressings composed of gelatin with or without gelatin-dendrimer conjugates could be fabricated by electrospinning. The scaffolds were successfully crosslinked by photo-polymerization using liquid or vapor form of PEG diacrylate for structure stability improvement. The characteristics in terms of morphology, fiber diameter, mechanical properties, porosity, permeability and swelling capability could be modulated by changing the composition of the scaffold. According to antimicrobial assay, silver-containing scaffolds could inhibit bacterial growth by 48 h. Silver could be released in a controlled manner over an extended period of time.

CHAPTER 6 SUMMARY AND FUTURE WORK

Tissue engineered scaffolds have a wide range of applications as a wound dressing, for tissue regeneration and development and as a vehicle for drug delivery. They mimic the natural extracellular matrix and facilitate cell growth and proliferation. We designed a novel gelatin-dendrimer nanofiber scaffold as a potential wound dressing. The scaffolds were characterized to quantify their mechanical properties, gas and nutrient flow capability, swelling capacity and drug release kinetics. The scaffolds which showed the desirable properties of a wound dressing are summarized in Table 9.

Table 9: Summary table

Properties	S1	S2	S3	S4	S5	S6	S7	S8
Stress	✓✓					✓		✓
Strain					✓	✓		
Porosity		✓				✓		✓✓
Permeability					✓			
Swelling	✓		✓	✓✓		✓		✓
Antimicrobial activity		✓✓	✓✓	✓		✓✓	✓✓	✓
Drug release						✓	✓	✓✓

The scaffolds were required to be crosslinked to acquire the properties of a tissue engineered scaffold. The scaffolds have a unique structural configuration in which covalently bound dendrimer is evenly distributed along the dimension of the nanofiber. The addition of dendrimer provides multiple functional groups for attachment of drugs and their controlled release. The scaffolds S2, S6 and S8 were highly porous in nature and the higher fiber diameter provided

greater surface area for diffusion and drug release. The scaffolds S1, S2, S4, S6 and S8 also exhibited high capacity of swelling and adsorption. The scaffolds S1 and S5 were found to be easily degradable when incubated in cell conditioned medium at 37°C. This could be due to gelatin which is easily soluble and needs higher density of crosslinking for stability. The concentration of PEG-diacrylate could be increased to improve the crosslinking density hence controlling the rate of degradation. We incorporated silver into the scaffold to determine its antimicrobial efficacy; various other antimicrobial agents can be used for future studies. The scaffolds with silver could effectively inhibit growth of bacteria by 24 h. Also the concentration of silver can be further reduced to avoid any potential accumulated toxicity. As future work, studies could be done to evaluate the effect and clearance of silver in vivo to get a better insight. The scaffolds fabricated show promise as a bioactive dressing to treat wounds. They exhibit the properties necessary to maintain a moist environment to facilitate wound healing.

The process of wound healing and wound closure involves growth factors like FGF, PDGF and TGF- β . As an extended study, growth factors like TGF- β could be incorporated into the scaffolds to increase the rate of healing and for release studies. TGF- β promotes the production of collagen framework thus helping in the proliferative phase of wound healing. Also the designed scaffold can be used to deliver other therapeutics for treating a variety of wounds, including chronic wounds, burns and skin cancer.

Literature cited

Bioactive products, in Development in Wound Care. *PJB Publications Ltd* 1994:43-60.

Agarwal A, Weis TL, Schurr MJ, Faith NG, Czuprynski CJ, McAnulty JF, Murphy CJ, Abbott NL: Surfaces modified with nanometer-thick silver-impregnated polymeric films that kill bacteria but support growth of mammalian cells. *Biomaterials* 2009; 31:680-690.

Bartlett RH: Skin Substitutes. *Journal of Trauma* 1981; 21:731.

Boateng JS, Matthews KH, Stevens HNE, Eccleston GM: Wound healing dressings and drug delivery systems: A review. *Journal of Pharmaceutical Sciences* 2008; 97:2892-2923.

Carr ME, Jr., Hardin CL: Fibrin has larger pores when formed in the presence of erythrocytes. *American Journal of Physiology* 1987; 253:H1069-1073.

Centegra hs: The importance of wound care.

Chardack W, Brueske D, Santamauro A, Fazekas G: Experimental studies on synthetic substitutes for skin and their use in treatment of burns. *Annals of Surgery* 1962; 155.

Debra J, Cheri O: Wound healing: Technological innovations and market overview. 1998; 2:1-185.

Doillon CJ, Silver FH: Collagen-based wound dressing: Effects of hyaluronic acid and fibronectin on wound healing. *Biomaterials* 1986; 7:3-8.

Epstein FH, Singer AJ, Clark RAF: Cutaneous Wound Healing. *The New England Journal of Medicine* 1999; 341:738-746.

Faler BJ, Macsata RA, Plummer D, Mishra L, Sidawy AN: Transforming Growth Factor- β and Wound Healing. 2006:55-62.

Freed LE, Vunjak-Novakovic G, Biron RJ, Eagles DB, Lesnoy DC, Barlow SK, Langer R: Biodegradable Polymer Scaffolds for Tissue Engineering. *Nat Biotech* 1994; 12:689-693.

Gilchrist T, Martin AM: Wound Treatment with Sorbsan - an Alginate Fiber Dressing. *Biomaterials* 1983; 4:317-320.

Gilliland E, Nathwani N, Dore C, Lewis J: Bacterial colonisation of leg ulcers and its effect on the success rate of skin grafting. *Annals of the Royal College of Surgeons of England* 1988; 70:105-108.

Greenhalgh DG: The Role of Growth Factors in Wound Healing. *Journal of Trauma* 1996; 41:159-167.

Grzybowski J, Oldak E, Antos-Bielska M, Janiak MK, Pojda Z: New cytokine dressings. I. Kinetics of the in vitro rhG-CSF, rhGM-CSF, and rhEGF release from the dressings. *International Journal of Pharmaceutics* 1999; 184:173-178.

Guo S, DiPietro LA: Factors Affecting Wound Healing. *Journal of Dental Research* 2010; 89:219-229.

Harding K, Cutting K, Price P: The cost effectiveness of wound management protocols of care. *British Journal of Nursing* 2000; 9:S6, S8, S10 passim-S16, S18, S10 passim.

.

Harding KG, Morris HL, Patel GK: Science, medicine, and the future - Healing chronic wounds. *British Medical Journal* 2002; 324:160-163.

Harihara Y, Konishi T, Kobayashi H, Furushima K, Ito K, Noie T, Nara S, Tanimura K: Effects of Applying Povidone-Iodine Just before Skin Closure. *Dermatology* 2006; 212:53-57.

Hemila H, Douglas R: Vitamin C and acute respiratory infections. *The International Journal of Tuberculosis and Lung Disease* 1999; 3:756-761.

Hromadka M, Collins JB, Reed C, Han L, Kolappa KK, Cairns BA, Andrady T, van Aalst JA: Nanofiber applications for burn care. *Journal of Burn Care & Research* 2008; 29:695-703.

Huang Z-M, Zhang YZ, Ramakrishna S, Lim CT: Electrospinning and mechanical characterization of gelatin nanofibers. *Polymer* 2004; 45:5361-5368.

Ip M, Lui SL, Poon VKM, Lung I, Burd A: Antimicrobial activities of silver dressings: an in vitro comparison. *Journal of Medical Microbiology* 2006; 55:59-63.

Keast D, Orsted H: The basic principles of wound healing.

Kerstein MD: The Scientific Basis of Healing. *Advanced Wound Care* 1997; 10:30-36.

Klajnert B, Bryszewska M: *Dendrimers in Medicine*: Nova Science Publishers, Inc., 2007.

Koempel JA, Gibson SE, O'Grady K, Toriumi DM: The effect of platelet-derived growth factor on tracheal wound healing. *International Journal of Pediatric Otorhinolaryngology* 1998; 46:1-8.

Kollenberg L: A new topical antibiotic delivery system. Surgical Materials Testing Laboratory, Wales, UK. *World Wide Wounds* 1998; Edition 1.0.

Komarcevic A: The modern approach to wound treatment. *Medicinski pregled* 2000; 53:363-368.

Kumbar SG, James R, Nukavarapu SP, Laurencin CT: Electrospun nanofiber scaffolds: engineering soft tissues. *Biomedical Materials* 2008; 3.

Lee J, Tae G, Kim YH, Park IS, Kim S-H, Kim SH: The effect of gelatin incorporation into electrospun poly(l-lactide-co-[var epsilon]-caprolactone) fibers on mechanical properties and cytocompatibility. *Biomaterials* 2008; 29:1872-1879.

Margolis DJ, Bilker W, Santanna J, Baumgarten M: Venous leg ulcer: incidence and prevalence in the elderly. *J Am Acad Dermatol* 2002; 46:381-386.

Martin P: Wound healing - Aiming for perfect skin regeneration. *Science* 1997; 276:75-81.

Mermet JM: Is it still possible, necessary and beneficial to perform research in ICP-atomic spectrometry? *Journal of analytical atomic spectrometry* 2005; 20.

Nelson EA, O'Meara S, Craig D, Iglesias C, Golder S, Dalton J, Claxton K, Bell-Syer SE, Jude E, Dowson C, Gadsby R, O'Hare P, Powell J: A series of systematic reviews to inform a decision analysis for sampling and treating infected diabetic foot ulcers. *Health technology assessment (Winchester, England)* 2006; 10:iii-iv, ix-x, 1-221.

Ngan V: Synthetic wound dressings Retrieved from <http://dermnetnz.org/procedures/dressings.html>.

Nicholas JP: Classification of Wounds and their Management. 2002; 20:114-117.

O'Meara S, Cullum N, Majid M, Sheldon T: Systematic reviews of wound care management: (3) antimicrobial agents for chronic wounds; (4) diabetic foot ulceration. *Health technology assessment (Winchester, England)* 2000; 4:1-237.

Park S-N, Kim JK, Suh H: Evaluation of antibiotic-loaded collagen-hyaluronic acid matrix as a skin substitute. *Biomaterials* 2004; 25:3689-3698.

Parsons D, Bowler P, Myles V, Jones S: Silver Antimicrobial Dressings in Wound Management: A Comparison of Antibacterial, Physical, and Chemical Characteristics. *Wounds* 2005.

Patel GK: The Role of Nutrition in the Management of Lower Extremity Wounds. *International Journal of Lower Extremity Wounds* 2005; 4:12-22.

Paul W, Sharma CP: Chitosan and alginate wound dressings: a short review. *Trends Biomater. Artificial organs* 2004; 18.

Percival S, Keith C: *Microbiology of Wounds*: CRC Press, Taylor and Francis Group, 2010.

Puolakkainen P, Twardzik D, Ranchalis J, Pankey S, Reed M, Gombotz W: The enhancement in wound healing by transforming growth factor $\beta 1$ (TGF $\beta 1$) depends on topical drug delivery system. *Journal of Surgical Research* 1995; 58:321-329.

Ratner BD: *Biomaterials science: An introduction to materials in medicine*: Elsevier Academic Press, 2004.

Rojas AI, Phillips TJ: Patients with Chronic Leg Ulcers Show Diminished Levels of Vitamins A and E, Carotenes, and Zinc. *Dermatologic Surgery* 1999; 25:601-604.

Sai P, Babu M: Collagen based dressings - a review. *Burns* 2000; 26:54-62.

Saltzman WM, Olbricht WL: Building drug delivery into tissue engineering design. *Nat Rev Drug Discov* 2002; 1:177-186.

Sell S, Barnes C, Simpson D, Bowlin G: Scaffold permeability as a means to determine fiber diameter and pore size of electrospun fibrinogen. *Journal of Biomedical Materials Research Part A* 2008; 85A:115-126.

Shanmugasundaram N, Sundaraseelan J, Uma S, Selvaraj D, Babu M: Design and delivery of silver sulfadiazine from alginate microspheres-impregnated collagen scaffold. *Journal of Biomedical Materials Research Part B-Applied Biomaterials* 2006; 77B:378-388.

Sill TJ, von Recum HA: Electrospinning: Applications in drug delivery and tissue engineering. *Biomaterials* 2008; 29:1989-2006.

Smith-Freshwater A: PREPARATION AND CHARACTERIZATION OF AN ELECTROSPUN GELATIN/DENDRIMER HYBRID NANOFIBER DRESSING, Virginia Commonwealth University, 2009.

Steenfos HH: Growth Factors and Wound Healing. *Scandinavian Journal of Plastic and Reconstructive Surgery and Hand Surgery* 1994; 28:95-105.

Stefánsson A, Gunnarsson I, Giroud N: New methods for the direct determination of dissolved inorganic, organic and total carbon in natural waters by Reagent-Free(TM) Ion Chromatography and inductively coupled plasma atomic emission spectrometry. *Analytica Chimica Acta* 2007; 582:69-74.

Thomas S: Alginate dressings in surgery and wound management - Part 1. *Journal of Wound care* 2000; 9:56-60.

Thomas S: Hydrocolloids update. *Journal of Wound care* 1992; 1:27-30.

Thomas S: Wounds and wound healing in: Wound Management and dressings. *London: Pharmaceutical Press* 1990:1-14.

Thomas S, Loveless P: A comparative study of twelve hydrocolloid dressings. *World Wide Wounds* 1997.

Tomalia DA, Baker H, Dewald J, Hall M, Kallos G, Martin S, Roeck J, Ryder J, Smith P: A New Class of Polymers - Starburst-Dendritic Macromolecules. *Polymer Journal* 1985; 17:117-132.

Ueno H, Yamada H, Tanaka I, Kaba N, Matsuura M, Okumura M, Kadosawa T, Fujinaga T: Accelerating effects of chitosan for healing at early phase of experimental open wound in dogs. *Biomaterials* 1999; 20:1407-1414.

Waldorf H, Fewkes J: Wound healing. *Advanced Dermatology* 1995; 10:77-96.

Warriner R, Burrell R: Infection and the Chronic Wound: A Focus on Silver. *Advances in skin and wound care* 2005; 18:2-12.

Wichterle O, Lim D: Hydrophilic Gels for Biological Use. *Nature* 1960; 185:117-118.

Winter GD: Formation of the Scab and the Rate of Epithelization of Superficial Wounds in the Skin of the Young Domestic Pig. *Nature* 1962; 193:293-294.

Zhang Y, Ouyang H, Lim CT, Ramakrishna S, Huang Z-M: Electrospinning of gelatin fibers and gelatin/PCL composite fibrous scaffolds. *Journal of Biomedical Materials Research Part B: Applied Biomaterials* 2005; 72B:156-165.

APPENDICES	Page
Appendix A – Statistical data for the scaffolds crosslinked by the solution method	50
Appendix B – Statistical data for the non-crosslinked scaffolds	81
Appendix C – Data for the scaffolds crosslinked by the vapor method	89

Interpretation of the statistical analysis shown in Appendix A, B and C

Analysis of Variance (ANOVA):

- $P < 0.05$ indicates that the data is statistically significant

Tukey's Pairwise Comparisons:

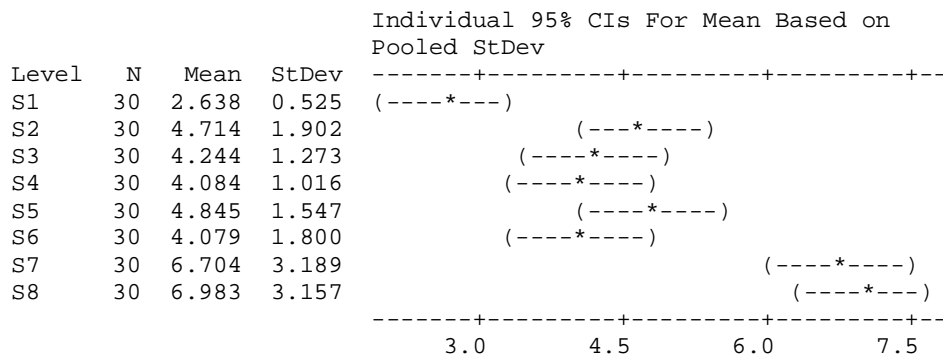
- Tukey's pairwise comparison is performed to determine if two data values is statistically different from one another
- If the confidence interval (lower to upper) between two data values does not include a zero, the difference between them is statistically significant
- If the confidence interval (lower to upper) between two data values includes a zero, the difference between them is not statistically significant

Appendix A (Data for the scaffolds crosslinked by the solution method)

One-way ANOVA: Fiber diameter

Source	DF	SS	MS	F	P
Factor	7	432.43	61.78	15.29	0.000
Error	232	937.12	4.04		
Total	239	1369.55			

S = 2.010 R-Sq = 31.57% R-Sq(adj) = 29.51%

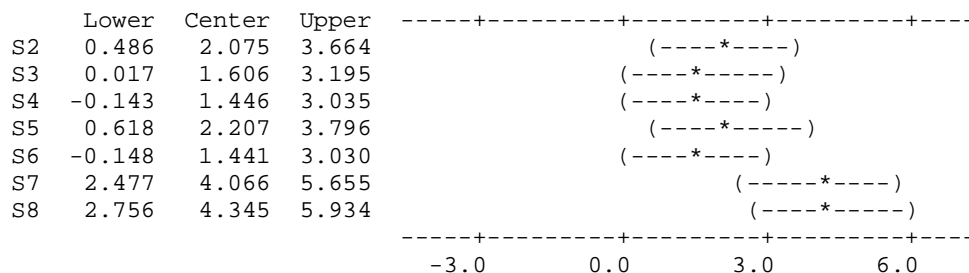


Pooled StDev = 2.010

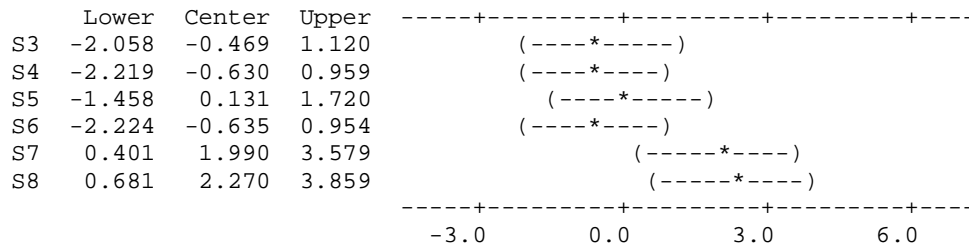
Tukey 95% Simultaneous Confidence Intervals
All Pairwise Comparisons

Individual confidence level = 99.75%

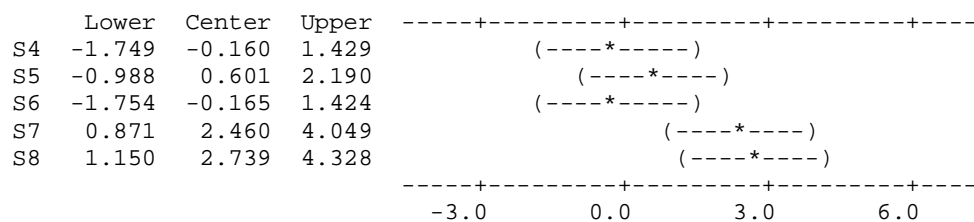
S1 subtracted from:



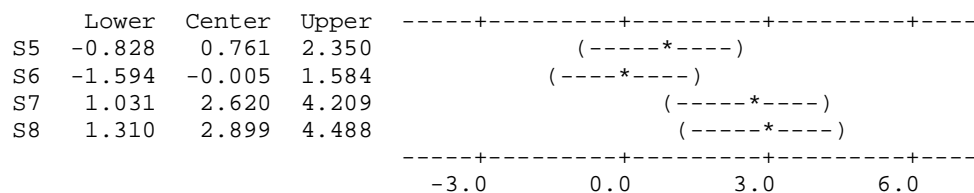
S2 subtracted from:



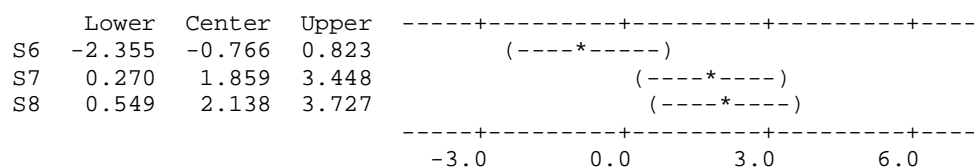
S3 subtracted from:



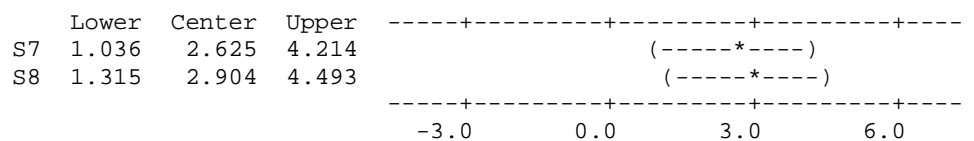
S4 subtracted from:



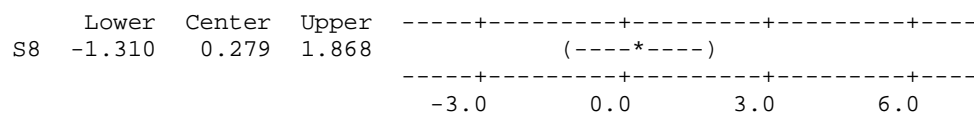
S5 subtracted from:



S6 subtracted from:



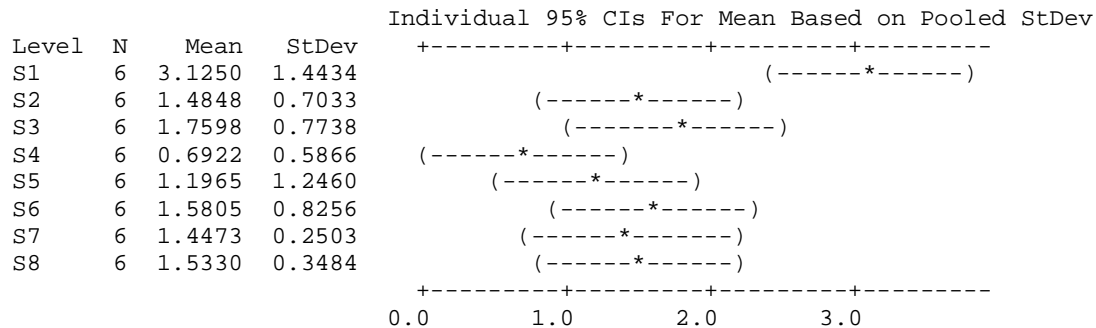
S7 subtracted from:



One-way ANOVA: Stress

Source	DF	SS	MS	F	P
Factor	7	20.277	2.897	3.90	0.002
Error	40	29.695	0.742		
Total	47	49.972			

S = 0.8616 R-Sq = 40.58% R-Sq(adj) = 30.18%

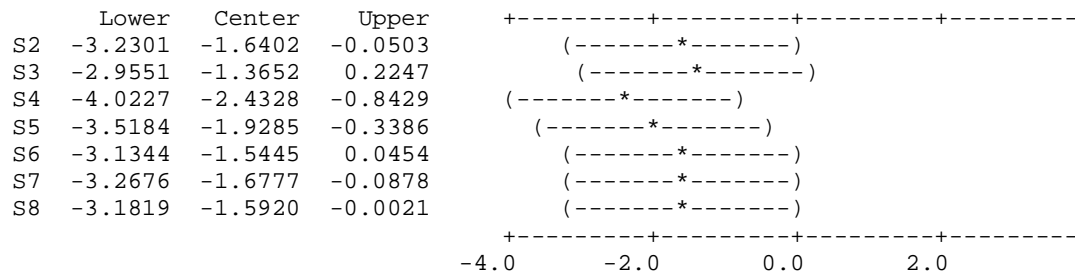


Pooled StDev = 0.8616

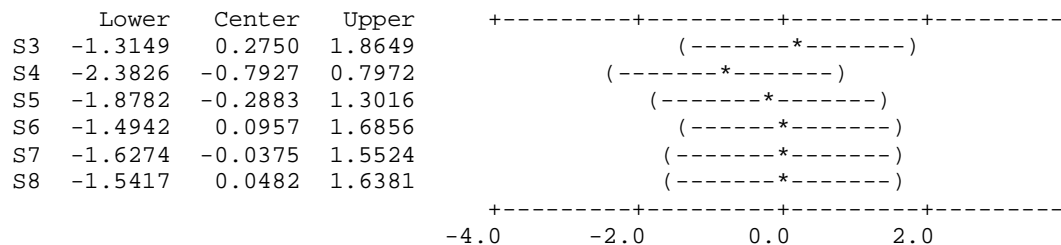
Tukey 95% Simultaneous Confidence Intervals
All Pairwise Comparisons

Individual confidence level = 99.73%

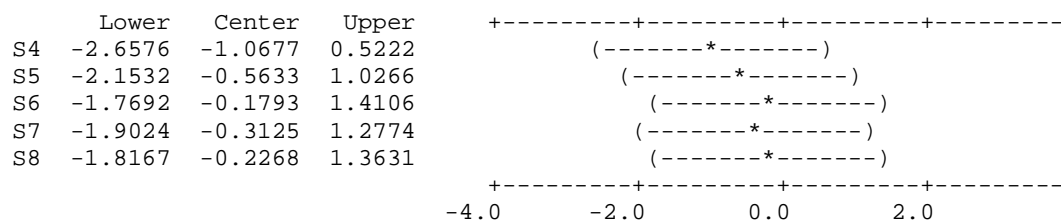
S1 subtracted from:



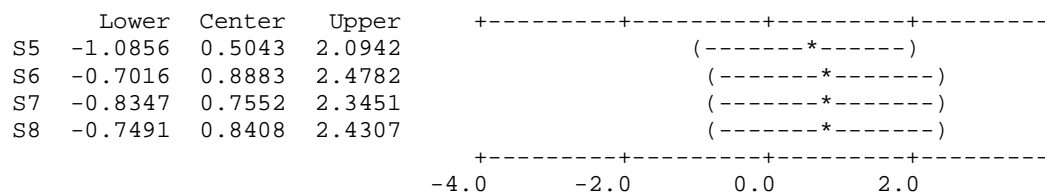
S2 subtracted from:



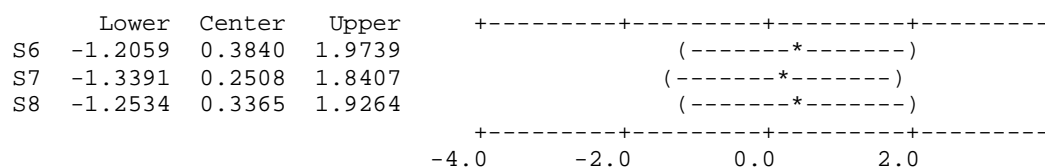
S3 subtracted from:



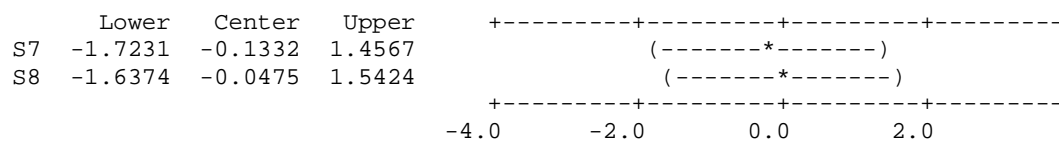
S4 subtracted from:



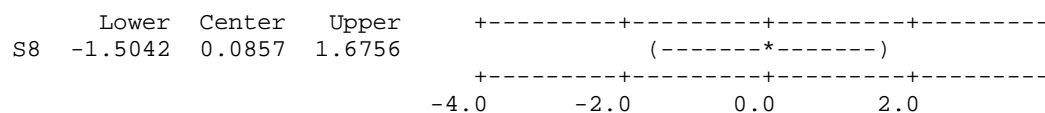
S5 subtracted from:



S6 subtracted from:



S7 subtracted from:



One-way ANOVA: Strain

Source	DF	SS	MS	F	P
Factor	7	0.012315	0.001759	3.53	0.005
Error	40	0.019907	0.000498		
Total	47	0.032222			

S = 0.02231 R-Sq = 38.22% R-Sq(adj) = 27.41%

Individual 95% CIs For Mean Based on Pooled StDev

Level	N	Mean	StDev
S1	6	0.04967	0.00937
S2	6	0.01983	0.01508
S3	6	0.03700	0.00780
S4	6	0.03267	0.01933
S5	6	0.05167	0.01147
S6	6	0.06317	0.05478
S7	6	0.06700	0.00897
S8	6	0.02650	0.00432

-----+-----+-----+-----+
 (-----*-----)
 (-----*-----)
 (-----*-----)
 (-----*-----)
 (-----*-----)
 (-----*-----)
 (-----*-----)
 -----+-----+-----+-----+
 0.025 0.050 0.075 0.100

Pooled StDev = 0.02231

Tukey 95% Simultaneous Confidence Intervals
 All Pairwise Comparisons

Individual confidence level = 99.73%

S1 subtracted from:

	Lower	Center	Upper
S2	-0.07100	-0.02983	0.01133
S3	-0.05383	-0.01267	0.02850
S4	-0.05817	-0.01700	0.02417
S5	-0.03917	0.00200	0.04317
S6	-0.02767	0.01350	0.05467
S7	-0.02383	0.01733	0.05850
S8	-0.06433	-0.02317	0.01800

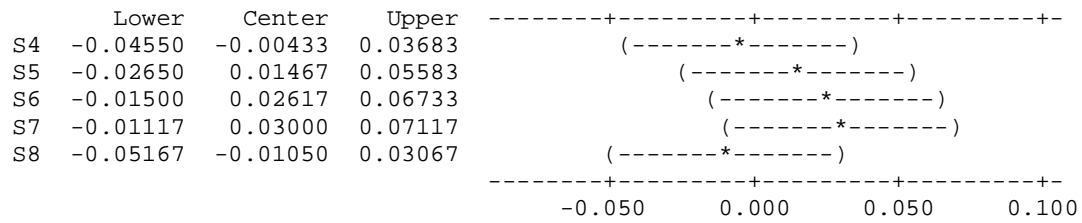
-----+-----+-----+-----+
 (-----*-----)
 (-----*-----)
 (-----*-----)
 (-----*-----)
 (-----*-----)
 (-----*-----)
 (-----*-----)
 -----+-----+-----+-----+
 -0.050 0.000 0.050 0.100

S2 subtracted from:

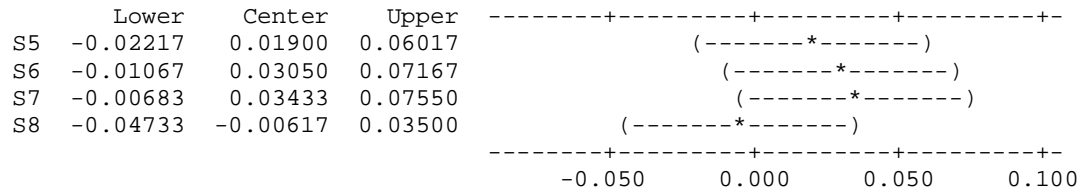
	Lower	Center	Upper
S3	-0.02400	0.01717	0.05833
S4	-0.02833	0.01283	0.05400
S5	-0.00933	0.03183	0.07300
S6	0.00217	0.04333	0.08450
S7	0.00600	0.04717	0.08833
S8	-0.03450	0.00667	0.04783

-----+-----+-----+-----+
 (-----*-----)
 (-----*-----)
 (-----*-----)
 (-----*-----)
 (-----*-----)
 (-----*-----)
 -----+-----+-----+-----+
 -0.050 0.000 0.050 0.100

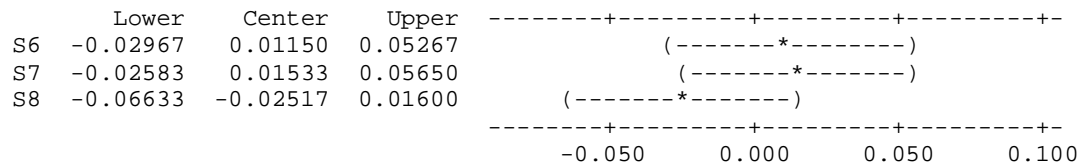
S3 subtracted from:



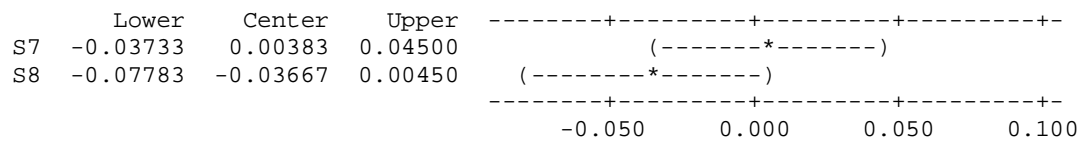
S4 subtracted from:



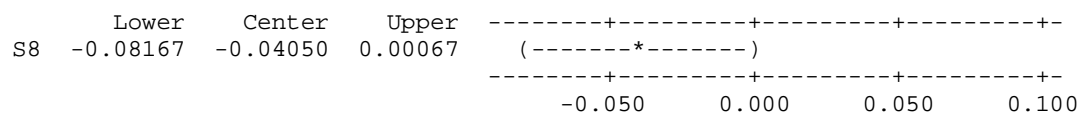
S5 subtracted from:



S6 subtracted from:



S7 subtracted from:



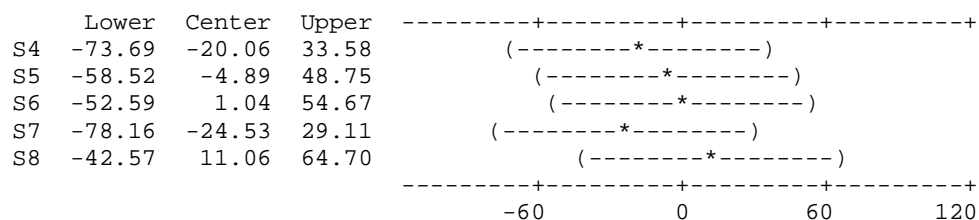
Source	DF	SS	MS	F	P
Factor	7	16752	2393	2.83	0.017
Error	40	33792	845		
Total	47	50544			

Level	N	Mean	StDev	Individual 95% CIs For Mean Based on Pooled StDev
S1	6	80.84	24.33	(-----+-----+-----+-----+-----+-----+)
S2	6	92.71	35.13	(-----*-----)
S3	6	58.33	20.24	(-----*-----)
S4	6	38.27	12.85	(-----*-----)
S5	6	53.44	55.34	(-----*-----)
S6	6	59.37	27.61	(-----*-----)
S7	6	33.80	8.91	(-----*-----)
S8	6	69.39	21.30	(-----*-----)

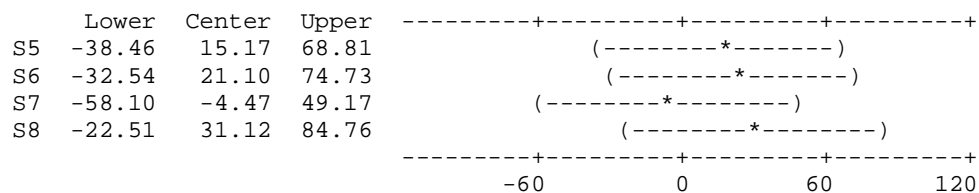
	Lower	Center	Upper	
S2	-41.76	11.87	65.51	(-----*-----)
S3	-76.14	-22.51	31.13	(-----*-----)
S4	-96.20	-42.56	11.07	(-----*-----)
S5	-81.03	-27.39	26.24	(-----*-----)
S6	-75.10	-21.46	32.17	(-----*-----)
S7	-100.66	-47.03	6.60	(-----*-----)
S8	-65.07	-11.44	42.19	(-----*-----)

	Lower	Center	Upper	
S3	-88.01	-34.38	19.25	(-----*-----)
S4	-108.07	-54.44	-0.80	(-----*-----)
S5	-92.90	-39.27	14.37	(-----*-----)
S6	-86.97	-33.34	20.30	(-----*-----)
S7	-112.54	-58.91	-5.27	(-----*-----)
S8	-76.95	-23.31	30.32	(-----*-----)

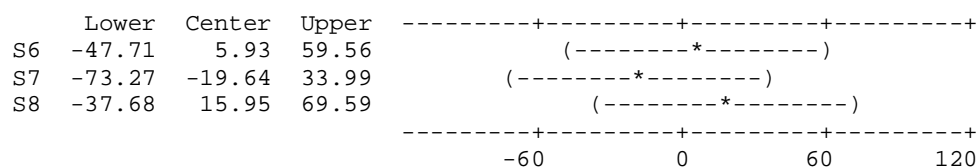
S3 subtracted from:



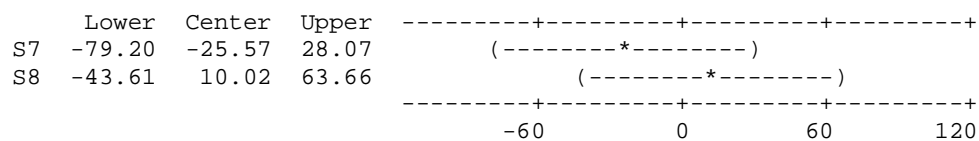
S4 subtracted from:



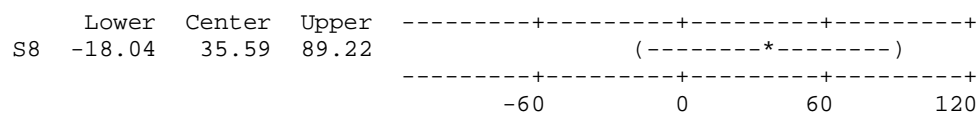
S5 subtracted from:



S6 subtracted from:



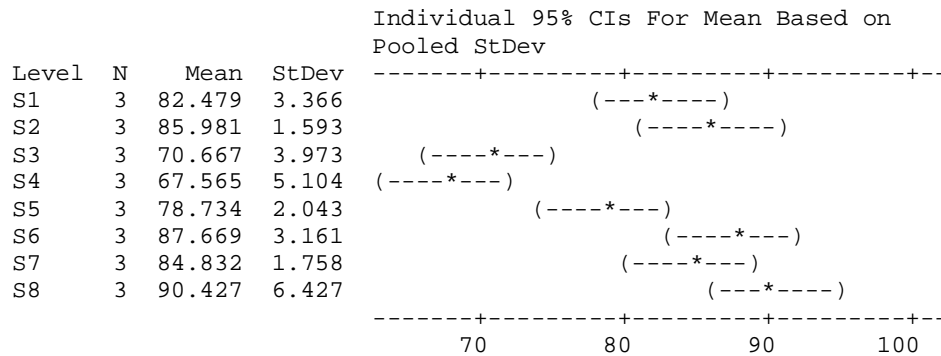
S7 subtracted from:



One-way ANOVA: Porosity

Source	DF	SS	MS	F	P
Factor	7	1402.2	200.3	14.02	0.000
Error	16	228.5	14.3		
Total	23	1630.7			

S = 3.779 R-Sq = 85.99% R-Sq(adj) = 79.85%

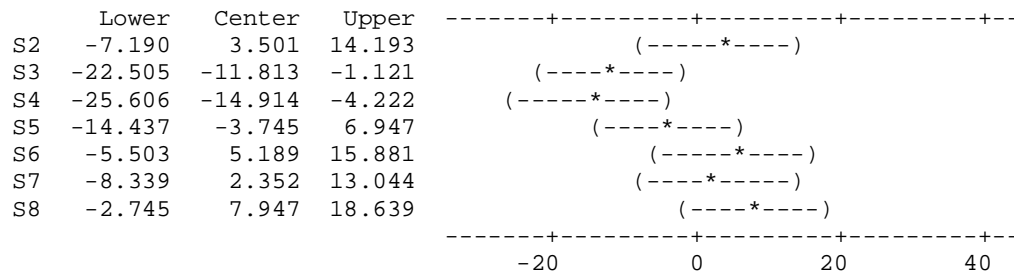


Pooled StDev = 3.779

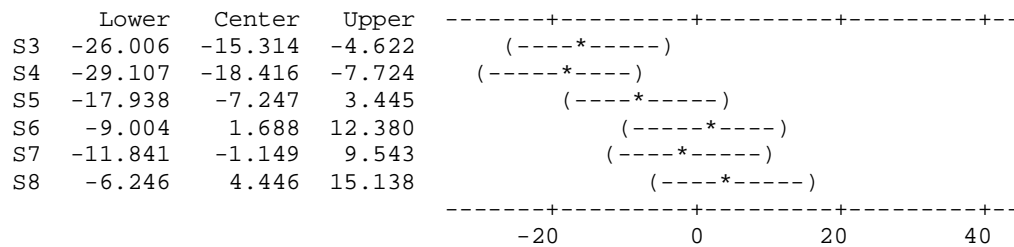
Tukey 95% Simultaneous Confidence Intervals
All Pairwise Comparisons

Individual confidence level = 99.68%

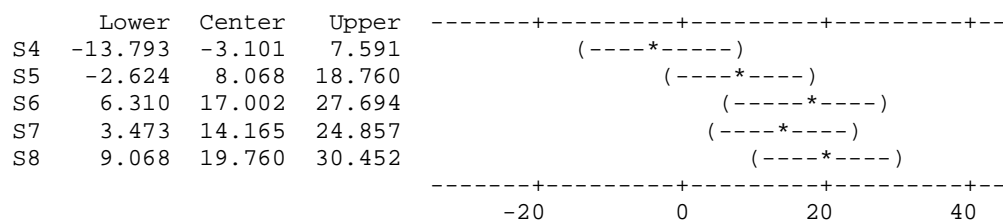
S1 subtracted from:



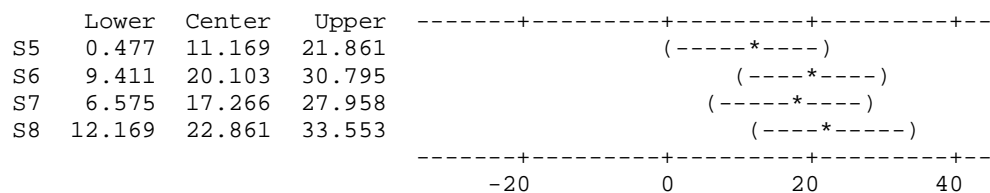
S2 subtracted from:



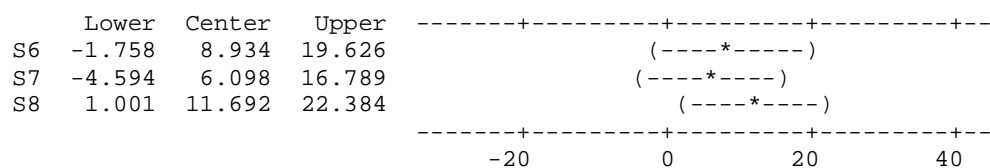
S3 subtracted from:



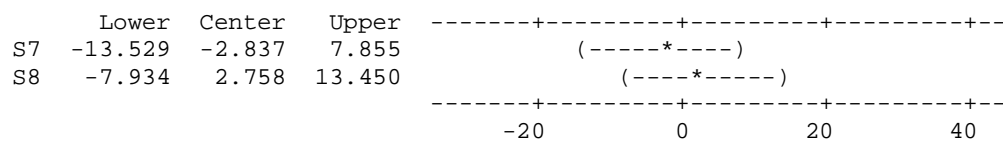
S4 subtracted from:



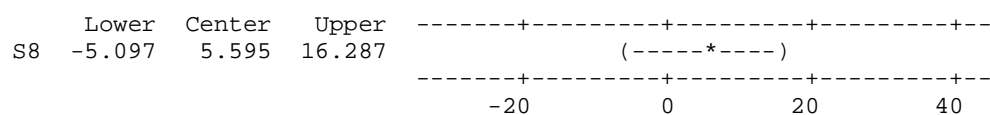
S5 subtracted from:



S6 subtracted from:



S7 subtracted from:



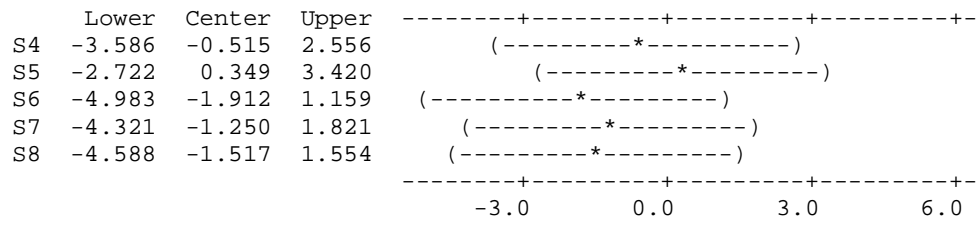
Source	DF	SS	MS	F	P
Factor	7	12.81	1.83	1.55	0.220
Error	16	18.86	1.18		
Total	23	31.67			

Level	N	Mean	StDev	Individual 95% CIs For Mean Based on Pooled StDev
S1	3	1.713	1.421	(-----*-----)
S2	3	1.690	1.343	(-----*-----)
S3	3	2.079	0.636	(-----*-----)
S4	3	1.564	1.115	(-----*-----)
S5	3	2.428	1.229	(-----*-----)
S6	3	0.167	0.014	(-----*-----)
S7	3	0.829	1.283	(-----*-----)
S8	3	0.562	0.896	(-----*-----)

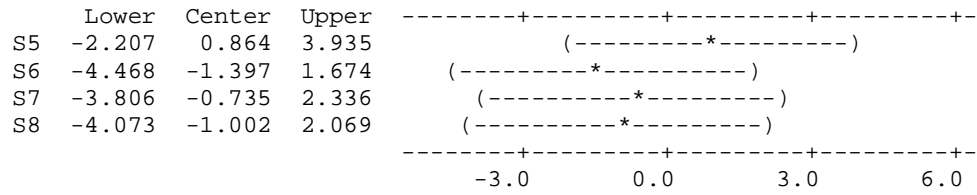
	Lower	Center	Upper	
S2	-3.095	-0.023	3.048	(-----*-----)
S3	-2.705	0.366	3.437	(-----*-----)
S4	-3.220	-0.149	2.922	(-----*-----)
S5	-2.356	0.715	3.786	(-----*-----)
S6	-4.617	-1.546	1.525	(-----*-----)
S7	-3.955	-0.884	2.187	(-----*-----)
S8	-4.222	-1.151	1.920	(-----*-----)

60

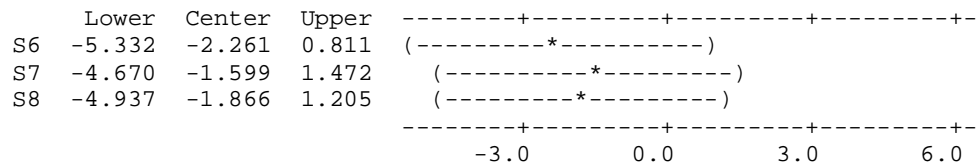
S3 subtracted from:



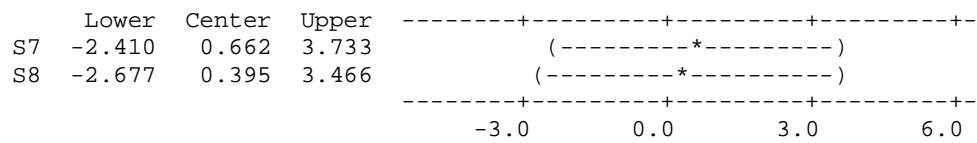
S4 subtracted from:



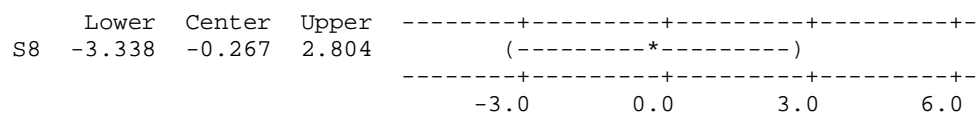
S5 subtracted from:



S6 subtracted from:



S7 subtracted from:



One-way ANOVA: Pore size

Source	DF	SS	MS	F	P
Factor	7	0.9393	0.1342	1.99	0.120
Error	16	1.0787	0.0674		
Total	23	2.0180			

S = 0.2596 R-Sq = 46.55% R-Sq(adj) = 23.16%

Individual 95% CIs For Mean Based on Pooled StDev

Level	N	Mean	StDev
S1	3	0.6106	0.3277
S2	3	0.6299	0.2496
S3	3	0.7286	0.1124
S4	3	0.5942	0.2810
S5	3	0.7729	0.2207
S6	3	0.2082	0.0088
S7	3	0.3583	0.3605
S8	3	0.2821	0.3151

0.00 0.35 0.70 1.05

Pooled StDev = 0.2596

Tukey 95% Simultaneous Confidence Intervals
All Pairwise Comparisons

Individual confidence level = 99.68%

S1 subtracted from:

	Lower	Center	Upper
S2	-0.7152	0.0193	0.7539
S3	-0.6165	0.1180	0.8526
S4	-0.7509	-0.0164	0.7182
S5	-0.5723	0.1623	0.8968
S6	-1.1369	-0.4024	0.3322
S7	-0.9868	-0.2523	0.4823
S8	-1.0630	-0.3284	0.4061

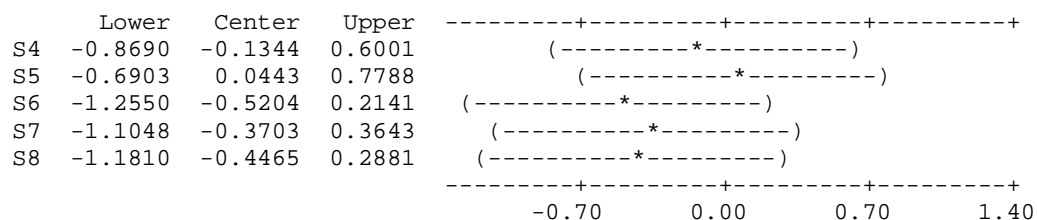
-0.70 0.00 0.70 1.40

S2 subtracted from:

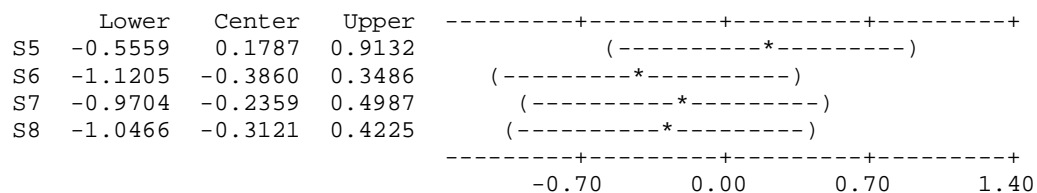
	Lower	Center	Upper
S3	-0.6358	0.0987	0.8333
S4	-0.7702	-0.0357	0.6989
S5	-0.5916	0.1430	0.8775
S6	-1.1562	-0.4217	0.3129
S7	-1.0061	-0.2716	0.4630
S8	-1.0823	-0.3478	0.3868

-0.70 0.00 0.70 1.40

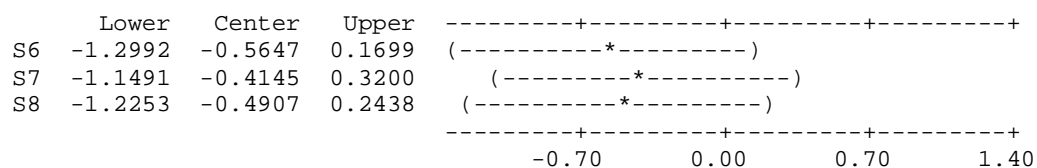
S3 subtracted from:



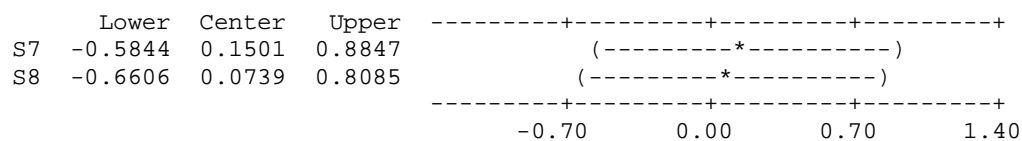
S4 subtracted from:



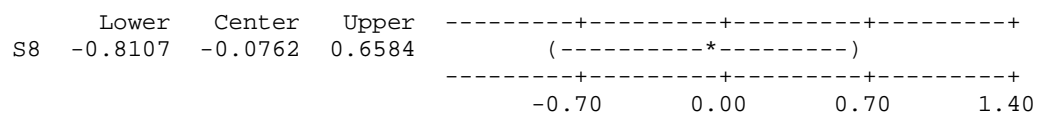
S5 subtracted from:



S6 subtracted from:



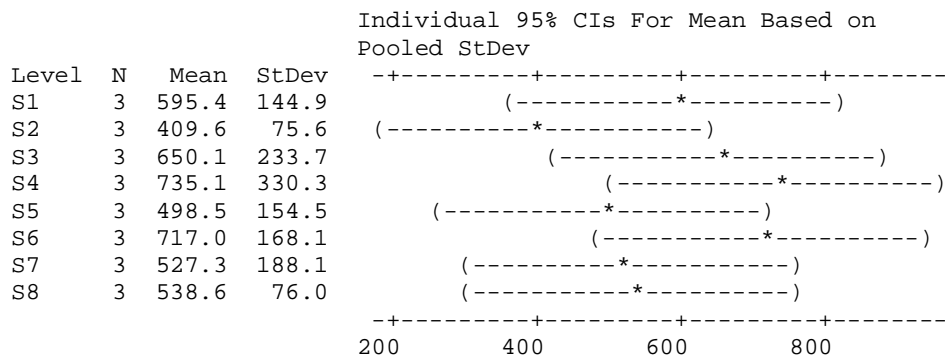
S7 subtracted from:



One-way ANOVA: Swelling studies (data points at 48 h)

Source	DF	SS	MS	F	P
Factor	7	264049	37721	1.06	0.429
Error	16	567362	35460		
Total	23	831410			

S = 188.3 R-Sq = 31.76% R-Sq(adj) = 1.90%

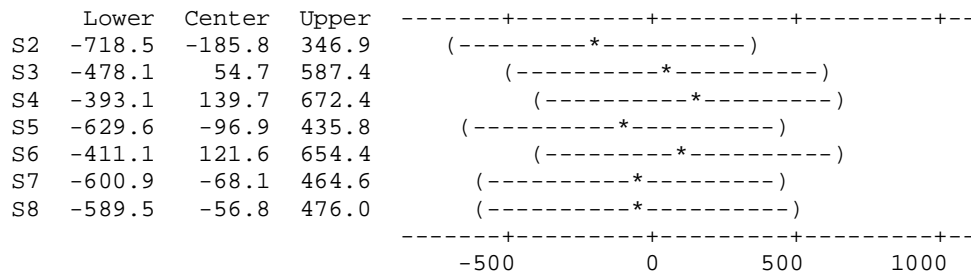


Pooled StDev = 188.3

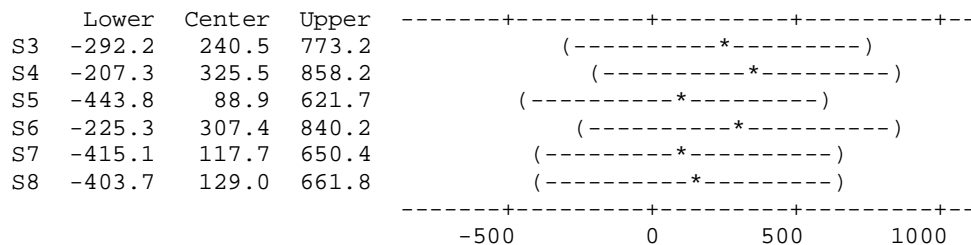
Tukey 95% Simultaneous Confidence Intervals
All Pairwise Comparisons

Individual confidence level = 99.68%

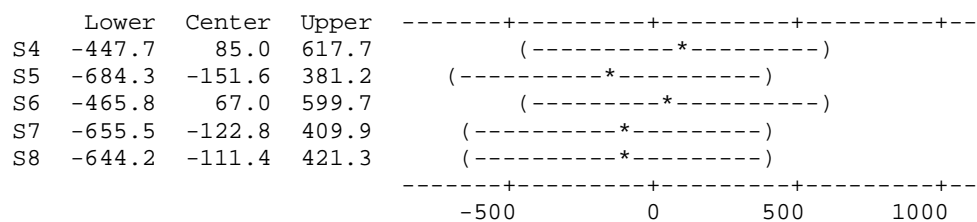
S1 subtracted from:



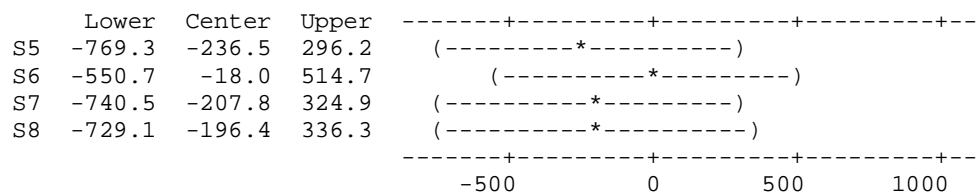
S2 subtracted from:



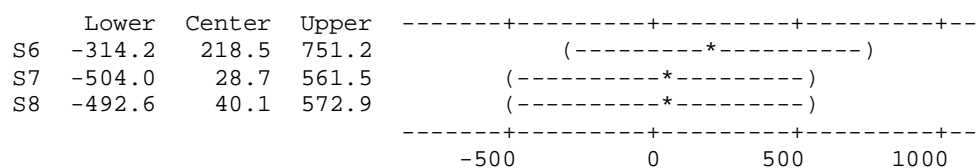
S3 subtracted from:



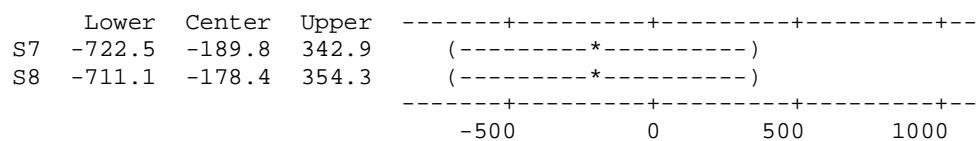
S4 subtracted from:



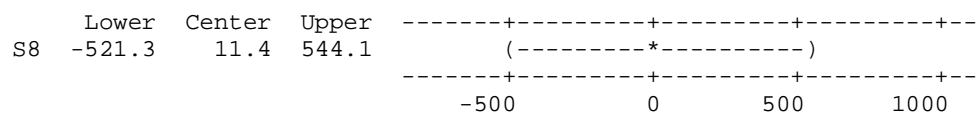
S5 subtracted from:



S6 subtracted from:



S7 subtracted from:



Degradation studies for scaffold S1
One-way ANOVA: cell conditioned medium at 37°C

Source	DF	SS	MS	F	P
Factor	2	765.3	382.7	9.04	0.015
Error	6	254.0	42.3		
Total	8	1019.3			

S = 6.506 R-Sq = 75.09% R-Sq(adj) = 66.78%

Level	N	Mean	StDev	Individual 95% CIs For Mean Based on Pooled StDev
CCM @ 37C 6h	3	80.44	11.27	(-----*-----)
CCM @ 37C 12h	3	100.00	0.00	(-----*-----)
CCM @ 37C 24h	3	100.00	0.00	(-----*-----)

80 90 100 110

Pooled StDev = 6.51

Tukey 95% Simultaneous Confidence Intervals
All Pairwise Comparisons

Individual confidence level = 97.80%

CCM @ 37C 6h subtracted from:

	Lower	Center	Upper	
CCM @ 37C 12h	3.260	19.562	35.864	(-----*-----)
CCM @ 37C 24h	3.260	19.562	35.864	(-----*-----)

-15 0 15 30

CCM @ 37C 12h subtracted from:

	Lower	Center	Upper	
CCM @ 37C 24h	-16.302	0.000	16.302	

CCM @ 37C 24h (-----*-----)

-15 0 15 30

One-way ANOVA: DMEM at 37°C

Source	DF	SS	MS	F	P
Factor	2	1372.1	686.1	17.12	0.003
Error	6	240.4	40.1		
Total	8	1612.5			

S = 6.330 R-Sq = 85.09% R-Sq(adj) = 80.12%

Individual 95% CIs For Mean Based on Pooled StDev

Level	N	Mean	StDev
DMEM @ 37C 6h	3	70.06	5.48
DMEM @ 37C 12h	3	81.31	9.49
DMEM @ 37C 24h	3	100.00	0.00

-----+-----+-----+-----+
 (-----*-----)
 (-----*-----)
 (-----*-----)
 -----+-----+-----+-----+
 72 84 96 108

Pooled StDev = 6.33

Tukey 95% Simultaneous Confidence Intervals
 All Pairwise Comparisons

Individual confidence level = 97.80%

DMEM @ 37C 6h subtracted from:

		Lower	Center	Upper
DMEM @ 37C 12h		-4.612	11.249	27.109
DMEM @ 37C 24h		14.078	29.938	45.799

-----+-----+-----+-----+
 DMEM @ 37C 12h (-----*-----)
 DMEM @ 37C 24h (-----*-----)
 -----+-----+-----+-----+
 -25 0 25 50

DMEM @ 37C 12h subtracted from:

		Lower	Center	Upper
DMEM @ 37C 24h		2.829	18.689	34.550

-----+-----+-----+-----+
 DMEM @ 37C 24h (-----*-----)
 -----+-----+-----+-----+
 -25 0 25 50

One-way ANOVA: DMEM at room temperature

Source	DF	SS	MS	F	P
Factor	2	17.0	8.5	0.35	0.715
Error	6	143.6	23.9		
Total	8	160.6			

S = 4.892 R-Sq = 10.56% R-Sq(adj) = 0.00%

Level	N	Mean	StDev	Individual 95% CIs For Mean Based on Pooled StDev
DMEM room tmp 6h	3	8.718	7.543	(-----*-----)
DMEM room tmp 12h	3	9.848	1.488	(-----*-----)
DMEM room tmp 24h	3	6.541	3.562	(-----*-----)

0.0 5.0 10.0 15.0

Pooled StDev = 4.892

Tukey 95% Simultaneous Confidence Intervals
All Pairwise Comparisons

Individual confidence level = 97.80%

DMEM room tmp 6h subtracted from:

	Lower	Center	Upper
DMEM room tmp 12h	-11.128	1.131	13.389
DMEM room tmp 24h	-14.435	-2.177	10.082

DMEM room tmp 12h (-----*-----)

DMEM room tmp 24h (-----*-----)

-8.0 0.0 8.0 16.0

DMEM room tmp 12h subtracted from:

	Lower	Center	Upper
DMEM room tmp 24h	-15.566	-3.307	8.951

DMEM room tmp 24h (-----*-----)

-8.0 0.0 8.0 16.0

One-way ANOVA: SWF at 37°C

Source	DF	SS	MS	F	P
Factor	2	6737.5	3368.7	49.58	0.000
Error	6	407.6	67.9		
Total	8	7145.1			

S = 8.243 R-Sq = 94.29% R-Sq(adj) = 92.39%

Individual 95% CIs For Mean Based on Pooled StDev

Level	N	Mean	StDev
SWF @ 37C 6h	3	33.48	10.10
SWF @ 37C 12h	3	73.81	10.09
SWF @ 37C 24h	3	100.00	0.00

25 50 75 100

Pooled StDev = 8.24

Tukey 95% Simultaneous Confidence Intervals
All Pairwise Comparisons

Individual confidence level = 97.80%

SWF @ 37C 6h subtracted from:

	Lower	Center	Upper
SWF @ 37C 12h	19.680	40.334	60.987
SWF @ 37C 24h	45.867	66.520	87.174

-35 0 35 70

SWF @ 37C 12h subtracted from:

	Lower	Center	Upper
SWF @ 37C 24h	5.533	26.186	46.840

-35 0 35 70

One-way ANOVA: Data at 6h from all media

Source	DF	SS	MS	F	P
Factor	3	9878.3	3292.8	41.70	0.000
Error	8	631.8	79.0		
Total	11	10510.1			

S = 8.887 R-Sq = 93.99% R-Sq(adj) = 91.73%

Individual 95% CIs For Mean Based on Pooled StDev

Level	N	Mean	StDev
CCM @ 37C 6h	3	80.438	11.268
DMEM @ 37C 6h	3	70.062	5.484
DMEM room tmp 6h	3	8.718	7.543
SWF @ 37C 6h	3	33.480	10.096

0 25 50 75

Pooled StDev = 8.887

Tukey 95% Simultaneous Confidence Intervals
All Pairwise Comparisons

Individual confidence level = 98.74%

CCM @ 37C 6h subtracted from:

	Lower	Center	Upper
DMEM @ 37C 6h	-33.62	-10.38	12.87
DMEM room tmp 6h	-94.96	-71.72	-48.48
SWF @ 37C 6h	-70.20	-46.96	-23.72

DMEM @ 37C 6h (----*----)

DMEM room tmp 6h (----*----)

SWF @ 37C 6h (----*----)

-50 0 50 100

DMEM @ 37C 6h subtracted from:

	Lower	Center	Upper
DMEM room tmp 6h	-84.59	-61.34	-38.10
SWF @ 37C 6h	-59.82	-36.58	-13.34

DMEM room tmp 6h (----*----)

SWF @ 37C 6h (----*----)

-50 0 50 100

DMEM room tmp 6h subtracted from:

	Lower	Center	Upper
SWF @ 37C 6h	1.52	24.76	48.00

(----*----)

-50 0 50 100

One-way ANOVA: Data at 12h from all media

Source	DF	SS	MS	F	P
Factor	3	13812.7	4604.2	94.82	0.000
Error	8	388.4	48.6		
Total	11	14201.1			

S = 6.968 R-Sq = 97.26% R-Sq(adj) = 96.24%

Individual 95% CIs For Mean Based on Pooled StDev

Level	N	Mean	StDev
CCM @ 37C 12h	3	100.00	0.00
DMEM @ 37C 12h	3	81.31	9.49
DMEM room tmp 12h	3	9.85	1.49
SWF @ 37C 12h	3	73.81	10.09

0 30 60 90

Pooled StDev = 6.97

Tukey 95% Simultaneous Confidence Intervals
All Pairwise Comparisons

Individual confidence level = 98.74%

CCM @ 37C 12h subtracted from:

	Lower	Center	Upper
DMEM @ 37C 12h	-36.91	-18.69	-0.46
DMEM room tmp 12h	-108.38	-90.15	-71.93
SWF @ 37C 12h	-44.41	-26.19	-7.96

DMEM @ 37C 12h (---*---)
DMEM room tmp 12h (---*---)
SWF @ 37C 12h (---*---)

-100 -50 0 50

DMEM @ 37C 12h subtracted from:

	Lower	Center	Upper
DMEM room tmp 12h	-89.69	-71.46	-53.24
SWF @ 37C 12h	-25.72	-7.50	10.73

DMEM room tmp 12h (---*---)
SWF @ 37C 12h (---*---)

-100 -50 0 50

DMEM room tmp 12h subtracted from:

	Lower	Center	Upper
SWF @ 37C 12h	45.74	63.97	82.19

SWF @ 37C 12h (---*---)

-100 -50 0 50

Source	DF	SS	MS	F	P
Factor	3	19652.72	6550.91	2065.00	0.000
Error	8	25.38	3.17		
Total	11	19678.10			

Level	N	Mean	StDev	Individual 95% CIs For Mean Based on Pooled StDev
CCM @ 37C 24h	3	100.00	0.00	(*)
DMEM @ 37C 24h	3	100.00	0.00	(*)
DMEM room tmp 24h	3	6.54	3.56	(*)
SWF @ 37C 24h	3	100.00	0.00	(*)

Tukey 95% Simultaneous Confidence Intervals
All Pairwise Comparisons

CCM @ 37C 24h subtracted from:

	Lower	Center	Upper
DMEM @ 37C 24h	-4.66	0.00	4.66
DMEM room tmp 24h	-98.12	-93.46	-88.80
SWF @ 37C 24h	-4.66	0.00	4.66

Condition	log10(FC) Difference (approx.)	Significance
DMEM @ 37C 24h	10	(*)
DMEM room tmp 24h	-10	(*)
SWF @ 37C 24h	10	(*)

DMEM @ 37C 24h subtracted from:

	Lower	Center	Upper
DMEM room tmp 24h	-98.12	-93.46	-88.80
SWF @ 37C 24h	-4.66	0.00	4.66

DMEM room tmp 24h subtracted from:

	Lower	Center	Upper
SWF @ 37C 24h	88.80	93.46	98.12

Degradation studies for scaffold S5
One-way ANOVA: Cell conditioned medium at 37°C

Source	DF	SS	MS	F	P
Factor	2	1092.70	546.35	166.19	0.000
Error	6	19.73	3.29		
Total	8	1112.42			

S = 1.813 R-Sq = 98.23% R-Sq(adj) = 97.64%

Individual 95% CIs For Mean Based on Pooled StDev

Level	N	Mean	StDev	
CCM 6h	3	76.63	3.14	(--*--)
CCM 12h	3	100.00	0.00	(--*--)
CCM 24h	3	100.00	0.00	(--*--)

80.0 88.0 96.0 104.0

Pooled StDev = 1.81

Tukey 95% Simultaneous Confidence Intervals
 All Pairwise Comparisons

Individual confidence level = 97.80%

CCM 6h subtracted from:

	Lower	Center	Upper	
CCM 12h	18.831	23.374	27.917	(---*---)
CCM 24h	18.831	23.374	27.917	(---*---)

0 10 20 30

CCM 12h subtracted from:

	Lower	Center	Upper	
CCM 24h	-4.543	0.000	4.543	(---*---)

0 10 20 30

Source	DF	SS	MS	F	P
Factor	2	7014	3507	13.76	0.006
Error	6	1529	255		
Total	8	8543			

Level	N	Mean	StDev	Individual 95% CIs For Mean Based on Pooled StDev
DMEM @ 37C 6h	3	37.52	9.95	(-----*-----)
DMEM @ 37C 12h	3	44.69	25.80	(-----*-----)
DMEM @ 37C 24h	3	100.00	0.00	(-----*-----)

		Lower	Center	Upper
DMEM @ 37C	12h	-32.83	7.17	47.17
DMEM @ 37C	24h	22.48	62.48	102.48

DMEM @ 37C 12h (-----*-----)

DMEM @ 37C 24h (-----*-----)

-----+-----+-----+-----+

-50 0 50 100

		Lower	Center	Upper	
DMEM @ 37C	24h	15.31	55.31	95.31	<div> <div>-----+-----+-----+-----+</div> <div>(-----*-----)</div> <div>-----+-----+-----+-----+</div> <div>-50 0 50 100</div> </div>

One-way ANOVA: DMEM at room temperature

Source	DF	SS	MS	F	P
Factor	2	88.0	44.0	0.72	0.524
Error	6	366.2	61.0		
Total	8	454.2			

S = 7.812 R-Sq = 19.38% R-Sq(adj) = 0.00%

Level	N	Mean	StDev	Individual 95% CIs For Mean Based on Pooled StDev
DMEM room tmp 6h	3	13.705	10.047	(-----+-----+-----+-----+-----+-----+-----+-----+-----+-----+)
DMEM room tmp 12h	3	16.939	9.025	(-----+-----+-----+-----+-----+-----+-----+-----+-----+-----+)
DMEM room tmp 24h	3	21.337	0.829	(-----+-----+-----+-----+-----+-----+-----+-----+-----+-----+)

8.0 16.0 24.0 32.0

Pooled StDev = 7.812

Tukey 95% Simultaneous Confidence Intervals
All Pairwise Comparisons

Individual confidence level = 97.80%

DMEM room tmp 6h subtracted from:

	Lower	Center	Upper
DMEM room tmp 12h	-16.342	3.234	22.809
DMEM room tmp 24h	-11.943	7.632	27.207

DMEM room tmp 12h (-----+-----+-----+-----+-----+-----+-----+-----+-----+-----+)

DMEM room tmp 24h (-----+-----+-----+-----+-----+-----+-----+-----+-----+-----+)

-15 0 15 30

DMEM room tmp 12h subtracted from:

	Lower	Center	Upper
DMEM room tmp 24h	-15.177	4.398	23.974

DMEM room tmp 24h (-----+-----+-----+-----+-----+-----+-----+-----+-----+-----+)

-15 0 15 30

One-way ANOVA: SWF at 37°C

Source	DF	SS	MS	F	P
Factor	2	7509.6	3754.8	187.64	0.000
Error	6	120.1	20.0		
Total	8	7629.7			

S = 4.473 R-Sq = 98.43% R-Sq(adj) = 97.90%

Individual 95% CIs For Mean Based on Pooled StDev

Level	N	Mean	StDev	
SWF @ 37C 6h	3	30.35	4.69	(- * - -)
SWF @ 37C 12h	3	54.39	6.17	(- - * -)
SWF @ 37C 24h	3	100.00	0.00	(- - * - -)

25 50 75 100

Pooled StDev = 4.47

Tukey 95% Simultaneous Confidence Intervals
All Pairwise Comparisons

Individual confidence level = 97.80%

SWF @ 37C 6h subtracted from:

	Lower	Center	Upper	
SWF @ 37C 12h	12.831	24.040	35.249	(- - * - -)
SWF @ 37C 24h	58.443	69.651	80.860	(- - * - -)

-35 0 35 70

SWF @ 37C 12h subtracted from:

	Lower	Center	Upper	
SWF @ 37C 24h	34.403	45.611	56.820	(- - * - -)

-35 0 35 70

One-way ANOVA: Data at 6h from all media

Source	DF	SS	MS	F	P
Factor	3	6394.0	2131.3	36.77	0.000
Error	8	463.8	58.0		
Total	11	6857.8			

S = 7.614 R-Sq = 93.24% R-Sq(adj) = 90.70%

Individual 95% CIs For Mean Based on Pooled StDev

Level	N	Mean	StDev
CCM 6h	3	76.626	3.140
DMEM @ 37C 6h	3	37.523	9.953
DMEM room tmp 6h	3	13.705	10.047
SWF @ 37C 6h	3	30.349	4.692

-----+-----+-----+-----+-----+
 (---*---) (---*---)
 (---*---) (---*---)
 -----+-----+-----+-----+-----+
 25 50 75 100

Pooled StDev = 7.614

Tukey 95% Simultaneous Confidence Intervals
 All Pairwise Comparisons

Individual confidence level = 98.74%

CCM 6h subtracted from:

	Lower	Center	Upper
DMEM @ 37C 6h	-59.016	-39.102	-19.189
DMEM room tmp 6h	-82.834	-62.921	-43.007
SWF @ 37C 6h	-66.190	-46.277	-26.364

-----+-----+-----+-----+-----+
 (-----*-----)
 (-----*-----)
 (-----*-----)
 -----+-----+-----+-----+-----+
 -70 -35 0 35

DMEM @ 37C 6h subtracted from:

	Lower	Center	Upper
DMEM room tmp 6h	-43.732	-23.818	-3.905
SWF @ 37C 6h	-27.088	-7.175	12.739

-----+-----+-----+-----+-----+
 (-----*-----)
 (-----*-----)
 -----+-----+-----+-----+-----+
 -70 -35 0 35

DMEM room tmp 6h subtracted from:

	Lower	Center	Upper
SWF @ 37C 6h	-3.270	16.643	36.557

-----+-----+-----+-----+-----+
 (-----*-----)
 -----+-----+-----+-----+-----+
 -70 -35 0 35

One-way ANOVA: Data at 12 h from all media

Source	DF	SS	MS	F	P
Factor	3	10729	3576	18.23	0.001
Error	8	1570	196		
Total	11	12299			

S = 14.01 R-Sq = 87.24% R-Sq(adj) = 82.45%

Individual 95% CIs For Mean Based on Pooled StDev

Level	N	Mean	StDev
CCM 12h	3	100.00	0.00
DMEM @ 37C 12h	3	44.69	25.80
DMEM room tmp 12h	3	16.94	9.03
SWF @ 37C 12h	3	54.39	6.17

0 35 70 105

Pooled StDev = 14.01

Tukey 95% Simultaneous Confidence Intervals
All Pairwise Comparisons

Individual confidence level = 98.74%

CCM 12h subtracted from:

	Lower	Center	Upper
DMEM @ 37C 12h	-91.94	-55.31	-18.67
DMEM room tmp 12h	-119.70	-83.06	-46.43
SWF @ 37C 12h	-82.25	-45.61	-8.98

-100 -50 0 50

DMEM @ 37C 12h subtracted from:

	Lower	Center	Upper
DMEM room tmp 12h	-64.39	-27.75	8.88
SWF @ 37C 12h	-26.94	9.70	46.33

-100 -50 0 50

DMEM room tmp 12h subtracted from:

	Lower	Center	Upper
SWF @ 37C 12h	0.81	37.45	74.09

-100 -50 0 50

One-way ANOVA: Data at 24h from all media

Source	DF	SS	MS	F	P
Factor	3	13922.63	4640.88	27025.15	0.000
Error	8	1.37	0.17		
Total	11	13924.01			

S = 0.4144 R-Sq = 99.99% R-Sq(adj) = 99.99%

Level	N	Mean	StDev
CCM 24h	3	100.000	0.000
DMEM @ 37C 24h	3	100.000	0.000
DMEM room tmp 24h	3	21.337	0.829
SWF @ 37C 24h	3	100.000	0.000

Individual 95% CIs For Mean Based on Pooled StDev

Level	
CCM 24h	+-----+-----+-----+-----*
DMEM @ 37C 24h	+-----+-----+-----+-----*
DMEM room tmp 24h	(* +-----+-----+-----+-----*
SWF @ 37C 24h	+-----+-----+-----+-----*

20 40 60 80

Pooled StDev = 0.414

Tukey 95% Simultaneous Confidence Intervals
All Pairwise Comparisons

Individual confidence level = 98.74%

CCM 24h subtracted from:

	Lower	Center	Upper
DMEM @ 37C 24h	-1.084	0.000	1.084
DMEM room tmp 24h	-79.747	-78.663	-77.579
SWF @ 37C 24h	-1.084	0.000	1.084

DMEM @ 37C 24h	+-----+-----+-----+-----*
DMEM room tmp 24h	(*) +-----+-----+-----+-----*
SWF @ 37C 24h	+-----+-----+-----+-----*

-80 -40 0 40

DMEM @ 37C 24h subtracted from:

	Lower	Center	Upper
DMEM room tmp 24h	-79.747	-78.663	-77.579
SWF @ 37C 24h	-1.084	0.000	1.084

DMEM room tmp 24h	(*) +-----+-----+-----+-----*
SWF @ 37C 24h	+-----+-----+-----+-----*

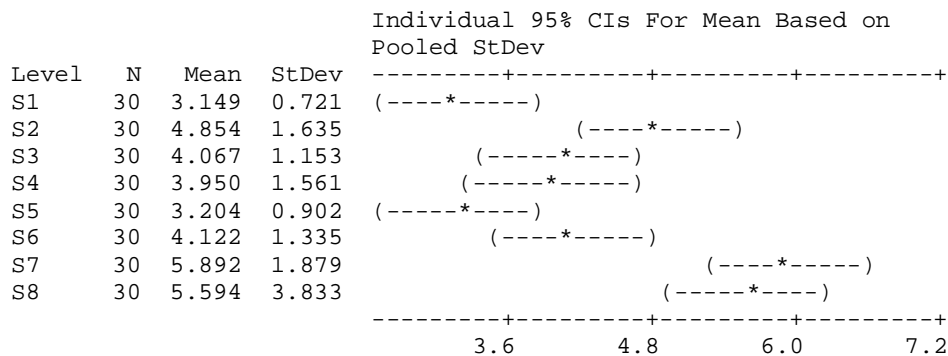
-80 -40 0 40

Appendix B (Data for the non-crosslinked scaffolds)

One-way ANOVA: fiber diameter

Source	DF	SS	MS	F	P
Factor	7	216.75	30.96	8.92	0.000
Error	232	805.50	3.47		
Total	239	1022.25			

S = 1.863 R-Sq = 21.20% R-Sq(adj) = 18.83%

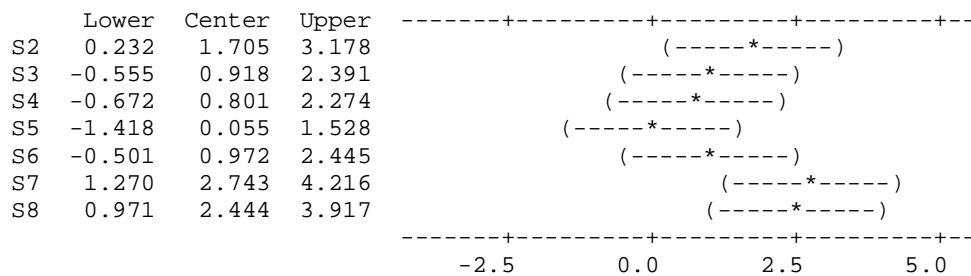


Pooled StDev = 1.863

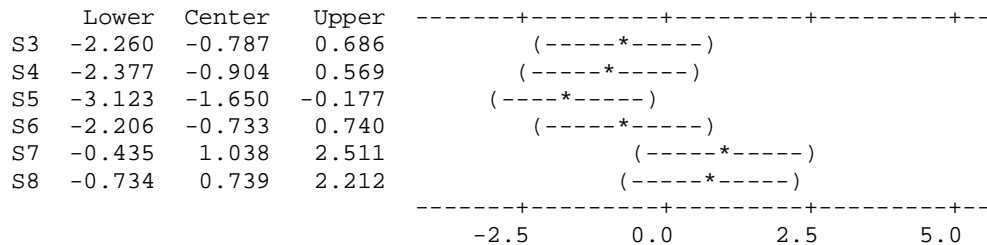
Tukey 95% Simultaneous Confidence Intervals
All Pairwise Comparisons

Individual confidence level = 99.75%

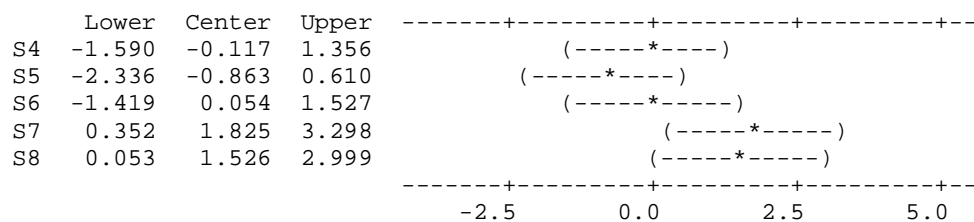
S1 subtracted from:



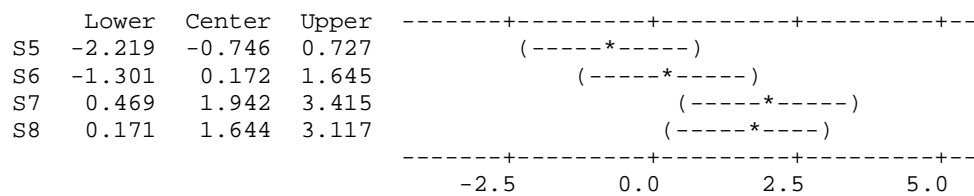
S2 subtracted from:



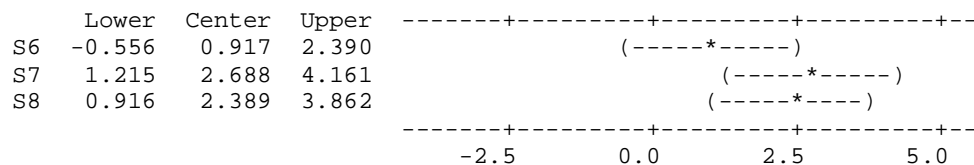
S3 subtracted from:



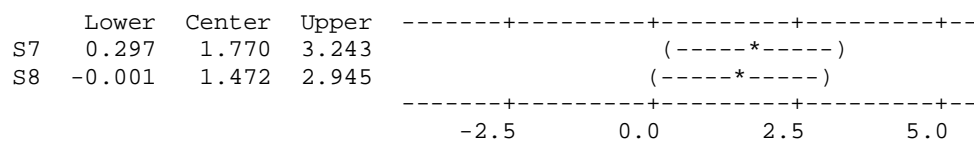
S4 subtracted from:



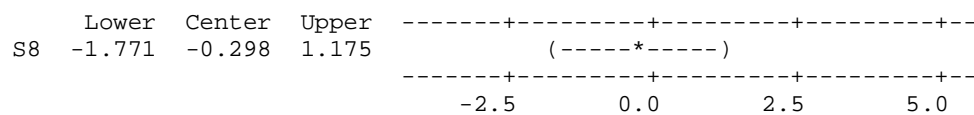
S5 subtracted from:



S6 subtracted from:



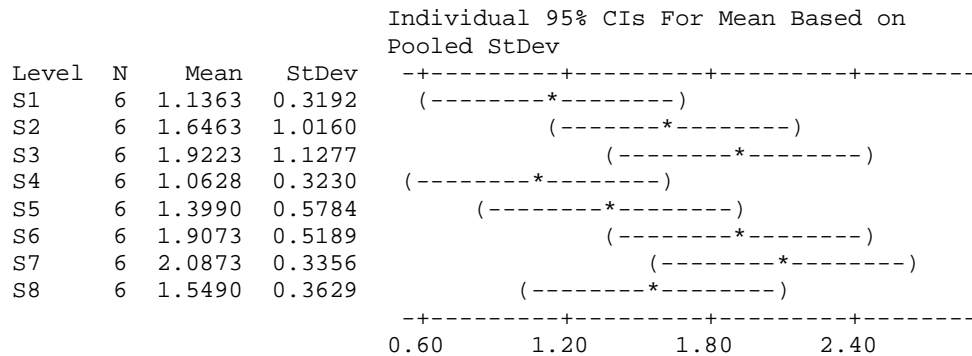
S7 subtracted from:



One-way ANOVA: Stress

Source	DF	SS	MS	F	P
Factor	7	5.901	0.843	2.01	0.078
Error	40	16.791	0.420		
Total	47	22.692			

S = 0.6479 R-Sq = 26.01% R-Sq(adj) = 13.06%

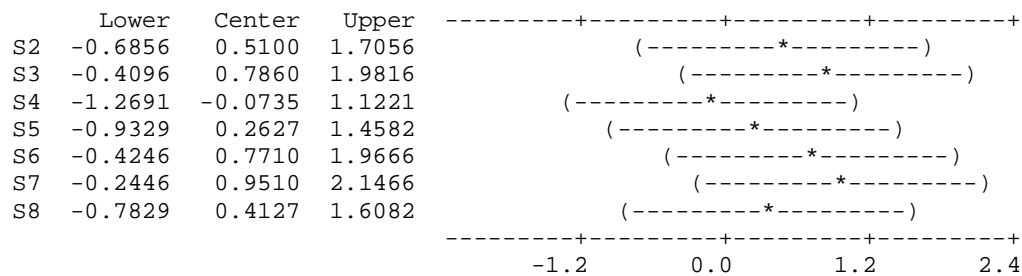


Pooled StDev = 0.6479

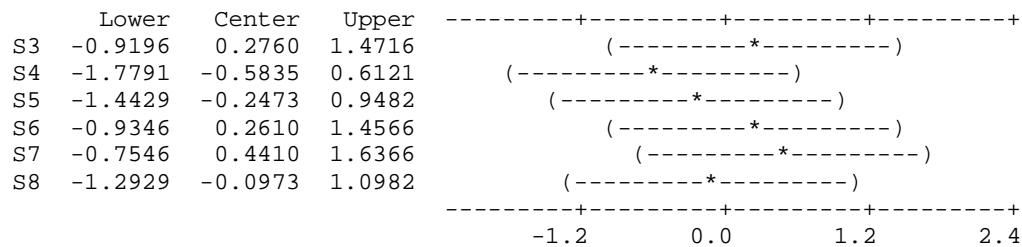
Tukey 95% Simultaneous Confidence Intervals
All Pairwise Comparisons

Individual confidence level = 99.73%

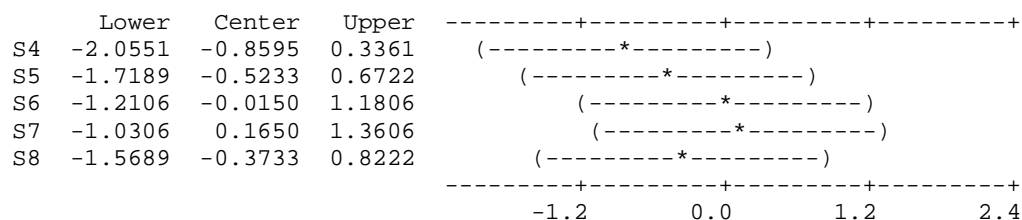
S1 subtracted from:



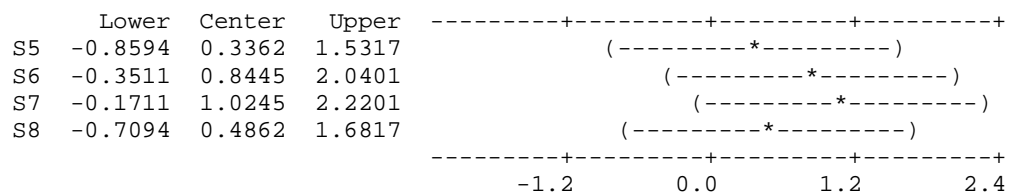
S2 subtracted from:



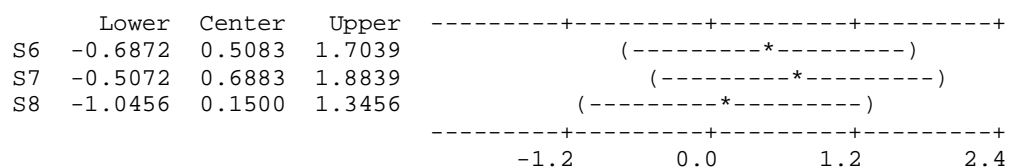
S3 subtracted from:



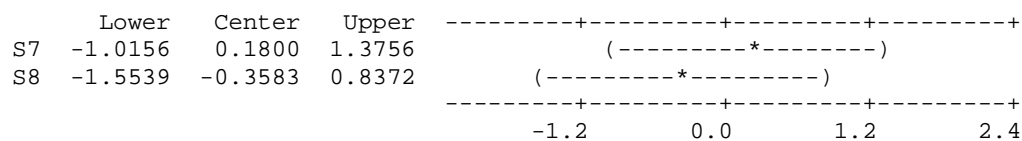
S4 subtracted from:



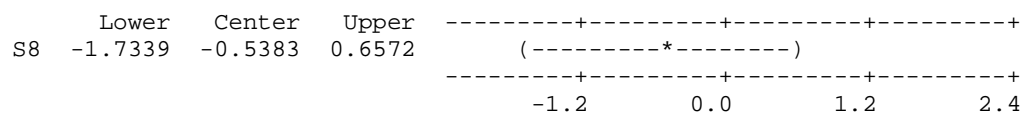
S5 subtracted from:



S6 subtracted from:



S7 subtracted from:



One-way ANOVA: Strain

Source	DF	SS	MS	F	P
Factor	7	0.003182	0.000455	2.04	0.073
Error	40	0.008901	0.000223		
Total	47	0.012083			

S = 0.01492 R-Sq = 26.34% R-Sq(adj) = 13.44%

Individual 95% CIs For Mean Based on Pooled StDev

Level	N	Mean	StDev
S1	6	0.02833	0.00665
S2	6	0.03967	0.03828
S3	6	0.02250	0.00723
S4	6	0.01767	0.00745
S5	6	0.02250	0.00509
S6	6	0.03667	0.00845
S7	6	0.02750	0.00606
S8	6	0.01467	0.00539

0.015 0.030 0.045 0.060

Pooled StDev = 0.01492

Tukey 95% Simultaneous Confidence Intervals
All Pairwise Comparisons

Individual confidence level = 99.73%

S1 subtracted from:

	Lower	Center	Upper
S2	-0.01619	0.01133	0.03886
S3	-0.03336	-0.00583	0.02169
S4	-0.03819	-0.01067	0.01686
S5	-0.03336	-0.00583	0.02169
S6	-0.01919	0.00833	0.03586
S7	-0.02836	-0.00083	0.02669
S8	-0.04119	-0.01367	0.01386

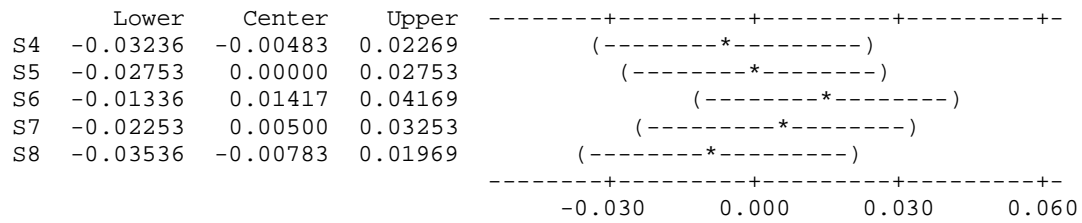
-0.030 0.000 0.030 0.060

S2 subtracted from:

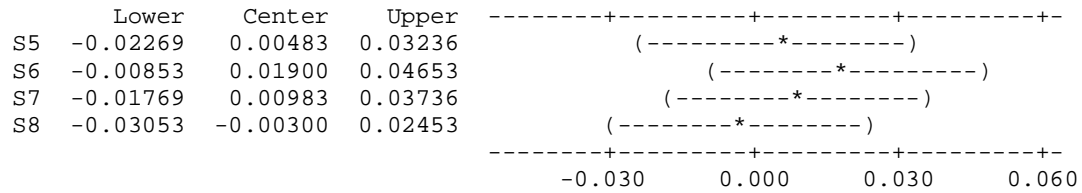
	Lower	Center	Upper
S3	-0.04469	-0.01717	0.01036
S4	-0.04953	-0.02200	0.00553
S5	-0.04469	-0.01717	0.01036
S6	-0.03053	-0.00300	0.02453
S7	-0.03969	-0.01217	0.01536
S8	-0.05253	-0.02500	0.00253

-0.030 0.000 0.030 0.060

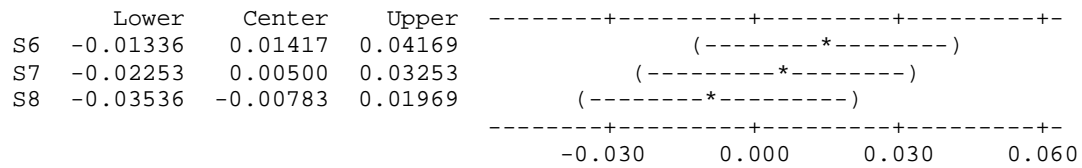
S3 subtracted from:



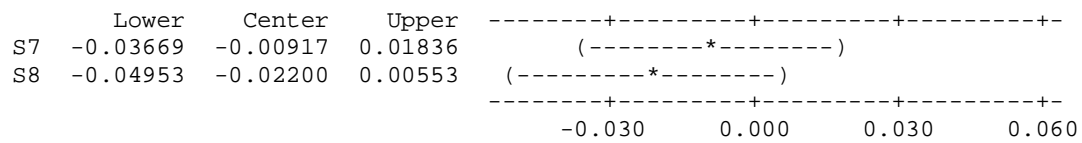
S4 subtracted from:



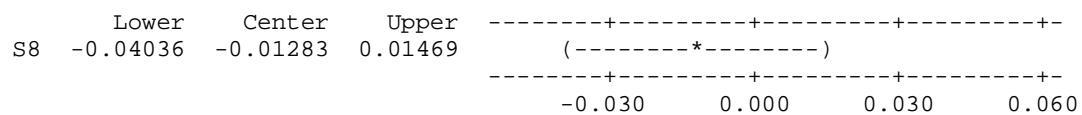
S5 subtracted from:



S6 subtracted from:



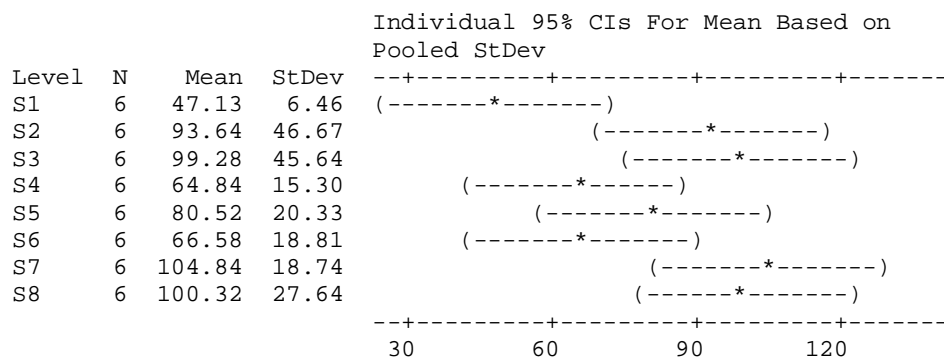
S7 subtracted from:



One-way ANOVA: Modulus

Source	DF	SS	MS	F	P
Factor	7	18245	2606	3.25	0.008
Error	40	32095	802		
Total	47	50340			

S = 28.33 R-Sq = 36.24% R-Sq(adj) = 25.09%

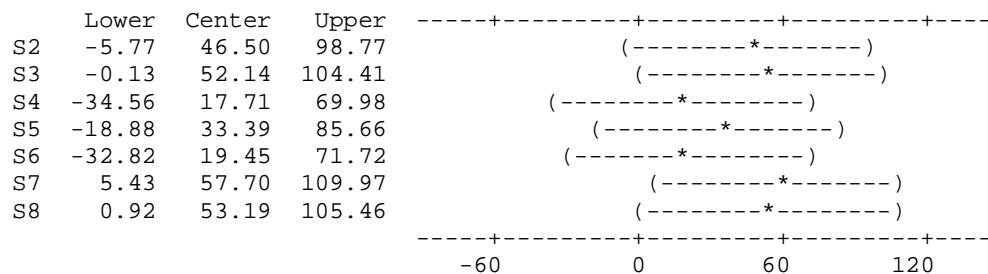


Pooled StDev = 28.33

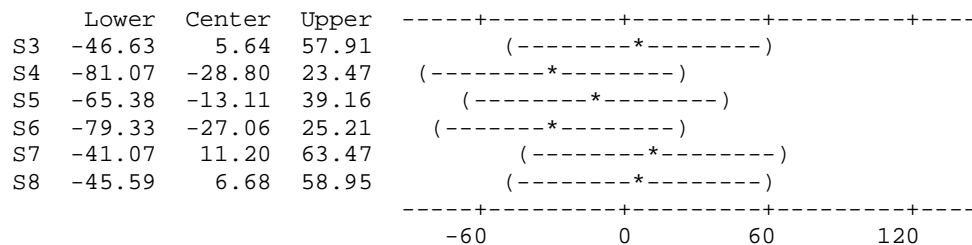
Tukey 95% Simultaneous Confidence Intervals
All Pairwise Comparisons

Individual confidence level = 99.73%

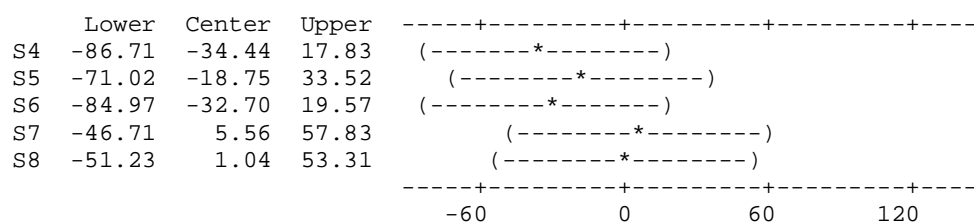
S1 subtracted from:



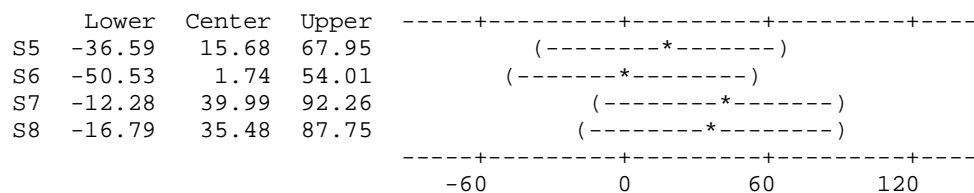
S2 subtracted from:



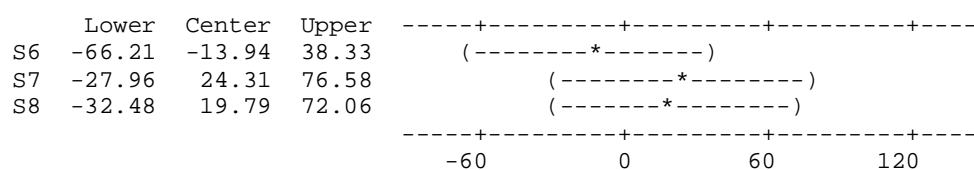
S3 subtracted from:



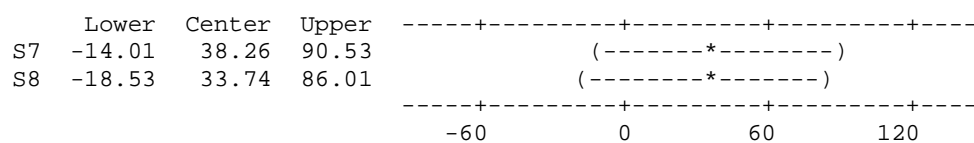
S4 subtracted from:



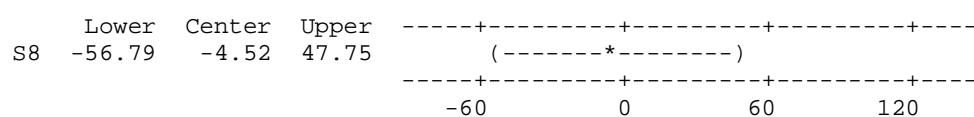
S5 subtracted from:



S6 subtracted from:

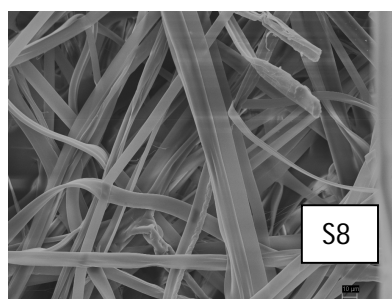
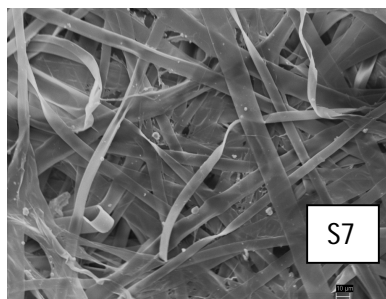
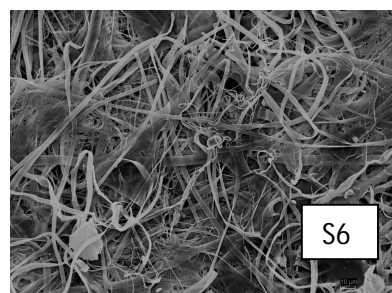
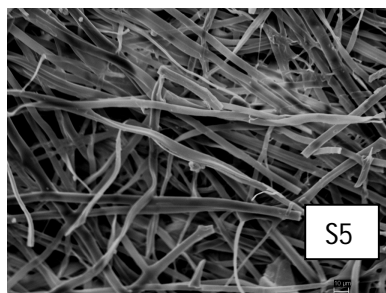
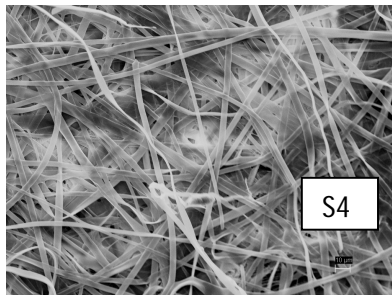
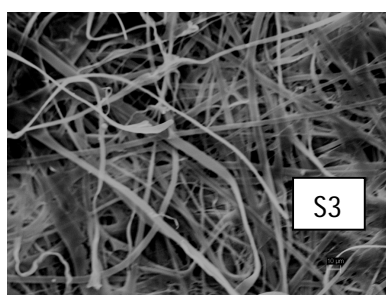
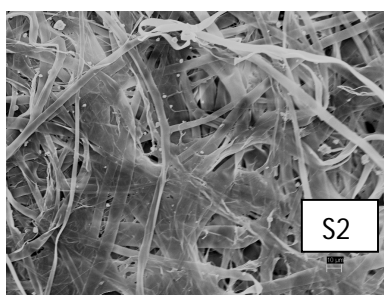
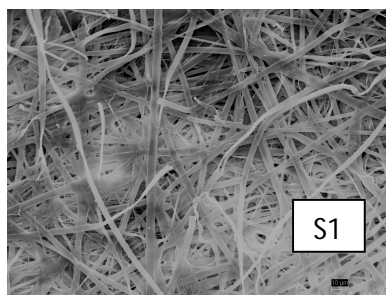


S7 subtracted from:

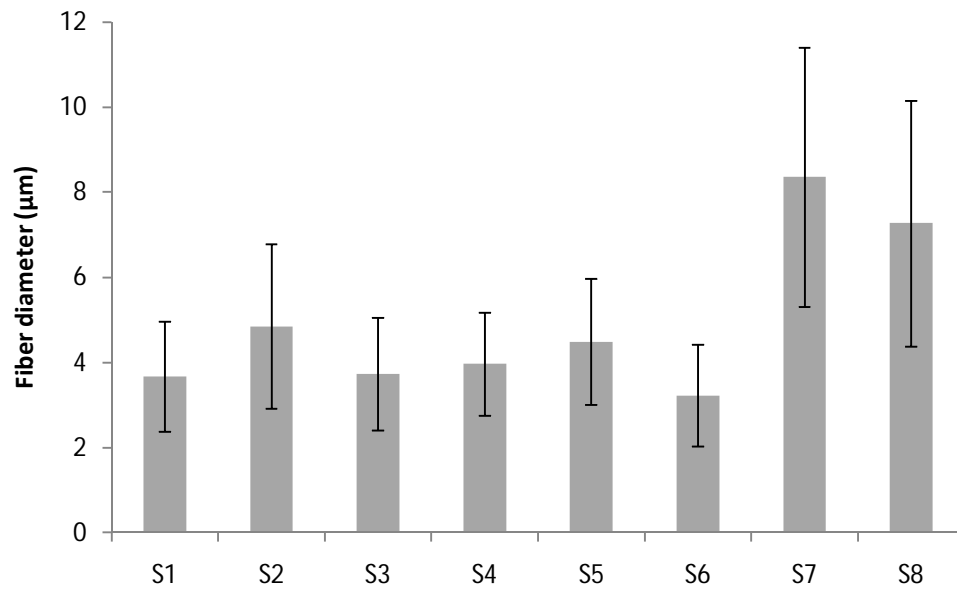


Appendix C (Data for the scaffolds crosslinked by the vapor method)

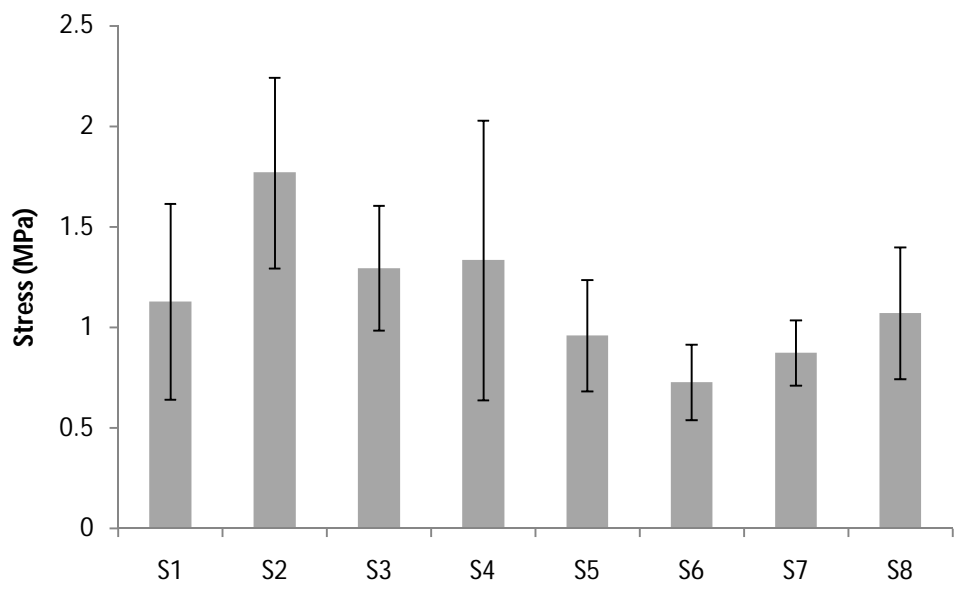
SEM images (The scale bar in all the images is 10 μm)



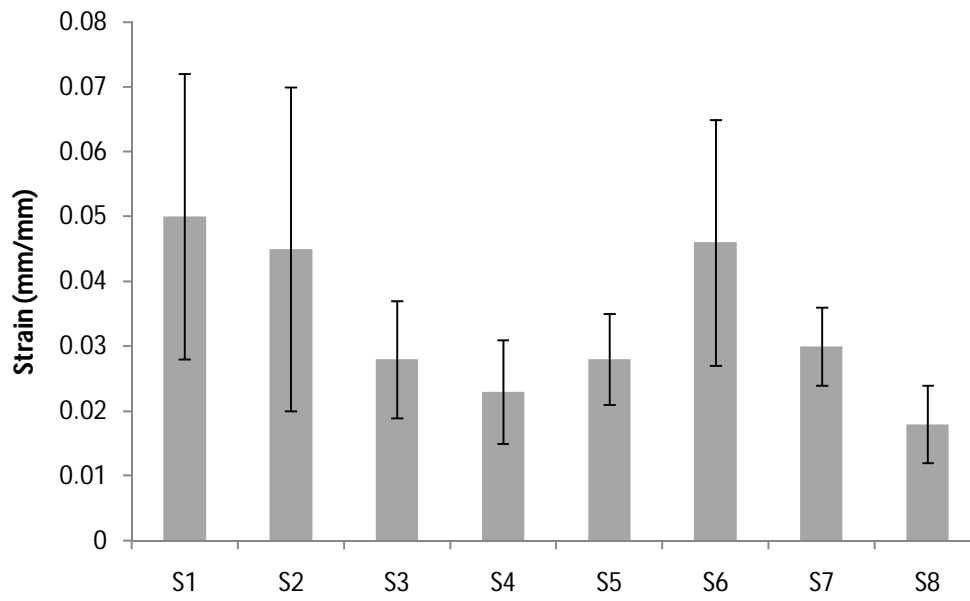
Fiber diameter



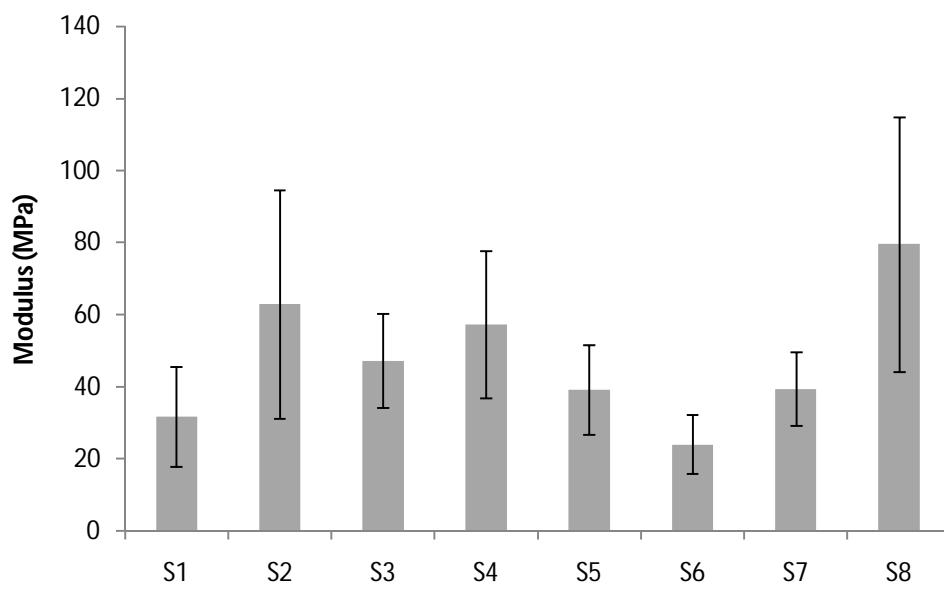
Stress



Strain



Modulus



One-way ANOVA: fiber diameter

Source	DF	SS	MS	F	P
Factor	7	728.15	104.02	27.89	0.000
Error	232	865.31	3.73		
Total	239	1593.46			

S = 1.931 R-Sq = 45.70% R-Sq(adj) = 44.06%

Individual 95% CIs For Mean Based on Pooled StDev

Level	N	Mean	StDev	
S1	30	3.666	1.287	(--*--)
S2	30	4.845	1.928	(--*--)
S3	30	3.727	1.318	(---*--)
S4	30	3.970	1.214	(---*--)
S5	30	4.486	1.481	(--*--)
S6	30	3.235	1.186	(--*--)
S7	30	8.360	3.047	(---*--)
S8	30	7.268	2.894	(--*--)

4.0 6.0 8.0 10.0

Pooled StDev = 1.931

Tukey 95% Simultaneous Confidence Intervals
All Pairwise Comparisons

Individual confidence level = 99.75%

S1 subtracted from:

	Lower	Center	Upper	
S2	-0.348	1.179	2.706	(---*---)
S3	-1.466	0.060	1.587	(---*---)
S4	-1.223	0.304	1.830	(---*---)
S5	-0.707	0.820	2.346	(---*---)
S6	-1.958	-0.431	1.095	(---*---)
S7	3.167	4.694	6.220	(---*---)
S8	2.075	3.601	5.128	(---*---)

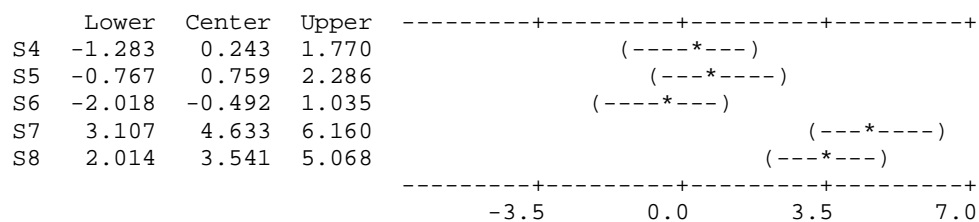
-3.5 0.0 3.5 7.0

S2 subtracted from:

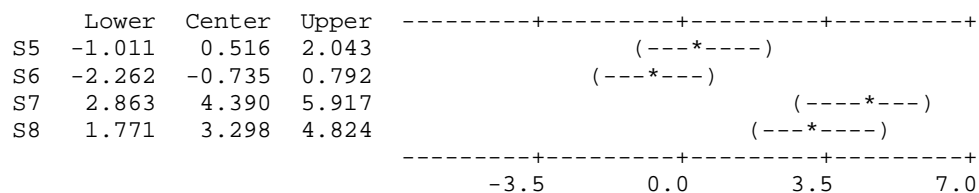
	Lower	Center	Upper	
S3	-2.645	-1.119	0.408	(---*---)
S4	-2.402	-0.875	0.651	(---*---)
S5	-1.886	-0.359	1.167	(---*---)
S6	-3.137	-1.610	-0.084	(---*---)
S7	1.988	3.515	5.041	(---*---)
S8	0.896	2.422	3.949	(---*---)

-3.5 0.0 3.5 7.0

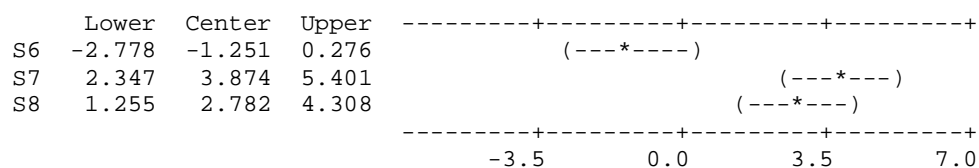
S3 subtracted from:



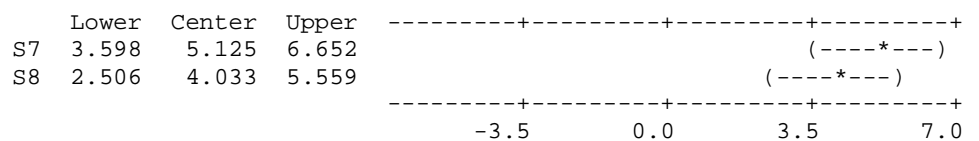
S4 subtracted from:



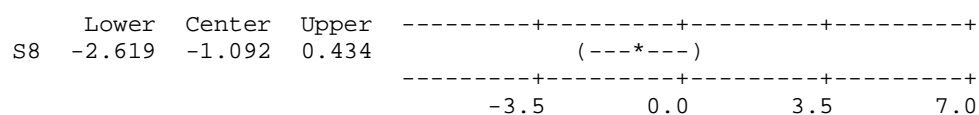
S5 subtracted from:



S6 subtracted from:



S7 subtracted from:



One-way ANOVA: Stress

Source	DF	SS	MS	F	P
Factor	7	4.406	0.629	3.91	0.002
Error	40	6.437	0.161		
Total	47	10.843			

S = 0.4011 R-Sq = 40.64% R-Sq(adj) = 30.25%

Individual 95% CIs For Mean Based on Pooled StDev

Level	N	Mean	StDev
S1	6	1.1302	0.4865
S2	6	1.7692	0.4763
S3	6	1.2947	0.3091
S4	6	1.3357	0.6963
S5	6	0.9598	0.2757
S6	6	0.7283	0.1873
S7	6	0.8755	0.1609
S8	6	1.0722	0.3263

0.50 1.00 1.50 2.00

Pooled StDev = 0.4011

Tukey 95% Simultaneous Confidence Intervals
All Pairwise Comparisons

Individual confidence level = 99.73%

S1 subtracted from:

	Lower	Center	Upper
S2	-0.1012	0.6390	1.3792
S3	-0.5757	0.1645	0.9047
S4	-0.5347	0.2055	0.9457
S5	-0.9106	-0.1703	0.5699
S6	-1.1421	-0.4018	0.3384
S7	-0.9949	-0.2547	0.4856
S8	-0.7982	-0.0580	0.6822

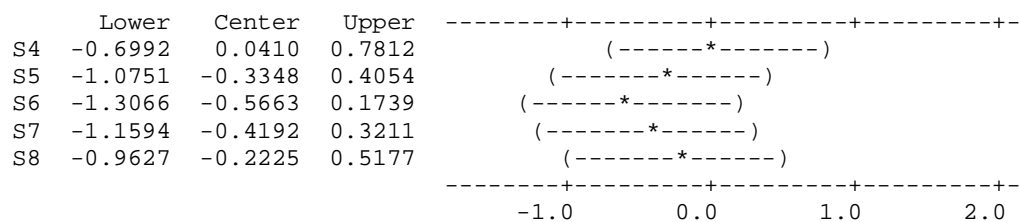
-1.0 0.0 1.0 2.0

S2 subtracted from:

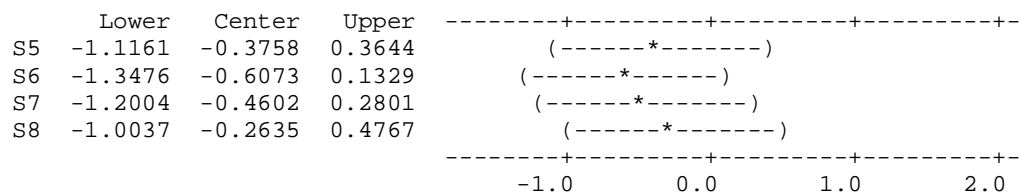
	Lower	Center	Upper
S3	-1.2147	-0.4745	0.2657
S4	-1.1737	-0.4335	0.3067
S5	-1.5496	-0.8093	-0.0691
S6	-1.7811	-1.0408	-0.3006
S7	-1.6339	-0.8937	-0.1534
S8	-1.4372	-0.6970	0.0432

-1.0 0.0 1.0 2.0

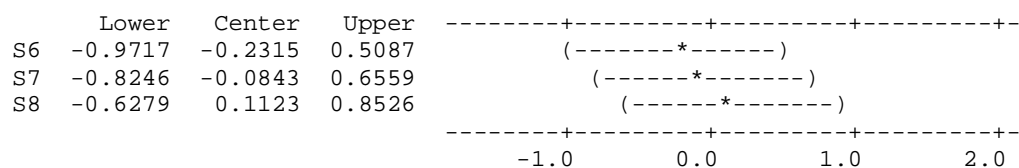
S3 subtracted from:



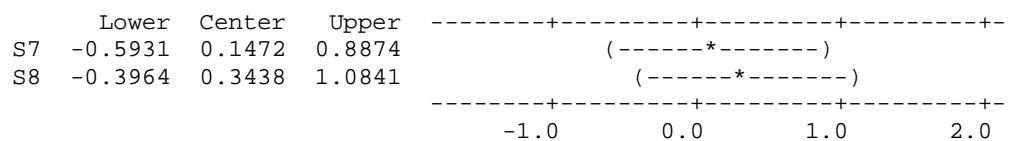
S4 subtracted from:



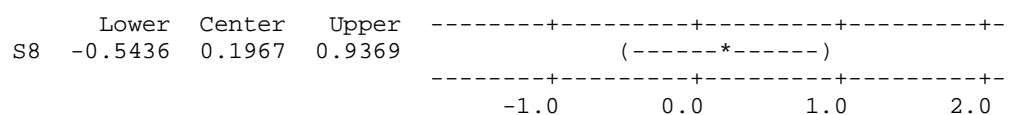
S5 subtracted from:



S6 subtracted from:



S7 subtracted from:



Source	DF	SS	MS	F	P
Factor	7	0.006165	0.000881	4.14	0.002
Error	40	0.008512	0.000213		
Total	47	0.014677			

S = 0.01459 R-Sq = 42.01% R-Sq(adj) = 31.86%

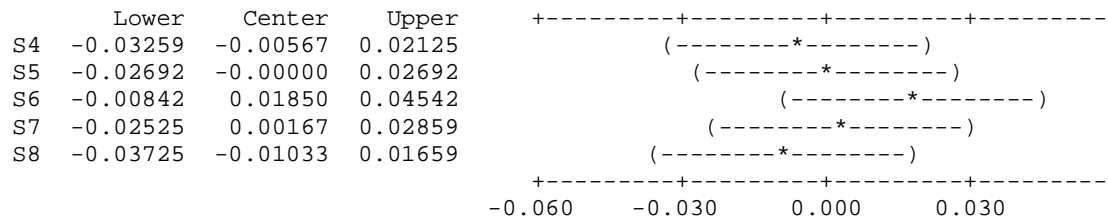
Pooled StDev = 0.01459

Individual confidence level = 99.73%

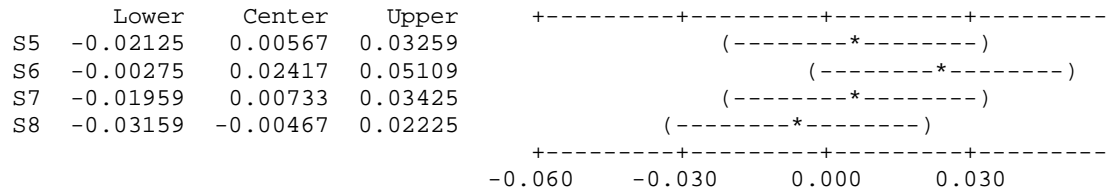
	Lower	Center	Upper	
S2	-0.03259	-0.00567	0.02125	(-----*-----)
S3	-0.04925	-0.02233	0.00459	(-----*-----)
S4	-0.05492	-0.02800	-0.00108	(-----*-----)
S5	-0.04925	-0.02233	0.00459	(-----*-----)
S6	-0.03075	-0.00383	0.02309	(-----*-----)
S7	-0.04759	-0.02067	0.00625	(-----*-----)
S8	-0.05959	-0.03267	-0.00575	(-----*-----)

	Lower	Center	Upper	
S3	-0.04359	-0.01667	0.01025	(-----*-----)
S4	-0.04925	-0.02233	0.00459	(-----*-----)
S5	-0.04359	-0.01667	0.01025	(-----*-----)
S6	-0.02509	0.00183	0.02875	(-----*-----)
S7	-0.04192	-0.01500	0.01192	(-----*-----)
S8	-0.05392	-0.02700	-0.00008	(-----*-----)

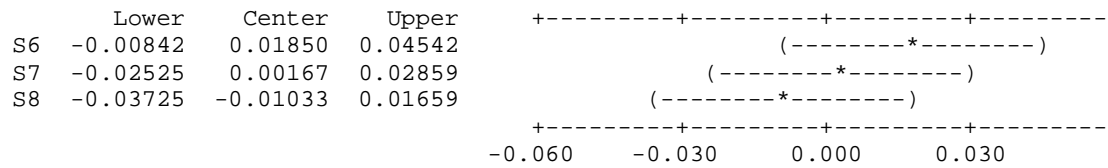
S3 subtracted from:



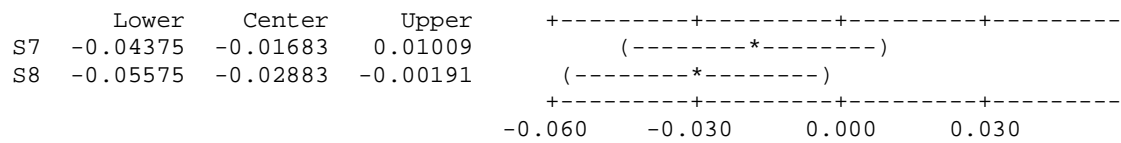
S4 subtracted from:



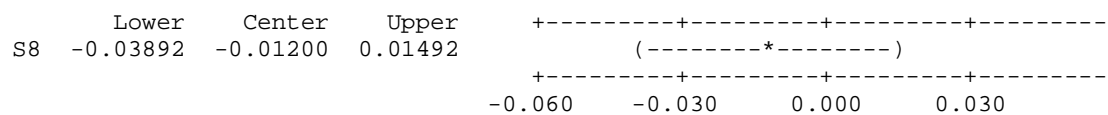
S5 subtracted from:



S6 subtracted from:



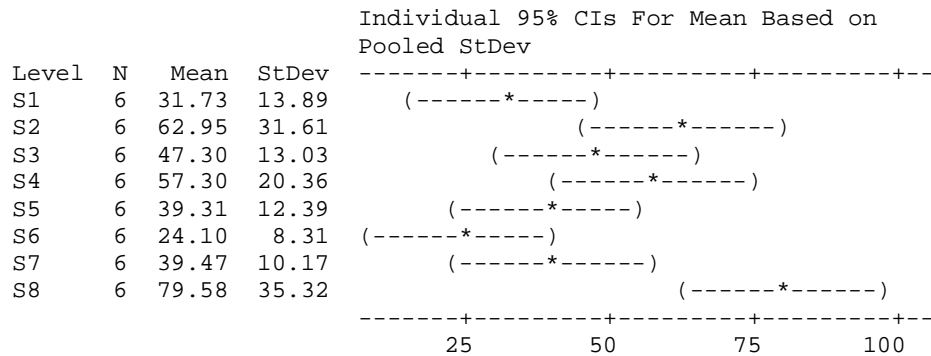
S7 subtracted from:



One-way ANOVA: modulus

Source	DF	SS	MS	F	P
Factor	7	13749	1964	4.69	0.001
Error	40	16753	419		
Total	47	30502			

S = 20.47 R-Sq = 45.08% R-Sq(adj) = 35.47%

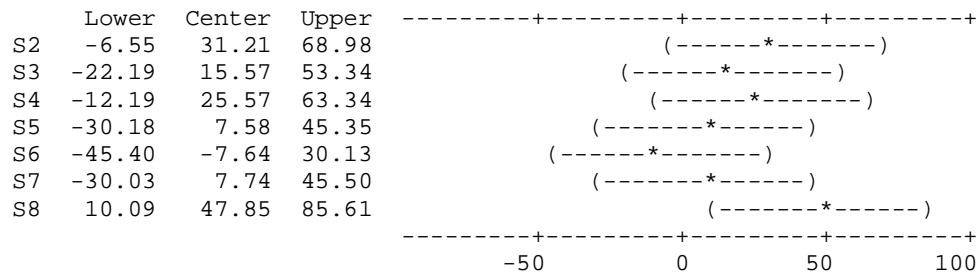


Pooled StDev = 20.47

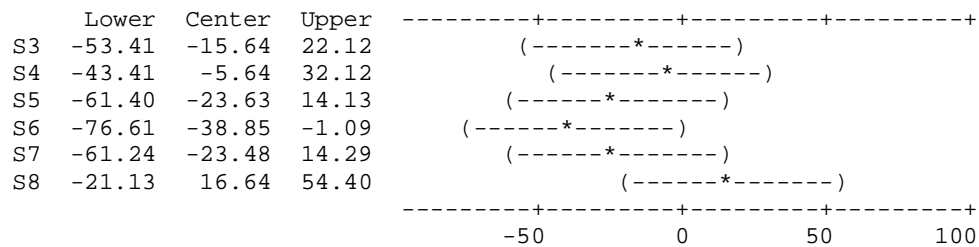
Tukey 95% Simultaneous Confidence Intervals
All Pairwise Comparisons

Individual confidence level = 99.73%

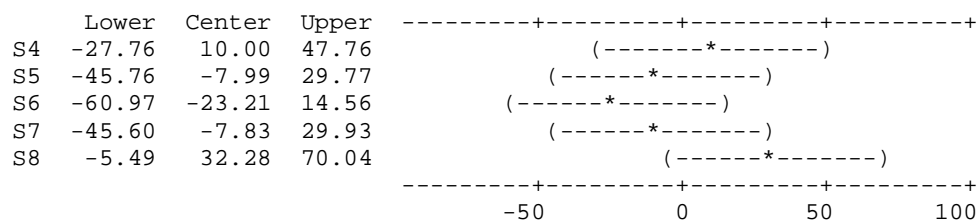
S1 subtracted from:



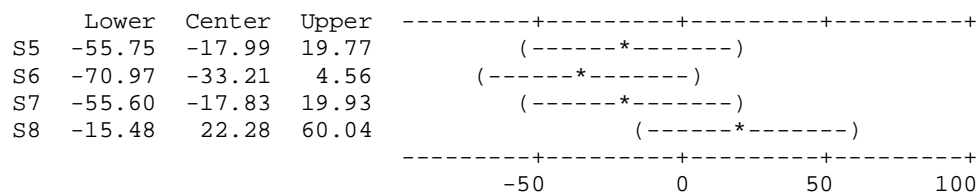
S2 subtracted from:



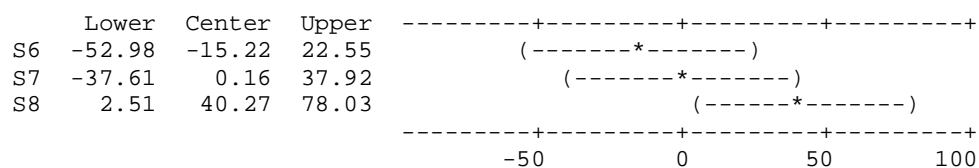
S3 subtracted from:



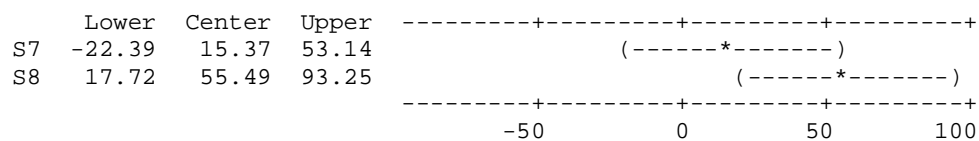
S4 subtracted from:



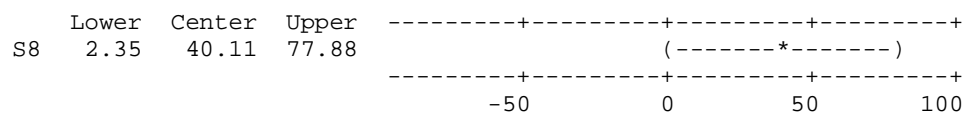
S5 subtracted from:



S6 subtracted from:



S7 subtracted from:



VITA

Alpana A. Dongargaonkar was born on October 24, 1985 in Mumbai, India. She graduated from Menon High School, Mumbai in 2003. She received her Bachelor of Technology in Biotechnology from ICFAI Institute of Science and Technology, Hyderabad, India in 2007. She began her graduate studies in Biomedical Engineering at Virginia Commonwealth University in Fall 2008. During her time at VCU, her research was focused on tissue engineering and drug delivery. She is very keen on expanding her knowledge in the field of stem cell and tissue engineering.